
Immobilized Catalysts for Alkene Oxidation

By

Nandi Malumbazo



A dissertation submitted in fulfillment of the requirements
For the degree of Master of Science in the Department of Chemistry,
University of the Western Cape

Supervisor: Prof. S. F. Mapolie (University of the Western Cape)

2007

DECLARATION

I declare that “**IMMOBILIZED CATALYSTS FOR ALKENE OXIDATION**” is my work and that all sources I have used or quoted have been indicated and acknowledged by means of references.



Signature:

ACKNOWLEDGEMENTS

I would like to extend my gratitude to the following:

God all mighty for his blessings and for giving me strength to continue with life and my studies even though there was no light shining upon my head.

My supervisor, Prof. S. F. Mapolie for his constant guidance, support and patience to develop my skills in research and also for believing in me.

My ancestors from my maternal side; Oonkomo, Oogolela, Oomasikela, Ooyongwane, Oomntungwa, Oomalinga, Oomasikane, Oonkumbuzo. To my ancestors from my paternal side; Oonyawuza, Oofaku, Oompondo, Oodayeli, Uziqelekazi uhlamba ngobubende, OoDakile.



To my family especially my mother (Bukelwa Ndayi), my late grandmother (Nombulelo Twala), my younger sister and brother.

To SASOL for financing my project and to give me a mentor, Dr Arno Nevelling

To DAAD NRF German Scholarship for financing my project.

To my friends who are always put a smile on my face at all times especially the following; Nanganmso Miti, Mvuselelo Matsebula, Fanelwa Ngece, Nothando Mungwe, Mteteleli Sibaca and Lucky Moni and colleagues who helped me with laboratory techniques.

ABSTRACT

Tertiary butyl substituted and unsubstituted Schiff base systems containing N,O donor ligands (Salicylaldimines) with aminotriethoxysilane tail were synthesized and complexed to Copper and Cobalt acetate. The ligands were characterized by FTIR and ¹H NMR Spectroscopy. The complexes were characterized by elemental analysis, ESI-Mass spectrometry and IR spectroscopy

Mesoporous silica supports (SBA-15 and MCM-41) were synthesized and characterized by X-ray diffraction, BET surface analysis and SEM. The tertiary butyl substituted and unsubstituted copper and cobalt salicylalimine complexes were immobilized on amorphous (Davisil silica gel) and mesoporous supports (SBA-15 and MCM-41). Immobilized catalysts were characterized with Atomic Absorption Spectroscopy, X-ray diffraction, BET surface analysis, IR spectroscopy and SEM.

Immobilized catalysts were tested for cyclohexene oxidation using molecular oxygen as co-oxidant and hydrogen peroxide as oxidant. In this study the effect of metal, reaction time, nature of oxidant (hydrogen peroxide tertiary butyl hydroperoxide), substituents on the ligand and substrate concentration were investigated. Allylic products were obtained at relatively high cyclohexene conversion. In addition to the above, homogeneous systems were compared with heterogeneous analogues. The former were found to have better selectivity than their heterogeneous analogues although there appears to be no significant difference in the activity of these two systems.

PUBLICATIONS

CONFERENCE CONTRIBUTIONS:

- ***OATA symposium (2006) – Water front, Cape Town***

Poster titled - Immobilisation of Salicylaldimine Complexes of Transition Metals on Silica Supports: Their Application in Alkene Oxidation.

- ***International Symposium Homogeneous Catalysis (2006) – Sun City***

Poster titled - Oxidation of Cyclohexene using Supported Salicylaldimine Complexes of Copper and Chromium.

- ***CATSA (2006) - Mosselbay***

Poster titled - Supported Salicylaldimine Complexes of Cu and Co as Catalysts in Alkene Oxidation.

- ***Inorg 007 (2007) – Langebaan, Cape Town***

Oral titled - Immobilized catalysts for Alkene Oxidation

- ***CATSA (2007) – KwaZulu Natal***

Poster titled - Mesoporous-Silica and Amorphous-Silica Supported Salicylaldimine Cu (II) and Co (II) Complexes as Catalysts for Cyclohexene Oxidation.

TABLE OF CONTENT

CHAPTER 1: Immobilized Catalysts for Alkene Oxidation

1. Background.....	2
1.1 Schiff Base Metal Complexes.....	4
1.1.1 Preparation of Schiff Bases.....	6
1.1.2 The Complexation Steps of Schiff Bases.....	7
1.1.3 Conformations of Metallosalen Complexes.....	9
1.2 Immobilization.....	12
1.2.1 Types of Support.....	13
1.2.2 Immobilization Methods.....	15
1.2.2 (a) Adsorption.....	16
1.2.2 (b) Encapsulation.....	16
1.2.2 (c) Covalent Tethering.....	18
1.2.2 (d) Electrostatic Interaction.....	23
1.2.3 Comparison of Methodologies and Advantages of Immobilization.....	24
1.3 Alkene Oxidation.....	25
1.3.1 Mechanistic Considerations for Formation of Epoxides.....	28
1.3.2 MCM-41 Supported Salen Complexes for Epoxidation.....	29
1.3.3 Co(II) Salen Functionalized Complexes for Styrene Oxidation with Hydrogen Peroxide.....	31

1.3.4 Allylic Oxidation of Cyclohexene Catalyzed by Schiff Base Complex	33
1.3.5 Comparison of Liquid Phase Olefin Epoxidation over MoO_x inserted within mesoporous silica and grafted onto silica	33
1.3.6 Preparation of Encapsulated and Anchored Alanine-Salicylaldehyde Schiff base Mn(III) (Sal-Ala-Mn) complexes by sol-gel method and their performance in aerobic epoxidation of cyclohexene.....	35
1.3.7 Allylic oxidation of cyclohexene over chromium containing mesoporous molecular sieves	36
1.3.8 Heterogeneous catalytic aerobic oxidation behavior of Co-Na heterodinuclear polymeric complex of Salen crown ether	38
1.3.9 Highly effective catalysts of natural polymer supported Salophen Mn(III) complexes for aerobic oxidation of cyclohexene ...	39
1.4 References.....	40

**CHAPTER 2: Synthesis and Characterization of Silica Immobilized Salicylaldimine
Copper (II) and Cobalt (II) Catalysts.**

2.1 Introduction	43
2.1.1 Salicylaldimine Complexes	43
2.2 Synthesis and Characterization of Silane Functionalized Salicylaldimine Ligands	44
2.2.1 Synthesis of Ligands	44
2.2.2 Characterization of Ligands	44
2.2.2.1 Characterization by means of ¹ H NMR Spectroscopy	44
2.2.2.2 Characterization by means of Infrared Spectroscopy	49
2.3 Synthesis and Characterization of Salicylaldimine Copper (II) and Cobalt (II) complexes	50
2.3.1 Complex Formation	50
2.3.2 Characterization of Complexes	51
2.3.2.1 Characterization by means of Infrared Spectroscopy	51
2.3.2.2 Characterization by means of Elemental Analysis	54
2.3.2.3 Characterization by means of Mass Spectroscopy	57
2.4 Synthesis and Characterization of Ordered Mesoporous Supports	58
2.4.1 Synthesis of MCM-41 and SBA-15	59
2.4.2 Characterization of MCM-41 and SBA-15	60
2.4.2.1 Characterization by means of X-ray Diffraction	60

2.4.2.2 Characterization by means of	
Infrared Spectroscopy	62
2.4.2.3 Characterization by means Scanning	
Electron Microscopy	63
2.4.2.4 Characterization by means of	
BET Surface Analysis	65
2.5 Synthesis and Characterization of Immobilized Cu(II) and Co(II) Catalysts.....	67
2.5.1 Immobilization of Complex 1 to 4 onto different Silica Supports.....	67
2.5.1.1 Immobilization of Metal Complexes onto Silica Supports.....	67
2.5.2 Characterization of Immobilized Metal Complexes	69
2.5.2.1 Characterization by means of X-ray Diffraction	69
2.5.2.2 Characterization by means of Infrared Spectroscopy	71
2.5.2.3 Characterization by means of Atomic Absorption Spectroscopy	73
2.5.2.4 Characterization by means of Scanning Electron Microscopy	75
2.5.2.5 Characterization by means of BET surface analysis.....	77
2.6 Conclusion	80
2.7 Experimental Method	80
2.7.1 Reagents.....	80
2.7.2 Apparatus.....	81
2.7.3 Synthesis of Ligands	81
2.7.4 Complex Formation	82
2.7.5 Synthesis of Inorganic Silica Supports	84
2.7.6 Immobilization of Complexes onto Inorganic Silica Supports.....	85

2.8 References.....	86
---------------------	----

CHAPTER 3: Alkene oxidation

3.1 Introduction	89
3.1.1 Salicylaldimine complexes as catalysts for alkene oxidation.....	89
3.1.2 Mechanism of Alkene Oxidation.....	90
3.1.2.1 Homolytic Oxidation	92
3.1.2.2 Heterolytic Oxidation	94
3.2 Evaluation of Catalytic Activity using Immobilized catalysts	95
3.2.1 The effect of metal.....	97
3.2.2 The effect of substituents	100
3.2.3 The effect of support.....	105
3.2.4 The effect of time	108
3.2.5 The effect of substrate concentration.....	112
3.2.6 The effect of changing oxidant	114
3.3 Evaluation of Catalytic Activity using Homogeneous Analogues	117
3.4 Conclusion	120
3.5 Experimental Method	121
3.6 References.....	122

LIST OF FIGURES

Figure 1.1: Some examples of different types of Schiff Base Ligands	5
Figure 1.2: Immobilization of $\text{Rh}^+[\text{R-R-BDPBzPSO}_3]^-$ complex by adsorption.....	17
Figure 1.3: Possible interactions of (-)-ephedrine with the surface of mesoporous micelle templated silica.	19
Figure 1.4: Proposed active site for the enantioselective dehydration of 2-butanol catalysed zeolites USY modified with dithiane oxide.	24
Figure 1.5: Structure of Sal-Ala-Mn.....	35
Figure 2.1: Typical Salicylaldimine complexes.	43
Figure 2.2: ^1H NMR of L1	48
Figure 2.3: FTIR spectrum of L1 recorded neat between NaCl plates.....	49
Figure 2.4: FTIR spectra showing change in bands after Complexation, ligand L1 was recorded neat between NaCl plates and Complex 1 was recorded as KBr pellets.	53
Figure 2.5: Proposed structures for Complexes 1, 2 and 6	56
Figure 2.6: ESI-Mass spectrum for Complex 1	57
Figure 2.7: Proposed synthetic pathway for MCM-41, by the liquid crystal templating approach.....	58
Figure 2.8: X-ray diffraction of MCM-41.	61
Figure 2.9: X-ray diffraction of SBA-15.	62
Figure 2.10: FTIR spectrum of MCM-41.	63

Figure 2.11: Scanning Electron Microscopy image of MCM-41.....	64
Figure 2.12: Scanning Electron Microscopy image of SBA-15.....	64
Figure 2.13: Nitrogen Adsorption Isotherm graph of MCM-41.....	65
Figure 2.14: Nitrogen Adsorption Isotherm graph of SBA-15.....	66
Figure 2.15: X-ray diffraction of Cat 5 to 7	69
Figure 2.16: X-ray diffraction of Cat 9 to 12	70
Figure 2.17: FTIR spectrum of the Immobilized Catalyst.....	72
Figure 2.18: Scanning Electron Microscopy of pure MCM-41 and MCM-41 immobilized Catalysts.....	75
Figure 2.19: Scanning Electron Microscopy of pure SBA-15 and SBA-15 immobilized Catalysts.....	76
Figure 2.20: Nitrogen Adsorption Isotherm graph of Cat 5 to 8	77
Figure 2.21: Nitrogen Adsorption Isotherm graph of Cat 9 to 12	78
Figure 3.1: Coordination of hydroperoxide molecule to the metal center.....	94

LIST OF SCHEMES

Scheme 1.1: A general schematic view of the synthesis of Schiff bases.....	7
Scheme 1.2: Various routes on the complexation of Schiff base ligands.....	8
Scheme 1.3: Different conformational isomers of Metallosalen.....	10
Scheme 1.4: Substitution of nucleophile on the Metallosalen.....	11
Scheme 1.5: Immobilization of (-)-ephedrine over mesoporous micelle templated silicas by covalent tethering.....	20
Scheme 1.6: Immobilization of Chromium Schiff base complexes.....	21
Scheme 1.7: Synthesis of covalently functionalized Copper-Schiff base MCM-41.....	22
Scheme 1.8: Cleavage pathways for the O-O bond in hydrogen peroxide: (A) Homolytic cleavage mechanism of hydrogen peroxide O-O bond; (B) Heterolytic cleavage mechanism of hydrogen peroxide O-O bond.....	27
Scheme 1.9: Peroxo and oxo metal pathways in olefin epoxidation.....	29
Scheme 2.1: Synthesis route of Salicylaldimine ligands.....	45
Scheme 2.2: General schematic route for the complex formation.....	52
Scheme 2.3: Schematic representation of the immobilization of metal complexes onto silica supports.....	68
Scheme 2.4: Condensation of adjacent silanols groups.....	74
Scheme 3.1: Peroxo and oxo metal pathways.....	91
Scheme 3.2: Homolytic decomposition of hydrogen peroxide; free radical mechanism of alkene oxidation.....	93

Scheme 3.3: Combination of Equation 6 and 7	94
Scheme 3.4: Schematic view of preparation of immobilized catalysts.....	96
Scheme 3.5: Possible products of cyclohexene oxidation.....	97
Scheme 3.6: Synthetic route of homogeneous analogues of the immobilized catalysts.	117



LIST OF TABLES

Table 2.1: ^1H NMR data of the ligand prepared.	46
Table 2.2: ^1H NMR of L1	50
Table 2.3: FTIR data for Complexes 2 to 8	53
Table 2.4: Elemental analysis for Complexes 1 to 8	54
Table 2.5: FTIR data of different catalysts.	72
Table 2.6: Metal content of immobilized catalysts.	74
Table 2.7: Physical properties of the immobilized catalysts.	79



LIST OF CHARTS

Chart 3.1: Effect of metal on cyclohexene conversion using immobilized catalysts.....	99
Chart 3.2: Effect of metal on product distribution using immobilized Cu and Co catalysts.	99
Chart 3.3: Cyclohexene conversion using immobilized Cu and Co unsubstituted and tertiary butyl substituted catalysts.....	103
Chart 3.4: Product distribution using immobilized unsubstituted and tertiary butyl Cu(II) and Co(II) catalysts.	105
Chart 3.5: Cyclohexene conversion using Cu(II) and Co(II) catalysts immobilized on different supports.	106
Chart 3.6: Effect of nature of support on product selectivity using unsubstituted Cu(II) and Co(II) immobilized catalysts.	107
Chart 3.7: The effect of time on cyclohexene conversion using immobilized Cu(II) and Co(II) catalysts.....	109
Chart 3.8: Product distribution of immobilized Cu(II) and Co(II) catalysts after 5 hrs and 24 hrs.....	110
Chart 3.9: Effect of decreasing substrate on cyclohexene conversion using immobilized unsubstituted Cu(II) catalysts.....	112
Chart 3.10: Effect of decreasing substrate on product selectivity using Cu(II) immobilized catalysts.....	113

Chart 3.11: Comparison of the use of hydrogen peroxide and tertiary butyl hydroperoxide as oxidants on cyclohexene conversion using unsubstituted Cu immobilized catalysts.....	115
Chart 3.12: Comparison on the effect of hydrogen peroxide against tertiary butyl hydroperoxide as oxidants on product selectivity using immobilized unsubstituted Cu catalysts.	116
Chart 3.13: Comparison of Cyclohexene conversion using homogeneous analogues against heterogeneous analogues.	118
Chart 3.14: Product distribution using homogeneous analogues.	119



CHAPTER 1

LITERATURE REVIEW



Immobilized Catalysts for Alkene Oxidation

1. General background

The need for cleaner chemical processes in industry is an obvious issue that has become important in recent times. In addition chemical transformations which produce large amounts of by-products and waste are less desirable. Selective transformation using catalytic processes can eliminate the requirement of stoichiometric auxiliary reagents in many current processes and can eventually help to decrease the amount of waste production. In recent times, more environmentally friendly processes for the oxidative transformations of organics have gained considerable interest. The catalytic transformation of hydrocarbons, mainly crude oil and natural gas constituents, into value added oxygenated derivatives such as alcohols, aldehydes, ketones, epoxides or carboxylic acids, using peroxides as oxidants have been extensively studied over the last few decades. This is primarily because such products are important intermediates in many industrial processes. Improvements can be made in many ways, such as the use of alternative reagents and catalysts, increasing the efficiency of the processes, easier separation of the products from the reactants and lastly the recycling of reagents or catalysts. This eliminates the requirement for laborious and inefficient extraction processes. One of the main contributions to waste in chemical processes is the separation of the product and catalyst from the reaction mixture. At the same time during the extraction, the catalysts can be easily destroyed. Thus elimination of these problems is highly desirable leading to so-called green chemistry.¹

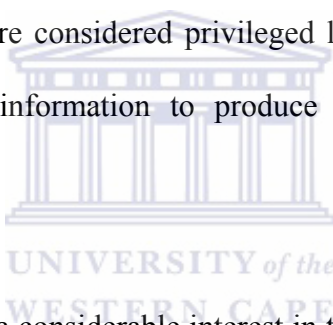
Homogeneous catalysis is not making as great an impact on the industrial synthesis of fine chemicals as may have been expected. One reason for this is that many of the ligands used in catalysis are expensive and there is a need for it to be recovered and re-used if the catalytic process is to be viable. Often this proves to be very difficult. A method for overcoming this problem is to combine the properties of homogeneous and heterogeneous catalysts by immobilizing the catalysts on a non-soluble support, thereby creating a heterogeneous type catalyst that can be readily recovered from the reaction mixture. The topic of immobilization has been a subject of several publications and several previous reviews. This strategy has been tested in recent years and many homogeneous catalysts have been immobilized. The catalytic properties of these immobilized catalysts have varied depending on the system. In many cases the performance was found to be significantly below those of the homogeneous analogues. Since the reasons of these differences in performance are still not well understood, there has been an ongoing interest to test different immobilization methods and different supports in order to get a better understanding of this strategy.²

The major part of this thesis describes our main efforts to develop new heterogenized catalytic systems that are capable of achieving oxidation of olefins at high activity using molecular oxygen as primary oxidant. We are focusing mainly on transition metals such as copper, manganese and cobalt since they are known to mediate the epoxidation of olefins in homogeneous systems. Also the nature of the ligand is very important in these types of catalytic systems. Schiff base ligands have been used because of their ability to stabilize many different metals in various oxidation states thus controlling the

performance of metals in a large variety of useful catalytic transformations. The main aim of this chapter is to give a clear overview of the use of immobilized Schiff base complexes in catalysis and the importance of alkene oxidation products.

1.1 Schiff base metal complexes

Hugo Schiff described the condensation between an aldehyde and an amine leading to imine formation in 1864. These so called Schiff bases are able to coordinate metals through the imine nitrogen and another group, usually linked to the parent aldehyde. Modern chemists still prepare Schiff base ligands and nowadays active and well-designed Schiff base ligands are considered privileged ligands. Some Schiff bases are also able to transmit chiral information to produce non-racemic products through catalytic processes.



In recent years, there has been a considerable interest in the chemistry of transition metal complexes of Schiff bases. This is due to the fact that Schiff bases offer opportunities for inducing substrate chirality, tuning the metal centered electronic behavior, enhancing the solubility of homogeneous and stability of heterogeneous catalysts. Schiff base complexes have been amongst the most widely studied coordination compounds in the past few years, since they are becoming increasingly important in a number of chemical industries. Generally active catalytic Schiff base metal complexes are obtained *in situ*, and are not well characterized. However, the appropriate choice of metal precursor and the reaction conditions are crucial for the catalytic properties.

A large number of reports are available on the chemistry of transition metal complexes containing O,N and S,N donor ligands. Transition metal complexes having oxygen and nitrogen donor Schiff bases possess unusual configurations, structural lability and are sensitive to their molecular environment.³

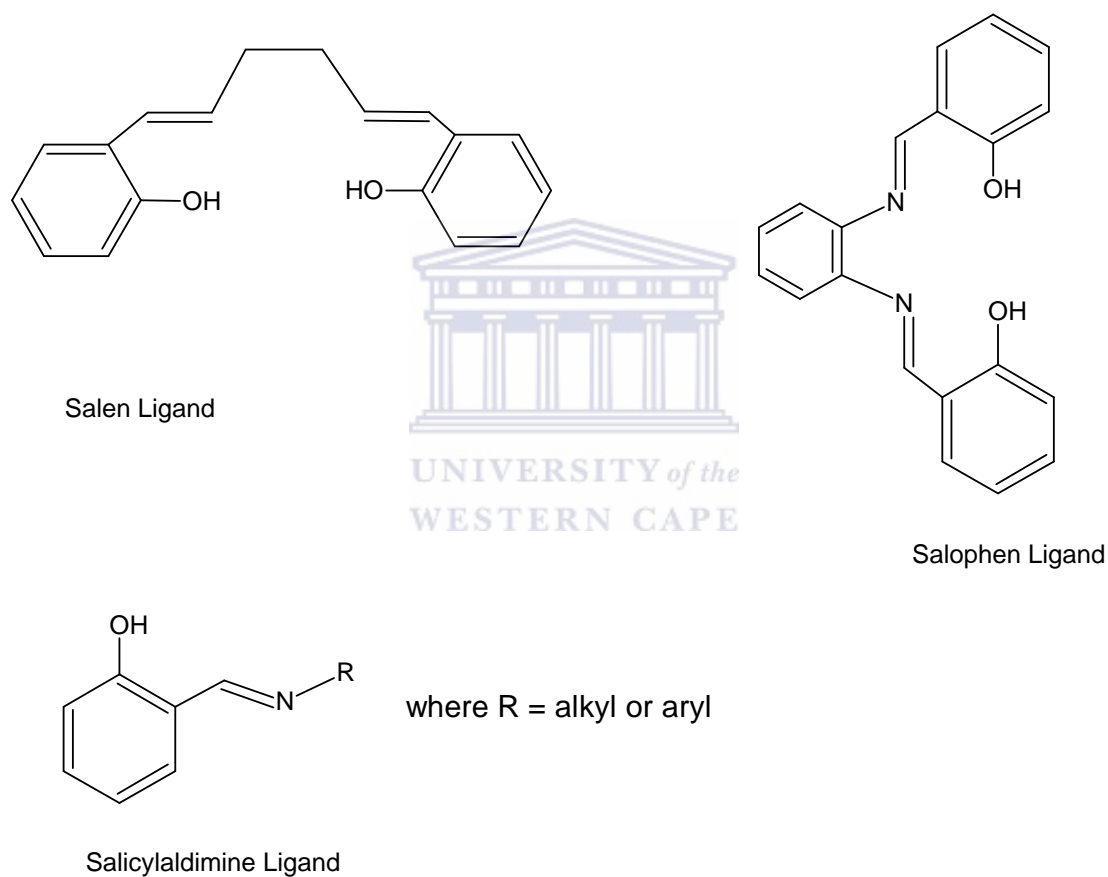


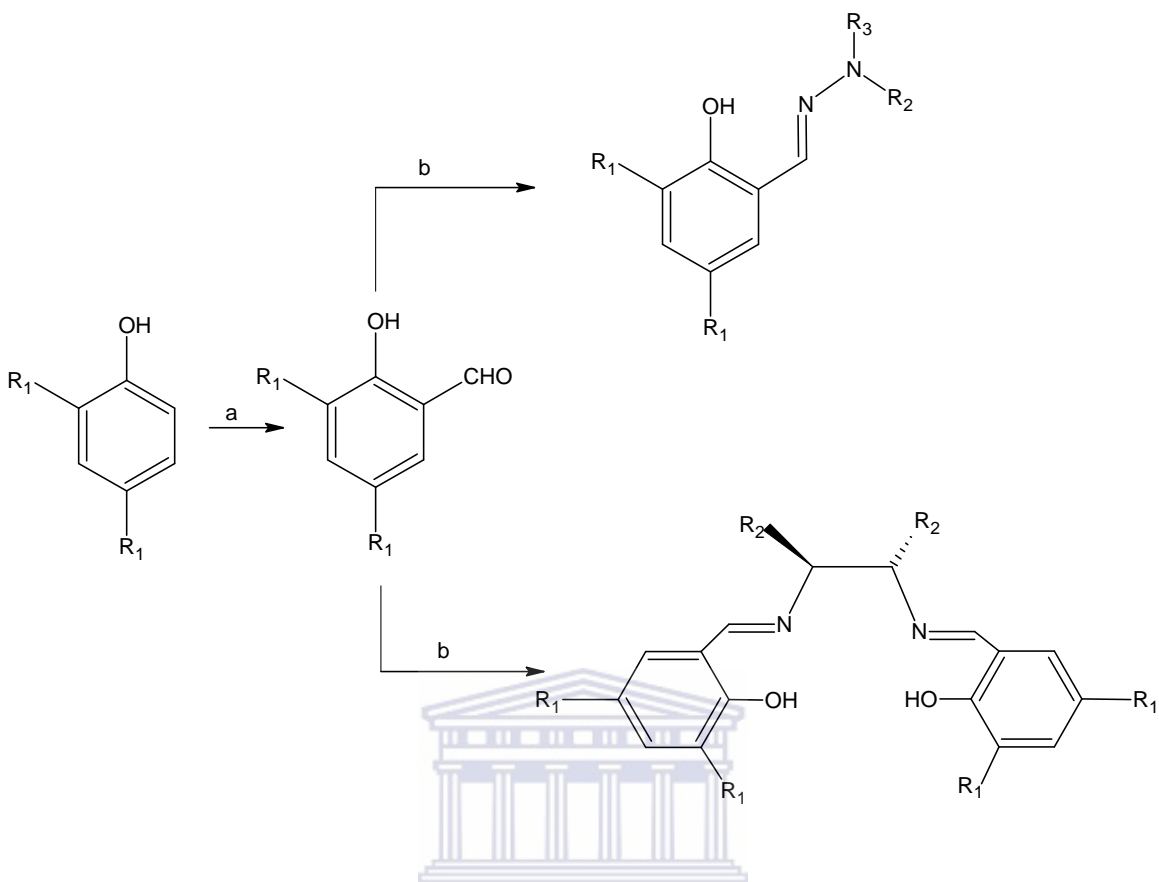
Figure 1.1: Some examples of different types of Schiff Base Ligands.

1.1.1 Preparation of Schiff bases

The condensation between aldehydes and imines is realized under different reaction conditions and using different solvents. The presence of dehydrating agents such as magnesium sulphate, formic acid, normally favors the formation of Schiff bases. Ethanol at room temperature or in refluxing conditions is also a valuable solvent for the preparation of Schiff bases. Degradation of the Schiff bases can occur during the purification step. Chromatography of Schiff bases on silica gel can cause degree of decomposition of the Schiff bases, through hydrolysis. In this case it is better to purify the Schiff base by recrystallization if possible.

If the Schiff bases are soluble in hexane or cyclohexane, they can be purified by stirring the crude reaction mixture in these solvents, sometimes adding a small portion of a more polar solvent such as dichloromethane or diethyl ether in order to eliminate impurities.

Condensation of salicylaldehydes with 1,2-diamines leads to the formation of Salens (**Scheme 1.1**). Salicylaldehydes bearing different substituents are obtained by the introduction of the formyl group, using a simple and well established reaction, of the corresponding phenol derivatives (**Scheme 1.1, a**).⁴ Schiff bases are suitable ligands for preparation of many catalytic precursors due to the straight forward reaction conditions and the availability of a variety of amines and aldehydes that can be used as precursors.



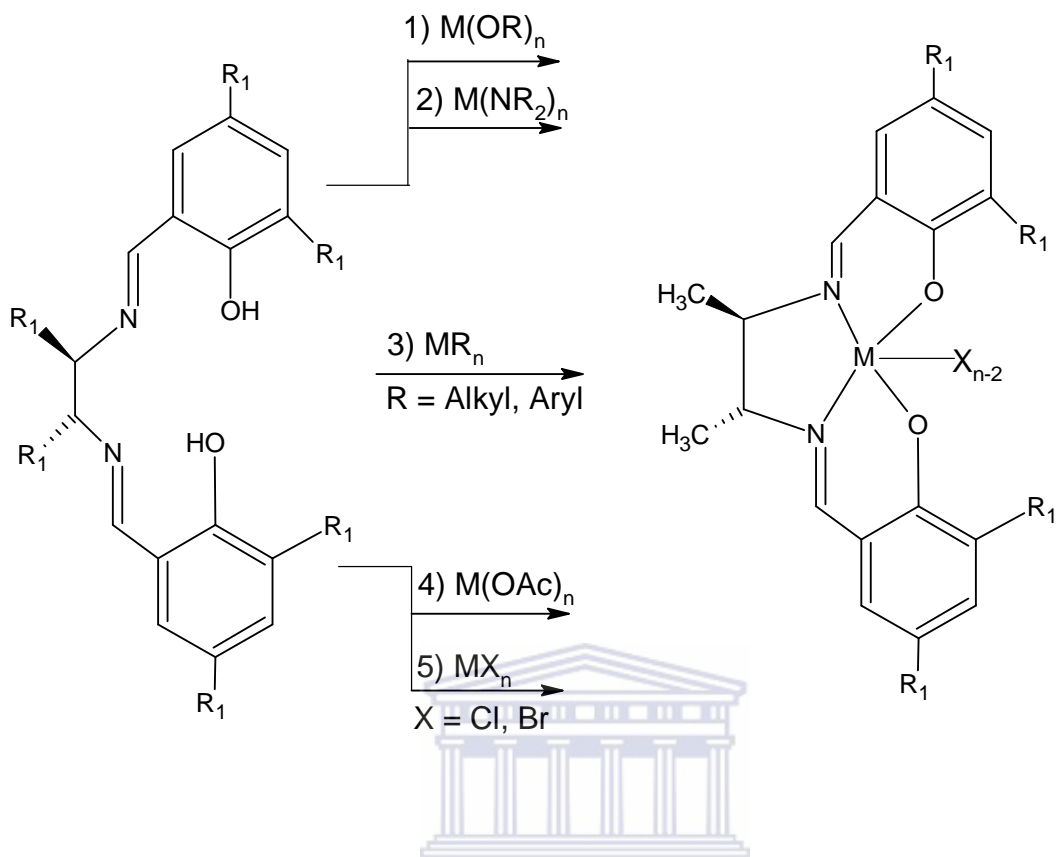
Where a = formaldehyde

Where b = secondary alkyl or aryl amine

Scheme 1.1: A general schematic view of the synthesis of Schiff bases.⁴

1.1.2 The complexation steps of Schiff bases

In many catalytic applications Schiff base metal complexes are prepared *in situ* by carrying out a reaction between the Schiff bases and the available and well defined metal precursors. This approach is clearly simple and suitable for catalytic applications. Essentially, five different synthetic routes can be identified for the preparation of Schiff base metal complexes.



Scheme 1.2: Various routes on the complexation of Schiff base ligands.⁴

Route 1 involves the use of metal alkoxides. For early transition metals ($M = \text{Ti, Zr}$), alkoxides derivatives are commercially available and easy to handle, while the use of other alkoxides is problematic. The introduction of a bulky group into the Schiff base can improve the solubility the complex. The disadvantage of using metal alkoxides is that they are very sensitive to hydrolysis and the presence of adventitious water can result in the formation of μ -oxo species. The formation of μ -oxo species can cause difficulties in reproducing the results of catalytic reactions.

Metal amides $M(NMe_2)_4$ ($M = Ti, Zr$) are highly suitable for the preparation of Schiff base metal complexes of early transition metals. The reaction occurs via the elimination of the acidic phenolic proton of the Schiff base, occurring at the same time as the formation of volatile $NHMe_2$. Disadvantage of this route is that this reaction produces two bisamido groups that can react further.

A Schiff base metal complex can be prepared in a clean and effective way using metal alkyl ($AlMe_3, GaMe_3, InMe_3$) complexes as precursors by a direct exchange reaction (route 3). These can be used as active catalysts for polymerization.

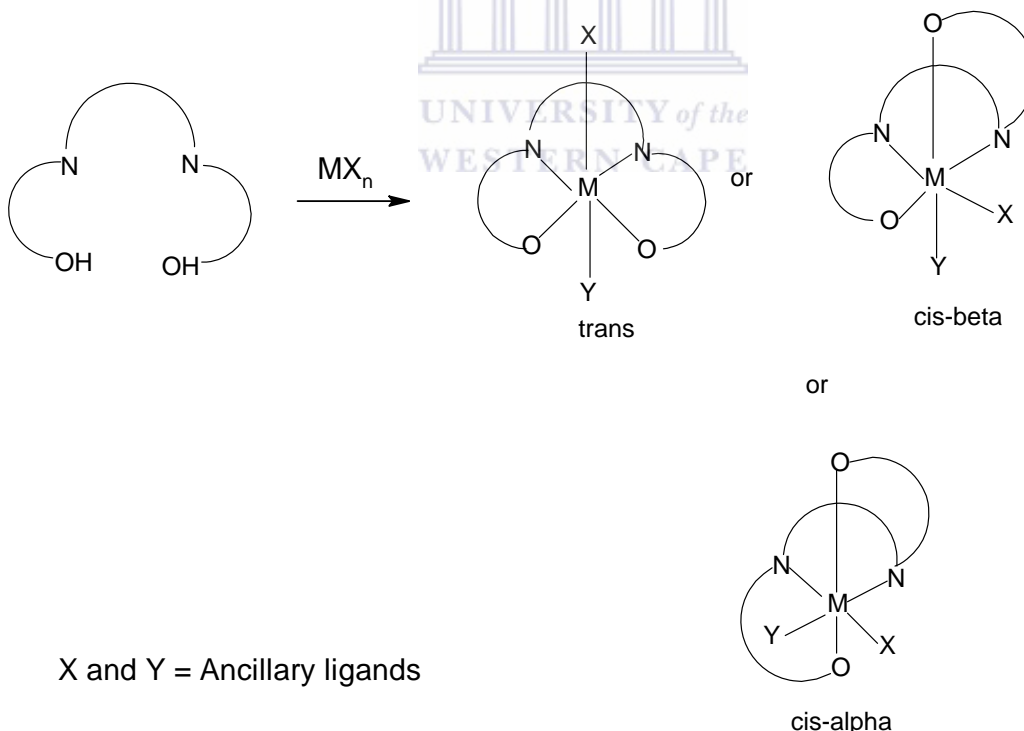
In route 4, the Schiff base metal complex can be obtained through the treatment of Schiff base with the corresponding metal acetate, normally by heating the Schiff base in the presence of metal salt under reflux conditions. Copper, cobalt and nickel Schiff bases are prepared by using the corresponding acetate $M(OAc)_2$ ($M = Ni, Cu, Co$).

In **scheme 1.2**, route 5, consists of a two-step reaction involving deprotonation of the Schiff Base and a successive reaction with metal halides. The deprotonation step is normally rapid at room temperature, but heating the reaction mixture to reflux does not cause decomposition.⁴

1.1.3 Conformations of metallosalen complexes

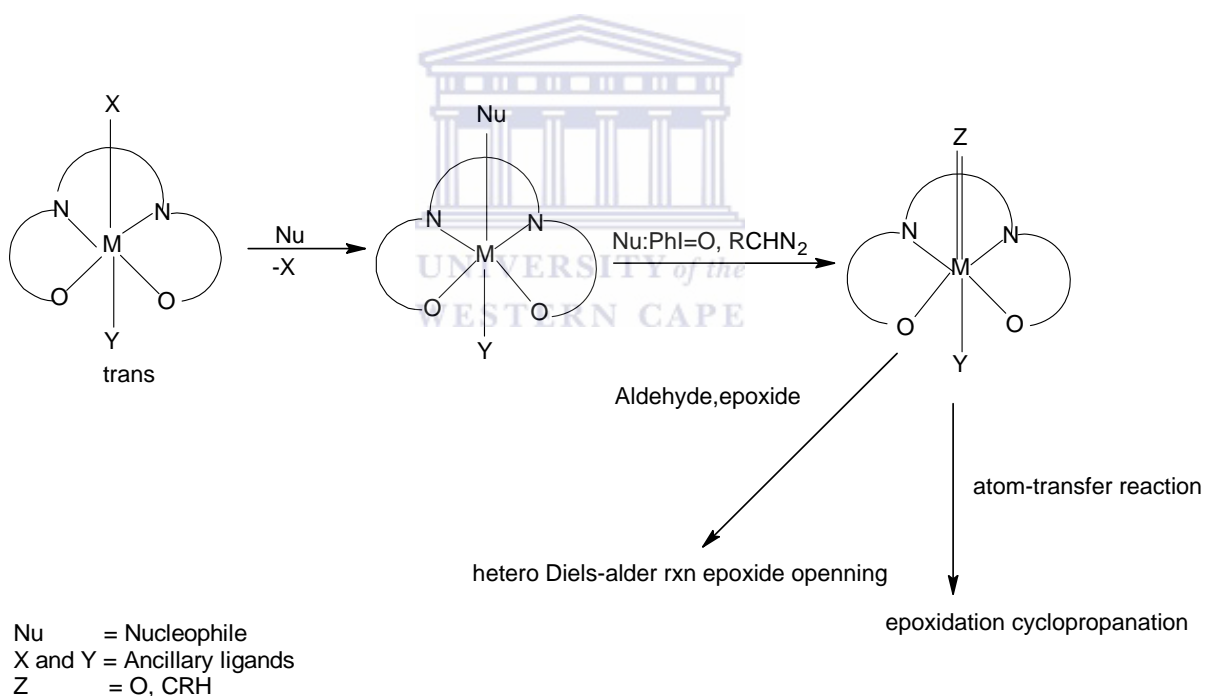
Studies of the catalysis of metallosalen complexes have been undertaken with the complexes of the first-row transition metals, such as chromium, manganese, cobalt and

vanadium. Due to the presence of two sp^3 carbons at the diamine unit (ethylenediamine has rotational freedom), a metallosalen complex exists as several stereoisomers (configurational and conformational isomers). Metallosalen complexes can adopt three configurations (*trans*, *cis-β* and *cis-α*): two ancillary ligands occupy the apical positions in *trans*-isomer, one equatorial and one apical position in *cis-β*-isomer and two equatorial positions in *cis-α*-isomer.⁵ The metallosalen adopt the *trans*-configuration when the ancillary ligands are monodentate. In general, the ancillary ligands of a *trans*-metallosalen complex can be readily substituted with a nucleophilic compound that might be a reagent or substrate. The coordinated nucleophile is activated by the Lewis acid metal ion or further transformed into an active species, depending on the nature of the nucleophilic compound.



Scheme 1.3: Different conformational isomers of metallosalen.⁵

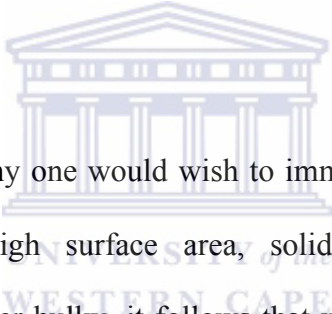
For an example, treatment of suitable metallosalen complex with nucleophile (Nu) such as iodosylbenzene and diazo ester, generates an active oxene ($Z = O$) and a carbene-metal complex ($Z = CRH$), respectively, via the corresponding additional compounds. These active species can undergo oxygen or carbon-atom transfer to a variety of substrates. On the other hand, when the coordinated Nu is an aldehyde or an epoxide, it undergoes hetero Diels-Alder reaction or epoxide-ring opening reaction, respectively. Thus, various reactions can be catalyzed by *trans*-metallosalen complexes. If the salen ligand is chiral, these reactions proceed in an enantioselective manner.⁶



Scheme 1.4: Substitution of a nucleophile on the metallosalen.

1.2 Immobilization

Heterogenization of homogeneous catalysts has become an important strategy for obtaining supported catalysts that retain the active catalytic sites of a homogeneous analogue while at the same time providing the advantages of easy separation and recycling of catalyst. Immobilization refers to the anchoring of the homogeneous catalysts onto the siliceous nanoporous support where the defined diameter of the pores may fall within the range of 30-500 Å. It also refers to the “ship in a bottle” construction in which an active organometallic catalyst is assembled within the cages of the zeolite or when a zeolite cage is built around the organometallic catalyst giving rise to what is known as “tea bag”.⁷



There are two main reasons why one would wish to immobilize catalytically significant organometallic species on high surface area, solid supports. Firstly, because organometallic species are rather bulky, it follows that when they are anchored at solid surfaces their points of attachments are rather far removed from one another. This means that when the organometallic species is subsequently converted, by appropriate post-immobilization treatment, to a smaller catalytically active entity these active sites are so far apart that the resulting solid may legitimately be designated a single site catalyst.

Secondly, an organometallic species that exhibits high catalytic activity and selectivity when in solution is even more desirable if it is immobilized because of the ensuring advantage of ease of separation of the catalyst itself from products and from unconverted reactants.

1.2.1 Types of support

Immobilization generally implies the use of any or all of the following materials as supports: silica, alumina, silica-alumina, magnesia, titania, zirconia, ceria, vanadia and various kinds of polymers. Two classes of materials that are extensively used as heterogeneous catalysts and adsorption media are microporous (pore diameter $< 20 \text{ \AA}$) and mesoporous ($20\text{-}500 \text{ \AA}$) inorganic solids. The utility of these materials is manifested in their microstructures which allow molecules access to large internal surfaces and cavities that enhance catalytic activity and adsorptive capacity. A major subclass of the microporous materials is molecular sieves. These materials are exemplified by the large family of aluminosilicates known as zeolites in which the micropores are regular arrays of uniformly sized arrays. Mesoporous materials are typically amorphous or paracrystalline solids such as silicas or transitional aluminas or modified layered materials such as pillared clays and silicates. The pores in these materials are generally irregularly spaced and broadly distributed in size.⁸

In the early 1990's, groups at the Mobil Co., USA and at the Toyota Co. and Waseda University, Japan were the ones who discovered a new family of ordered mesoporous silica materials which are called M41S and FMS families. The most frequently used mesoporous support is silica. This offers a variety of pore sizes, surfaces, and shapes of particles and this support is very affordable (cheap). A draw back is the broad pore size distribution; even the so-called wide-pore silica contains substantial numbers of micropores, which form the main part of the specific surface area.⁹ On the other hand it is an advantageous material to use. The merits of having readily available high surface

area (*ca.* 600-1500 m²g⁻¹) silica with well defined pore dimensions are obviously attractive for use in catalysis. Also owing to its excellent thermal and chemical stability, ease of handling and the exposed silanol groups (for binding of homogeneous catalysts), and silica is an ideal material for heterogenization of catalysts. Silica as a support material has a rigid structure and it does not swell when immersed in solvents so it may be used conveniently at both high and low temperatures and at high pressure.⁷

Since 1992, much research has focused on the synthesis of mesoporous molecular sieves, whose structures are similar to those of mesophases formed by self assembly of molecular inorganic solutions with surfactant molecules. MCM-41 is one of the widely used mesoporous silica materials that belong to a family of M41S. MCM-41 has one-dimensional pores with uniform size. Researchers at Mobil have proposed that MCM-41 forms via a liquid crystal templating mechanism. That is, a liquid crystalline phase forms initially and organizes silicates species in the continuous water region to create the inorganic walls of MCM-41, that is when the hexagonally close packed cylindrical are formed upon removal of the surfactant.

The stability of these materials is an important aspect for use in almost any application. MCM-41 has high stability in air, has low stability in water and aqueous solutions. The hydrothermal and thermal stability decreases when incorporated with metals such as titanium and aluminium. Synthesis of MCM-41 in various salts and ion-exchange after synthesis results in an improvement in the stability of MCM-41. Hexagonal mesopores produced via templating with neutral surfactants have shown to have thicker and more

condensed walls than materials synthesized with cationic surfactants, and this helps to improve thermal stability. Studies of the effects of pressure upon calcined materials have shown that the materials lose structure under pressure owing to hydrolysis of Si-O-Si bonds in the walls. It is also well known that these materials will break down over the course of the month when stored under ambient conditions.¹⁰

Pure silica mesoporous materials are of limited use in many catalytic applications because of their lack of active sites. According to the requirement of various catalytic reactions, various active species were introduced into the ordered mesoporous silica materials by various methods.¹¹



1.2.2 Immobilization methods

The topic of immobilization has been the subject of several publications and several previous reviews and most of them have focused on the extensive range of reactions exemplified by immobilized asymmetric catalysts. The silica surface consists of two types of functional groups, siloxane (Si-O-Si) and silanol (Si-OH). Immobilization can occur via a reaction of a particular molecule with either the siloxane (nucleophilic substitution at the Si) or silanol groups (direct reaction with the hydroxyl group). Although it is accepted that it is the reaction with the silanol function that constitutes the main modification.¹²

Four distinct methodologies have been developed for the heterogenization of homogeneous catalysts.

1.2.2 (a) Adsorption

Catalysts immobilized by this method can sometimes rely on weak van der Waals interactions between the catalyst and the support. This is a weak interaction with the result that the catalyst can readily leach into the solution as the system reaches equilibrium between the surface adsorbed species and the solution species. The stability of the supported catalyst can be improved by modifying the catalyst and support to allow hydrogen bonding to occur.

Rhodium phosphine catalysts have been immobilized on silica in this way where the phosphine ligand was modified to incorporate sulfonic acid groups which hydrogen bonded with the silanols present on the silica surface (**Figure 1.2**).¹³

Catalysts which contain a sulfonic counterion can also be immobilized in this way. In this case the sulfonate counterion interacts with both the support and the catalyst giving rise to an immobilization strategy more in keeping with electrostatic immobilization.

1.2.2 (b) Encapsulation

Encapsulation is the only catalyst immobilization method which does not require any interaction between the catalyst and the support and because of this, it is the only method which attempts to mimic the homogeneously catalysed reaction process. Other methods, by necessity lead to changes in the catalyst. To satisfy the condition of encapsulation, the catalyst must be larger than the pores of the support material to prevent loss of the catalyst into the solution during the course of the reaction.

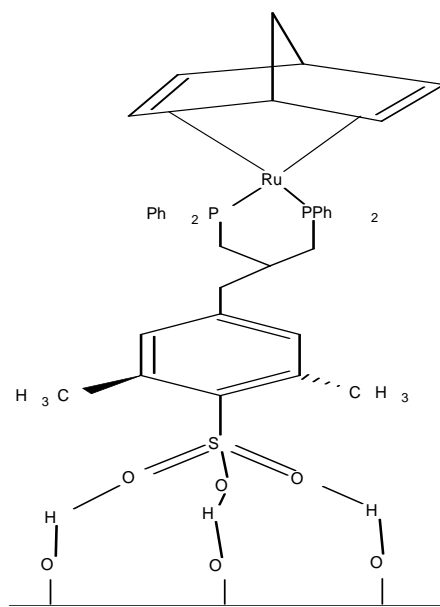


Figure 1.2: Immobilization of Rh^+ $[R-R-BDPBPzPSO_3]^-$ complex by adsorption.¹³

As the catalyst complex is larger than the pores of the support, techniques such as impregnation cannot be used to prepare these catalysts. The supported catalysts can be prepared by either i) assembling the catalyst within the pores of the support or ii) assembling the support around the catalyst and both of these methods have been used to encapsulate the catalyst. The route used for the catalyst encapsulation is dictated by the chemistry of the support and the catalysts complex. If the catalyst is to be assembled within the pores of the support, then the support needs to be stable under the reaction conditions used. The materials normally used as supports tend to be inert so this is generally not a problem. The chemical processes used to prepare a catalyst are of crucial importance and side reactions need to be avoided and each step must have high yields. If many different species are present in addition to the catalyst (due to side reactions in the ligand synthesis), it is likely that reduced yields and enantio-selectivity will be obtained

and because these moieties are encapsulated they are difficult to remove selectively from the support. If the support is assembled around the catalyst then the catalyst needs to be stable to the synthesis conditions of that support. Hence, if the catalyst can be made easily in a small number of steps then assembly within the pores is preferred. If the catalyst is difficult to make but is stable then formation of the support around the catalyst is preferred.¹³

1.2.2 (c) Covalent tethering

This is the most widely used method to design stable heterogeneous asymmetric catalysts. Different strategies have been developed depending upon the reaction being catalyzed.



Using this approach, the complex is grafted onto the surface of a support material (usually mesoporous silica). Where the complex contains suitable functional groups, this is normally grafted directly onto the surface of the silica as shown in **Figure 1.3**. If no such groups exist then the ligand is modified to include $\text{Si}(\text{OR})_3$ moieties, which can be grafted onto the surface of the support by condensation (**Scheme 1.5**).

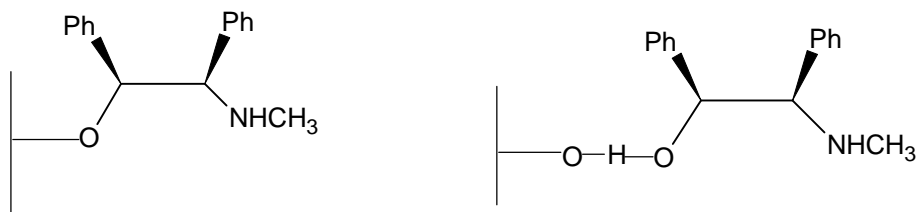
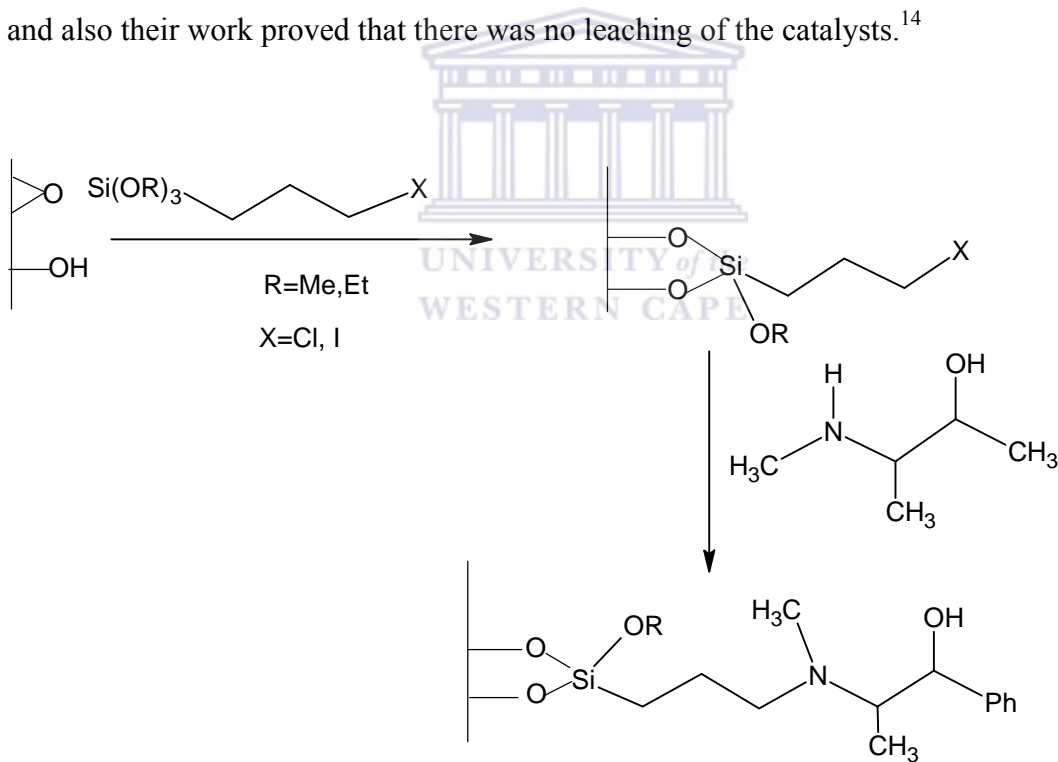


Figure 1.3: Possible interactions of (-)-ephedrine with the surface of mesoporous micelle templated silica.

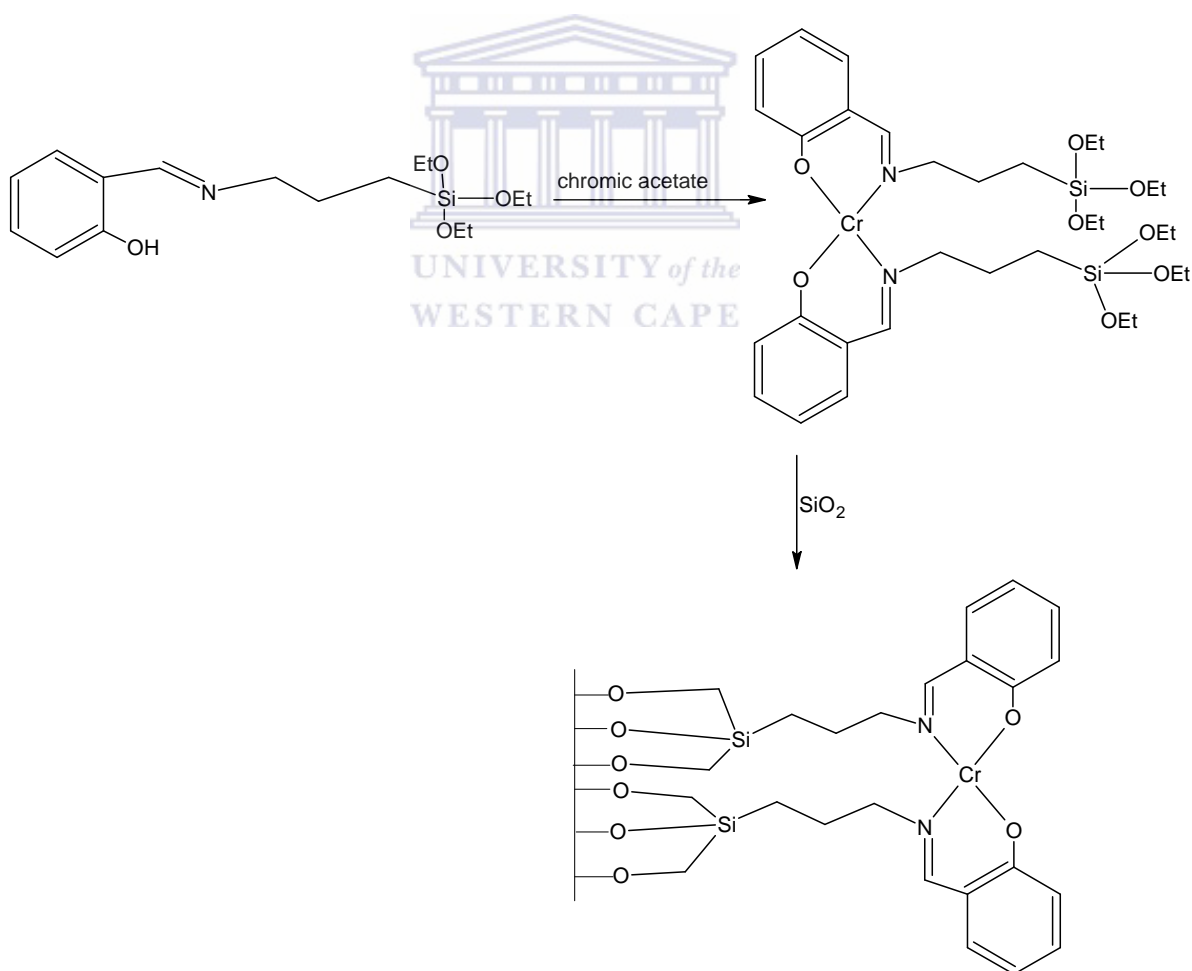
One of the most widely studied systems using this approach is the immobilization of chromium Schiff base complex for the catalytic oxidation of alkyl aromatics using novel silica as support.

The first step was to modify the ligand by reacting Salicylaldehydes with 3-aminopropytrimethoxysilane which gave Salicylaldimine ligands and this was further reacted with Chromium(III) acetate resulting in chromium Schiff base complex, this is shown in **Scheme 1.6**. The silica was then used as a support. The linkage was via surface silanols. Reasonable results were obtained for the oxidation of methyl aromatics and also their work proved that there was no leaching of the catalysts.¹⁴



Scheme 1.5: Immobilization of (-)-ephedrine over mesoporous micelle templated silicas by covalent tethering.

The synthesized of copper-Schiff base complexes were covalently anchored onto the Si-MCM-41 surface by the condensation of siloxane groups and the surface silanol groups of MCM-41. A series of copper-Schiff base MCM-41 materials were synthesized to study the effect of copper loadings and the reaction times on the surface properties of the material. The grafting of copper-Schiff base complex was carried out by preparing and characterizing Schiff base ligand followed by metal complexation. The complex was then immobilized on MCM-41 (**Scheme 1.7**).

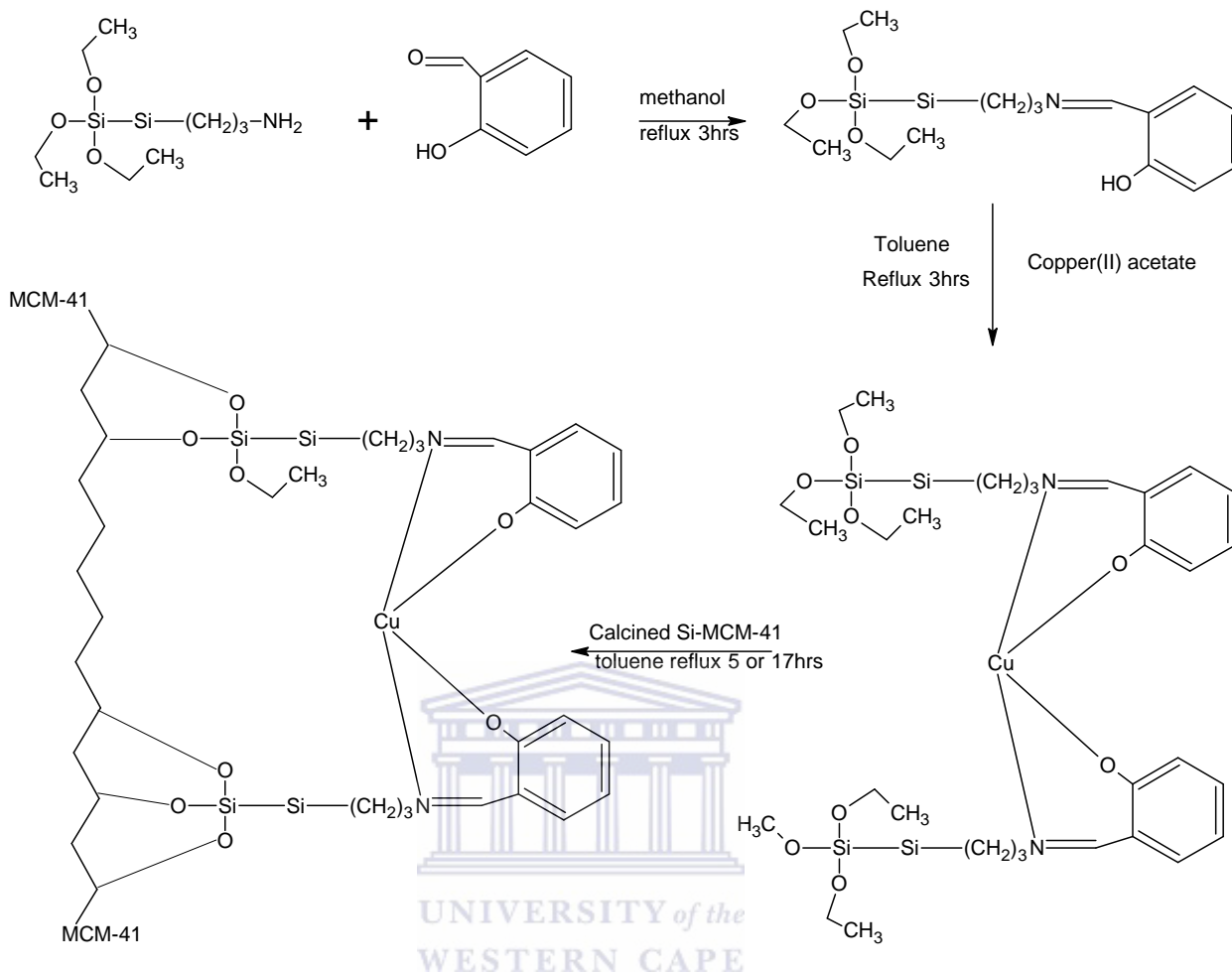


Scheme 1.6: Immobilization of Chromium Schiff base complexes.¹⁴

Another coordination approach in immobilization is the modification of mesoporous silica with a surface modifier by the covalent bonding method.

Chiral Mn(III) salen complexes were prepared using these two approaches. Chiral Mn(III) salen complexes were supported onto mesoporous supports such as MCM-41 and SBA-15 and the reactive surface modifier used is 3-aminopropyltriethoxysilane. The anchoring of the chiral Mn(III) salen complex was made through the fifth position of the salen complex onto the surface modifier of MCM-41 and SBA-15. The coordination sphere of the manganese ion is not involved in the anchoring of the complex to the support and this makes the activity of this complex to be akin to the one of homogeneous complexes.¹⁶





Scheme 1.7: Synthesis of covalently functionalized copper-Schiff base MCM-41.¹⁵

1.2.2 (d) Electrostatic interaction

Many porous solids, including zeolites, zeotypes, ordered mesoporous silicates and layered materials, including clays can act as ion exchangers. This method presents a relatively facile mechanism for the immobilization of metal cations and complexes through electrostatic interaction. At first sight, many would consider that this interaction does not have sufficient strength to ensure that the catalyst remains truly heterogeneous, yet the approach has been used to produce stable heterogeneous, enantioselective

catalysts that can exhibit significantly improved catalytic performance when compared with the homogeneous counterparts.

The design of this approach involves the ion exchange of suitable cations into the intracrystalline pores of zeolites, e.g. zeolites Y or mesoporous solids, e.g. MCM-41, and the subsequent modification of the cation with a chiral ligand prior to reaction. The initial studies used the acidic form of zeolites Y with chiral dithiane 1-oxides as chiral ligands for the catalyst for the enantioselective dehydration of butan-2-ol. Although only one active center per zeolite supercage was modified, the modified sites were several orders of magnitude more active than the non-modified sites. As a result, the catalysts were effective for the enantioselective and catalysed dehydration reaction.

At low conversion, the chiral catalyst modified with the *R*-dithiane 1-oxide preferentially reacted *S*-butan-2-ol in the presence of both enantiomers. Unfortunately, the enantioselective reaction was short-lived, but the enhancement in the rate of reaction with the modified catalysts was long-lived. Detailed spectroscopic studies of active catalysts showed that the extra framework alumina, present in the pores of the zeolite, were an integral part of the active site. The rate enhancement was proposed to be due to activation of the Bronsted OH group of the zeolites through interaction with the oxygen of the dithiane 1-oxide and the extra framework of the alumina moiety (**Figure 1.4**).¹⁷

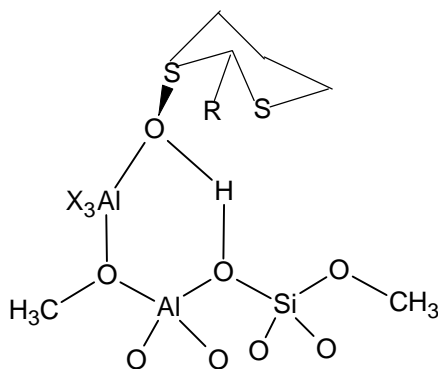


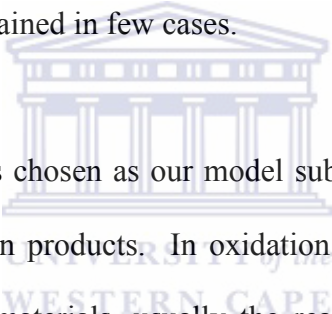
Figure 1.4: Proposed active site for the enantioselective dehydration of 2-butanol catalysed by zeolites USY modified with dithiane oxide.¹⁷

1.2.3 Comparison of methodologies and advantages of immobilization

Of the four immobilization strategies developed to date for the preparation of heterogeneous catalysts, two, namely immobilization by covalent tethering and electrostatic interaction, have been shown to form reasonably stable catalysts that are capable of re-use. Adsorption methodologies offer a relatively facile method of immobilization but tend to produce non-stable catalysts. Encapsulation of complexes during the preparation methods provides a very elegant methodology but is relatively complex compared with the more recently developed covalent tethering methods. Covalent tethering will undoubtedly produce stable catalysts and can be considered the preferred methodology for catalysts which do not lend themselves to immobilization through electrostatic interaction. Immobilization via ionic interaction is conceptually simple and is a facile method of immobilizing ionic catalysts. This approach has been shown to produce stable catalysts that are capable of re-use, but it has been noted recently by Rechavi and Lemaire that the methodology of catalyst synthesis is crucial if stable catalysts are to be obtained.¹⁸

1.3 Alkene Oxidation

Catalytic transformations of hydrocarbons, the main component of crude oil and natural constituents, into value added oxygenated derivatives such as alcohols, aldehydes, ketones or carboxylic acids, using peroxides as oxidants have been very useful primarily because such products are important intermediates in many industrial processes. Oxidation of alkenes under mild conditions is the subject of great interest from both academic and industrial points of view. Among several catalytic oxidation (oxidation of 1-hexene) products, 1,2-cyclohexanediol is commonly found in most reactions, whereas adipic acid formed through carbon-carbon bond cleavage in the presence of very strong oxidants and allylic oxidation products is obtained in few cases.

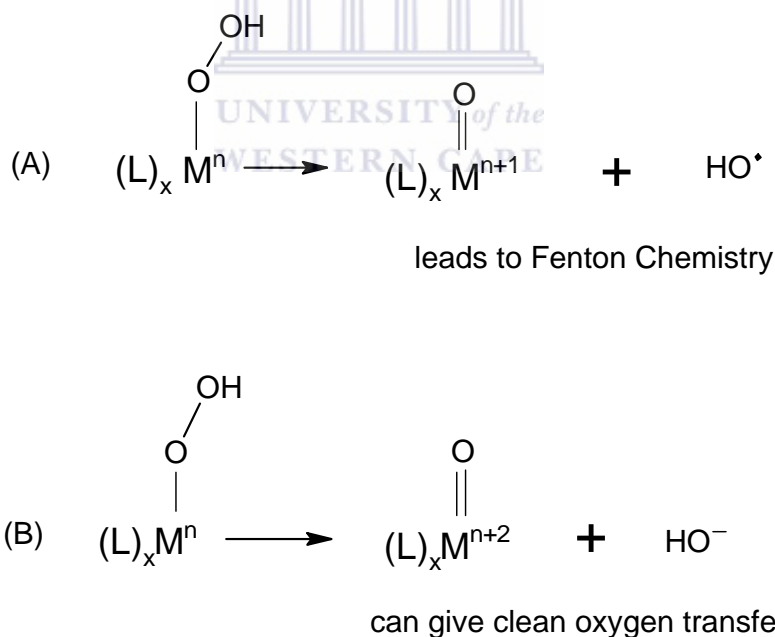


In our project cyclohexene was chosen as our model substrate because it produces both allylic products and epoxidation products. In oxidation of cyclohexene over transition metal containing mesoporous materials, usually the reaction proceeds via epoxidation followed by its hydrolysis in the presence of hydroperoxides to yield diols. This process can also yield alcohols and ketones depending on the reaction mechanism that is favoured. Examples of catalytic allylic oxidations of cyclohexene in the presence of peroxides are rare, although these allylic oxidation products of cyclohexene could act as building blocks for the synthesis of various functional macromolecules and fine chemicals.¹

Hydrogen peroxide is probably the best terminal oxidant after dioxygen with respect to environmental and economic considerations. As a result, an epoxidation system that uses

hydrogen peroxide in conjunction with cheap, relatively non-toxic metals is potentially viable for large scale production of inexpensive products and for specialized applications in development, process and research. The literature in this area is extensive and difficult to segregate into sharply delineated categories, but a fair way to attempt this is according to the catalyst precursors is heterogeneous coordination complexes.¹⁸

Good epoxidation catalysts must activate hydrogen peroxide without radical production. The key to clean activation seems to be the fact that the O-O bond must be cleaved heterolytically because homolytic cleavage generates free radicals in solution, leading to spurious reactions (formation allylic products; ketone and alcohol) that can degrade the catalyst, and unproductive consumption of the substrate and product (**Scheme 1.8**).



Scheme 1.8: Cleavage pathways for the O-O bond in hydrogen peroxide: (A) Homolytic cleavage mechanism of hydrogen peroxide O-O bond; (B) Heterolytic cleavage mechanism of hydrogen peroxide O-O bond.

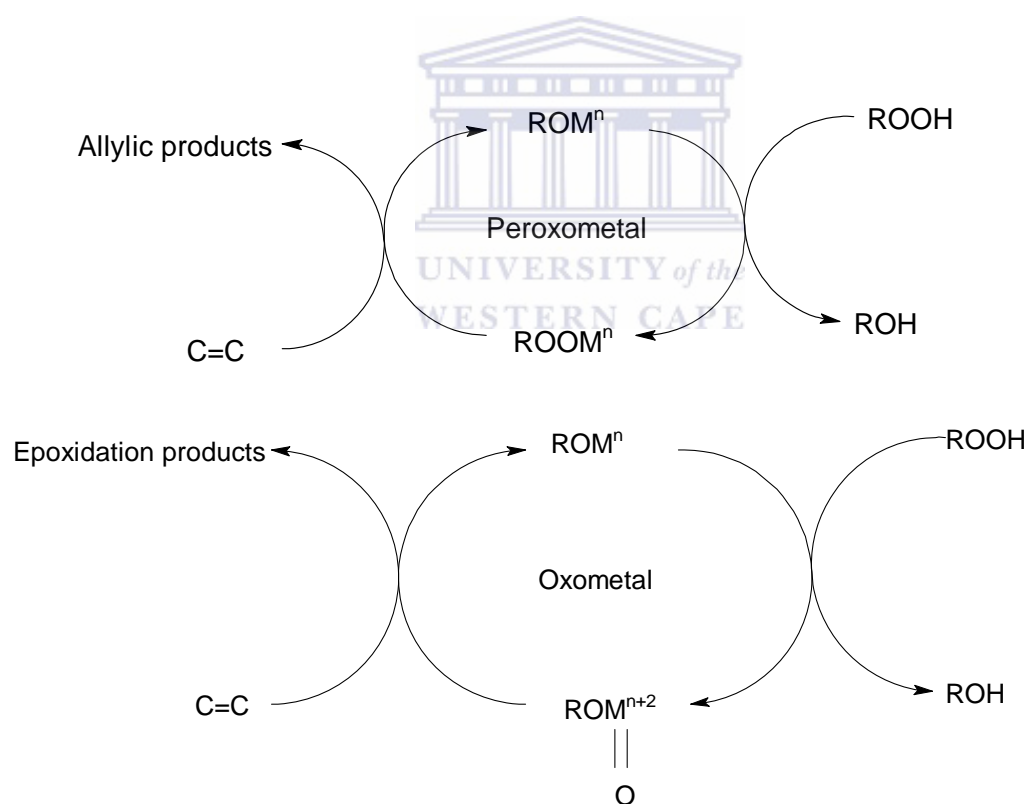
Various non-obvious strategies have emerged to facilitate clean heterolytic activation of hydrogen peroxide. Once the activated catalyst-peroxide adduct has been formed, efficient transfer of oxygen to the alkene substrate is important. Oxygen transfer from a metal can be achieved directly, or in two steps. The direct transfer is better with respect to minimization of reaction byproducts. Direct transfer of oxygen from M=O systems to alkenes is further complicated by the fact that more than one mechanism must be operative because some systems are stereospecific for *cis*-epoxide formation while others are not.

Often, the physical properties of catalysts are critical for developing epoxidation conditions. Partition coefficients between two solvents, or the solubilities in homogeneous media, can differentiate well from poor epoxidation systems. There are other important, but subtle properties of catalysts that must be optimized to obtain useful reactivities in epoxidation reactions.¹⁸

1.3.1 Mechanistic considerations for formation of epoxides

Oxygen transfer processes have various examples one which is the metal catalyzed epoxidation with hydrogen peroxide or RO₂H. In the oxygen transfer processes the active oxidant can be oxo-metal or a peroxo-metal species. Early transition metals react via peroxo-metal intermediates whereas catalysis by the late or many first row transition elements (Cr, Mn, Fe) involves high valent oxo-metal intermediates. Some elements react via oxo-metal or peroxo-metal intermediates depending on the substrate. The oxo-metal intermediate can be formed via heterolysis of the O-O bond of an initially formed

peroxo-metal species. The major difference between these two pathways is that in the peroxo-metal pathway there is no change in the oxidation state of the metal center during the reaction. The metal ion increases the oxidizing power (electrophilicity) of the peroxo by withdrawing electrons i.e. by acting as a Lewis acid. Hence, the peroxo-metal pathway is not limited to variable valence elements. In the oxo-metal pathway, the metal center undergoes a two-electron reduction and is subsequently re-oxidized by the oxygen donor.¹⁹



Scheme 1.9: Peroxo-metal and oxo-metal pathways in olefin epoxidation.

1.3.2 MCM-41 supported Salen Complexes for epoxidation

Organosilane-modified mesoporous materials have been prepared by a solvent evaporation method using C₁₆TMABr surfactant as a template under mild and acidic conditions. Mesoporous material synthesized by using the solvent evaporation method show fully disordered pore system, but those synthesized under hydrothermal conditions have highly ordered pores. Since MCM-41 possesses a large surface area and uniform mesopores with a controllable diameter of 2-10 nm, it is expected as a good material for catalytic applications.

In most cases, siliceous mesoporous materials do not have intrinsic activity as catalysts and thus many studies have concentrated on introducing catalytically active sites, such as metals, metal ions and metal complexes into mesoporous silica. The most popular method for the introduction of the active sites is the direct hydrothermal method (DHT); this method cannot ensure the incorporation of the active species into the mesopore of MCM-41, usually accompanied by some contraction of channels during wet impregnation.

In 1998, Kim *et al.* carried out the immobilization of new tetra dentate chelates of bis-Schiff bases onto mesoporous MCM-41 by template ion exchange method. Although the salen ligand with an appropriate size (10-11 Å) trapped in the supercage (13 Å) of zeolite Y cannot escape through the pore opening (7 Å), this encapsulation method could be unsuitable for MCM-41 system because of its one-dimensional large pore (30 Å). Active salen Mn(III) complexes in the cationic form have been found to be efficient catalysts for

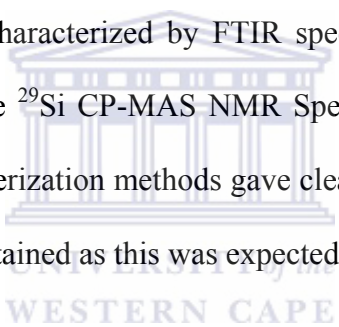
epoxidation of simple alkenes, however, these bulky chiral salen ligands are too large to form in the supercage of zeolite Y. Ion exchange ability of MCM-41 mesoporous material makes it capable of anchoring the chiral salen ligands in the cationic form as the heterogeneous catalyst, without any steric hindrance effect. Thus the prepared catalysts have been used for the epoxidation of styrene and α -methyl styrene to obtain high level of enantioselectivity.

Also, there were attempts that were made to immobilize onto the unmodified MCM-41, which lacks $-\text{NH}_2$ groups, but this was unsuccessful. Additionally, to make clear whether the environment, inside or outside the channels, is responsible for the enhancement of chiral induction, the complex was anchored inside the channels of another modified MCM-41, designated MCM-41 (m-in), whose external surface was passivated with Ph_2SiCl_2 , through the same surface-bound tether of terminal $-\text{NH}_2$ groups used in MCM-41 (m). Under the same conditions, with *p*-chlorostyrene as the substrate, both MCM-41 (m-in) and MCM-41 (m) catalysts afforded the corresponding epoxides in almost the same yield and ee value, showing that the environment inside the channels of the support led to the enhancement of the chiral induction.²⁰

1.3.3 Co(II) Salen functionalized complexes for styrene oxidation with hydrogen peroxide.

To obtain the good promising properties of mesoporous materials such as MCM-41, functionality should be added to the silica surface. There are two ways to do this; firstly the functional group is linked to the silica surface by covalent grafting after elimination

of the surfactant template by calcination. The second is that a hybrid material can be obtained by co-condensation of siloxane and organosiloxane in the presence of surfactants, which are then eliminated by an acidic solvent extraction technique. Compared with the first method, more homogeneous distribution, higher loading of functional groups and easier one-pot process make the latter more preferred, which was used in this project. As far as this method is concerned, there is some debate as to whether the organic groups lie embedded in the wall or are distributed within the channels of the mesoporous silica. As catalysts there should be as much active organic groups within the channels of the mesoporous silica so that the catalysts is efficient. The immobilized catalyst can be characterized by FTIR spectroscopy, ^{13}C CP-MAS NMR spectroscopy, XRD, Solid state ^{29}Si CP-MAS NMR Spectroscopy, Nitrogen adsorption and TEM. All of these characterization methods gave clear analysis that the Co(II) Salen functionalized complex was obtained as this was expected.



In the catalysis, the homogeneous catalysts ($\text{Co}(\text{Salen})_2$) were compared with the heterogeneous catalysts ($\text{MCM-41-Co}(\text{Salen})_2$) for oxidation of styrene using hydrogen peroxide as oxidant. Conversion of styrene was determined by GC after 1 hr. The heterogeneous was active for this reaction with 57% conversion after 1ht with turnover frequencies (TOF) of $36 \text{ /mol}(\text{styrene}) \text{ mol}(\text{Co})^{-1}\text{h}^{-1}$ (TOF determined after 1hr, $(\text{mol}(\text{styrene}) \text{ mol}(\text{Co})^{-1}\text{h}^{-1})$). The oxidation reactions based on homogeneous catalysts showed lower conversion of 42% and TOF of $15 \text{ /mol}(\text{styrene}) \text{ mol}(\text{M})^{-1}\text{h}^{-1}$. This is due to the loading of active homogeneous catalysts sites in the silica matrix of MCM-41. Thus, encapsulation of complexes into MCM-41 is found to increase the activation of the

catalyst by reducing dimerization due to the restriction within the internal framework structure.

Leaching of active species was investigated by filtrating the immobilization of the catalyst and the metal content was done by AAS, the absence of a metal ion in the solution phase indicated that no leaching of complexes occurred during reaction. Also recyclability of catalysts was investigated, and it was found out that the catalysts has lost its activity due to dimerization of $\text{Co}(\text{Salen})_2$ groups which are still close enough in the heterogeneous catalysts of $\text{MCM-41-Co}(\text{Salen})_2$.²¹

1.3.4 Allylic oxidation of cyclohexene catalysed by Schiff base complex.

The catalysts preparation was done by reacting a functionalized group (aminopropyl silica) onto the amorphous silica surface, and then the homogeneous Cu catalyst was added. The immobilized catalyst was characterized by FTIR, SEM, differential thermal analysis, UV-VIS diffuse reflectance spectra and EPR spectroscopy and the data obtained from these analyses suggested that the Cu-amp complex was formed and that it was strongly anchored with the modified silica surface.

Both the complex and the immobilized material have been used as catalysts in the liquid phase partial oxidation of cyclohexene. In the catalysis reactions the immobilized catalyst showed better conversion of cyclohexene than the soluble Cu-amp complex under the same conditions. Catalytic data suggested that the allylic oxidation products predominate and that both the conversion and the selectivity of products increased

through the immobilization of the copper catalyst over modified silica surface. The immobilized copper catalyst is reactive when dispersed in water, compared to the soluble Cu-amp catalyst under homogeneous condition, thus opening an avenue for greener chemistry.¹

1.3.5 Comparison of liquid-phase olefin epoxidation over MoO_x inserted within mesoporous silica (MCM-41 and SBA-15) and grafted onto silica

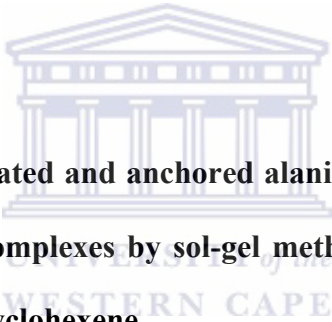
Molybdenum(VI) containing siliceous MCM-41 and SBA-15 mesoporous molecular sieves. The silica supported molybdenum was synthesized by reacting the molybdenum with the silica precursors such as tetraethylorthosilicate, silica beads or precipitated silica in acid. The immobilized molybdenum was characterized by XRD, and it was observed from this analysis that the Mo-SBA-15 has one broad peak at a very low angle and Mo-MCM-41 has a very sharp peak at a high angle and the other two small peaks that are observed further away from the sharp peak. Analysis of the Mo content was done by EDX. BET analysis was done and it indicated that Mo-MCM-41 and Mo-SBA-15 are mesoporous and that the SBA-15 displays microporosity with significant contribution of the micropore area to the total surface area. It also gave a clear indication that SBA-15 has thicker walls than MCM-41 but the pore diameter is similar.

Catalysis was performed with TBHP (5-6 mol L⁻¹ in decane, 4% H₂O) which did not give good reproducible results, the cyclooctene conversion fluctuating between 40 and 70% after 24 hrs with Mo-MCM-41. It was observed that Mo-MCM-41 and Mo-SBA-15 are active at 40⁰C in hexane. It was also noticed that cyclooctene oxide is produced very

quickly resulting in high epoxidation activity of Mo catalytic species. Comparison of Mo-MCM-41, Mo-SBA-15 and Mo-SiO₂-bead shows that Mo-SBA-15 is one of the most effective catalysts, with the lowest mesopore surface area. Moreover it was found out that Mo-SBA-15 has fewer active sites per gram than Mo-MCM-41 and Mo-SiO₂-bead.

The effect of different solvents was observed, cyclooctene conversion increased in the order of; acetonitrile (polar) < hexane < decane (apolar). This result can be explained by the fact that the more polar the solvent the more water is soluble. Acetonitrile contains more water than decane and water must be removed to make all these catalysts efficient.

22



1.3.6 Preparation of encapsulated and anchored alanine-salicylaldehyde Schiff base Mn(III) (Sal-Ala-Mn) complexes by sol-gel method and their performance in aerobic epoxidation of cyclohexene.

Alanine-salicylaldehyde Schiff base Mn(III) complex was entrapped into silica matrix by direct physical encapsulation and copolymerization of the functionally modified complex and tetraethoxysilane. The heterogenized catalysts were characterized by FTIR, XPS, nitrogen adsorption and ICP.

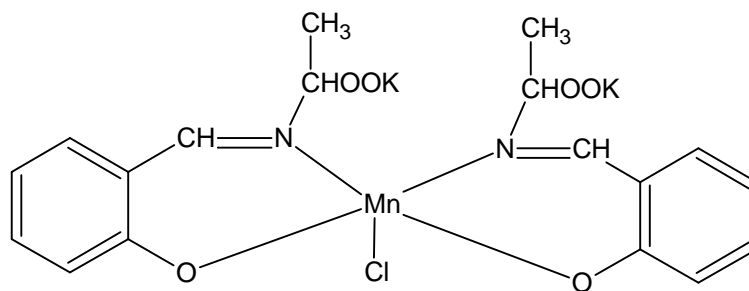


Figure 1.5: The structure of Sal-Ala-Mn.

Catalytic performance of epoxidation of cyclohexene was investigated. The results show that the both the cyclohexene conversion and epoxide selectivity increased sharply with time in the first 6 hrs. Then after 6hrs the increase in conversion became slow and the epoxide selectivity decreased. The products that were produced were epoxide, several by-products including 2-cyclohexene-ol, 2-cyclohexene-1-one, 1,2-cyclohexanedione and H₂O. Then H₂O reacts with epoxide to give 1,2-cyclohexanediol, which can be easily converted to 1,2-cyclohexanedione by oxygen.

The effect of temperature on the conversion of cyclohexene in the ranges from 25 to 55 °C. It was found that the epoxide selectivity strongly depends on temperature because as the temperature increases from 25 to 35 °C, the selectivity also increases from 74 to 79%, then it decreased sharply to 61% at 55 °C which indicates that higher temperature could enhance the oxidation and the ring opening reactions.²³

1.3.7 Allylic oxidation of cyclohexene over chromium containing mesoporous molecular sieves.

Oxidation of cyclohexene was carried out over mesoporous (Cr)/MCM-41 and (Cr)/MCM-48 molecular sieve catalysts. The catalysts preparation was done together with the preparation of the support material. All the synthesized samples were initially green and changed to yellow upon calcination. The former was due to the presence of trivalent chromium ions and the latter is due to the presence of higher valent chromium ions. The catalysts were characterized by X-ray diffraction, thermal analysis, ICP, UV-Vis and EPR. The oxidation of cyclohexene was done using 70% of tert-butyl hydrogen

peroxide (TBHP) (16 mmol) in the presence of chlorobenzene (5 ml) as solvent and 50 mg of (Cr)/MCM-41 and (Cr)/MCM-48. The substrate to oxidant ratio was 1:2. Cyclohexene was purified by washing with successive portions of dilute acidified ferrous sulphate solution followed by distilled water. It was then dried under calcium chloride and distilled under nitrogen atmosphere. The reaction products were analyzed by gas chromatography and the results were further confirmed using gas chromatography-mass spectrometry.

High selectivity of 2-cyclohexen-1-one was observed, and this may be explained with the fact that TBHP interacts with chromate species to produce chromium peroxo species. The latter further reacts with cyclohexene, by abstraction of hydrogen from allylic position, leading to allylic free-radical. The resulting species is then oxidized to 2-cyclohexen-1-one via the formation of cyclohexenyl chromate ester.

However, the selectivity of 2-cyclohexen-1-one decreases with time, due to the formation of side products, cyclohexene oxide and 1,2-cyclohexanediol. The cyclohexene conversion increases when the ratio substrate to oxidant was increased to 3:1. It was noted that the TBHP efficiency was found to be higher for the 2:1 ratio. At higher ratios, a competitive reaction of double bond oxidation favors the formation of 1,2-cyclohexanediol and hence, a decrease in 2-cyclohexen-1-one selectivity.

Likewise, at lower oxidant: substrate ratio (1:1), a considerable amount of cyclohexene oxide is formed, but it decreases continuously with increase in oxidant amount, which

may be accounted for additional oxidation of cyclohexene oxide into 1,2-cyclohexanediol. This may be explained due to the fact that TBHP interacts with the chromate species, leading to a tertiary butyl peroxy radical. The interaction of the tertiary butyl peroxy radical with the double bond of cyclohexene results in the formation of epoxide, which can be further oxidized into diols (1,2-cyclohexanediol).²⁴

1.3.8 Heterogeneous catalytic aerobic oxidation behavior of Co-Na heterodinuclear polymeric complex of Salen crown ether.

A Co-Na heterodinuclear polymer complex was prepared from Salen Schiff base ligand and crown ether by a condensation polymerization process reaction. This polymeric complex was characterized by Scanning Electron microscopy, TG-DTA analysis for thermal stability, X-ray photoelectron microscopy in order to confirm coordination of polymer ligand with cobalt and sodium ions and IR spectra was also used to analyze the polymer complex.

Cyclohexene oxidation by molecular oxygen using the Co-Na heterodinuclear polymeric complex was evaluated. It was found that cyclohexene oxidation preferred the formation of 2-cyclohexene-1-one, 2-cyclohexene-1-ol and 2-cyclohexen-1-hydroperoxide and only a little of epoxide was afforded by this reaction. It was observed that at first, 2-cyclohexen-1-hydroperoxide was formed in high concentrations but the 2-cyclohexene-1-one and 2-cyclohexene-1-ol were formed in small amounts. As the time progressed it was found that the selectivity of 2-cyclohexene-1-ol and 2-cyclohexene-1-one increased as the selectivity of 2-cyclohexen-1-hydroperoxide decreased. It was deduced that the

two main products, 2-cyclohexene-1-ol and 2-cyclohexene-one were derived from the decomposition of 2-cyclohexen-1-hydroperoxide.²⁵

1.3.9 Highly effective catalysts of natural polymer supported Salophen Mn(III) complexes for aerobic oxidation of cyclohexene.

Salophen Mn(III) complexes were supported on chitosan and these supported complexes were characterized by FT-IR and XPS. Allylic oxidation of cyclohexene by chitosan supported Mn(III) complexes with oxygen was tested in the absence of solvent. The effect of temperature and time were taken into good consideration. The supported Salophen Mn(III) complexes and the unsupported Salophen Mn(III) complexes were compared. It was observed that the supported catalysts had much greater activity and good turnover numbers as compared to the unsupported catalysts. The reasoning of this difference is that the supported catalysts has the active sites isolating the effect of macromolecular supports which makes Salophen Mn(III) complexes to be disperse molecularly to chitosan as compared to the unsupported Salophen complexes which are not disperse molecularly in the reaction mixture. It was indicated that between 60 °C and 70 °C the product selectivity of 2-cyclohexene-1-one increased but cyclohexene oxide, 2-cyclohexene-1-ol and 2-cyclohexen-1-hydroperoxide decreased. As the reaction time was prolonged, it was observed that the selectivity of 2-cyclohexene-1-one increases as the time is increases but for the other three products this was not the case especially after 8 hrs these seems to decompose to form more of 2-cyclohexene-1-one.²⁶

1.4 References

1. S. Mukherjee, S. Samanta, B. C. Roy and A. Bhaumik, *Appl Catal. A: Gen.*, **301** (2006), 79.
2. I. Steiner, R. Aufdenblatten, A. Togni, H. Blaser, B. Pugin, *Tetrahedron: Asymm.*, **15** (2004), 2307.
3. A. Golcu, M. Tumer, H. Demirelli, R. A. Wheatley, *Inorg. Chimica Acta*, **358** (2005), 1785.
4. P. G. Cozzi, *Chem. Soc. Rev.*, **33** (2004), 410.
5. M. M. Ali, *Rev. Inorg. Chem.*, **16** (1996), 315.
6. T. Katsuki, *Chem. Soc. Rev.*, **33** (2004), 437.
7. J. M. Thomas, R. Raja, *J. Organomet. Chem.*, **689** (2004), 4110.
8. J. S. Berk, J. C. Vartuli, W. J. Roth, M. E. Leonowicz, C. T. Kregse, K. D. Schmitt, C. T. W. Chu, D. H. Olson, E. W. Sheppard, S. B. McCullen, J. B. Higgins, J. L. Schlenker, *J. Am. Chem. Soc.*, **114** (1992), 10834.
9. H. M. Hultman, *J. Cat.*, **217** (2003), 264.
10. K. J. Edler, J. W. White, *J. Mat. Chem.*, **9** (1999), 2611.
11. Y. Sun, S. Walspurger, J. Tessonier, B. Louis, J. Sommer, *Appl. Cat. A: Gen.*, **300** (2006), 1.
12. P. M. Price, J. H. Clark, D. J. Macquarrie, J., *Chem. Soc., Dalton Trans.*, **11** (2000), 101.
13. P. McMorn, G. J. Hutchings, *Chem. Soc. Rev.*, **33** (2004), 108.
14. I. C. Chisem, J. Rafelt, M. T. Sheih, J. Chisem, J. H. Clark, R. Jachuck, D. Macquarrie, C. Ramshaw, K. Scott, *Chem. Commun.*, 1998, 1949.

-
15. U. G. Singh, R. T. Williams, K. R. Hallam, G. C. Allen, *J. Sol. St. Chem.*, **178** (2005), 3405.
 16. R. I. Kureshy, I. A., N. H. Khan, S. H. R. Abdi, K. Pathak, *J. Cat.*, **238** (2006), 134.
 17. S. Feast, M. R. Siddiqui, R. P. K. Wells, D. J. Willock, F. King, C. H. Rochester, D. Bethell, P. C. B. Page, G. J. Hutchings, *J. Cat.*, **167** (1997), 533.
 18. D. Rechavi, M. Lamaire, *Chem. Rev.*, **102** (2002), 3467.
 19. B. S. Lane, K. Burgess, *Chem. Rev.*, **103** (2002), 2457.
 20. Q.-H. Xia, H.-Q. Ge, C.-P. Ye, Z.-M. Liu, K.-X. Su, *Chem. Rev.*, **105** (2005), 1603.
 21. Y. Luo, J. Lin, *Micro. and Meso. Mat.*, **86** (2005), 23.
 22. P. C. Bakala, E. Briot, L. Salles, J. M. Bregeault, *Appl. Cat. A: Gen.*, **300** (2006), 91.
 23. J. Zhao, J. Han, Y. Zhang, *J. Mol. Cat. A: Chem.*, **231** (2005), 129.
 24. A. Shakthivel, S. E. Dapurkar, P. Selvam, *Appl. Cat. A: Gen.*, **246** (2003), 283.
 25. R. Wang, Z. Duan, Y. He, Z. Lei, *J. Mol. Cat. A: Chemical*, **260** (2006), 280.
 26. J. Tong, Y. Zhang, Z. Li, C. Xia, *J. Mol. Cat. A: Chemical*, **249** (2006), 47.

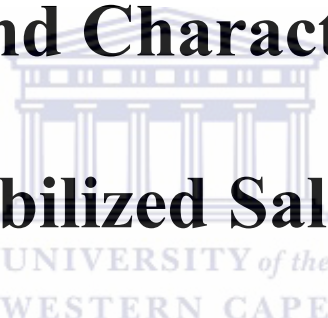
CHAPTER 2

Synthesis and Characterization of

Silica Immobilized Salicylaldimine

Copper (II) and Cobalt (II)

catalysts.

The logo of the University of the Western Cape is centered in the background. It features a classical building with a portico supported by columns, with the text "UNIVERSITY of the WESTERN CAPE" below it.

2.1 INTRODUCTION

2.1.1 Salicylaldimine Complexes

Salicylaldimines belong to the group of Schiff base complexes. Schiff bases are compounds containing the azomethine group (-RC=N) and are usually formed by the condensation of a primary amine with an active carbonyl compound.¹ These Schiff bases are also formed when two equivalents of a salicylaldehyde are combined with a diamine leading to so-called Salen type ligands.² It is advantageous to use salicylaldimines because of the flexibility of the synthetic procedure, which allows a variety of complexes with a given metal whose properties are dependent on the detailed ligand structure. The most significant structures of salicylaldimines are illustrated in **Figure 2.1**. Salicylaldimines may act as bidentate chelating agents, coordinating through their *cis*-oxygen atoms to form bi- and tri-nuclear metal complexes and these metal complexes are known as tetradentate Schiff bases complexes (TSB).^{3,4}

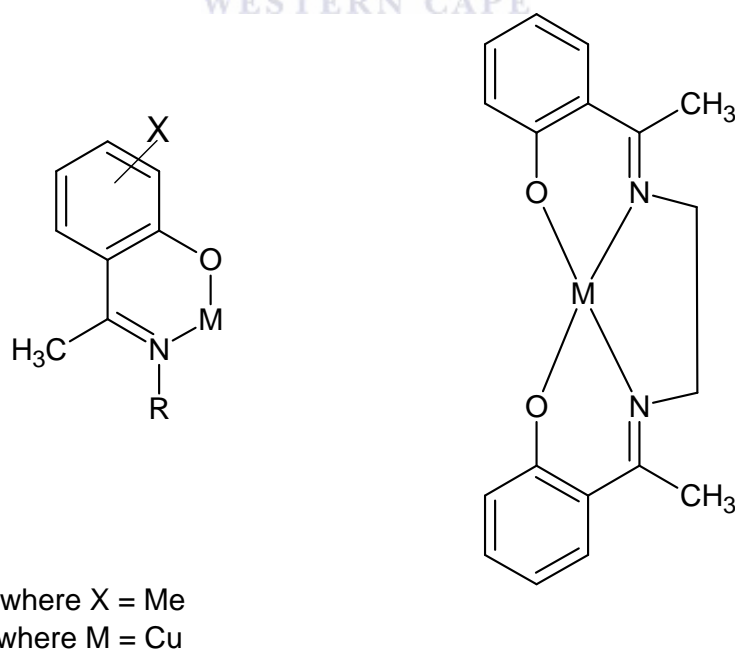
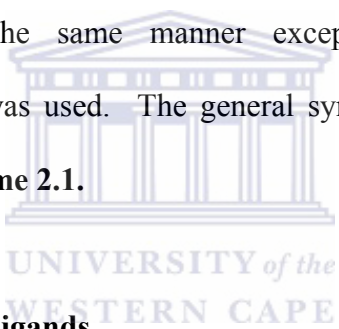


Figure 2.1: Typical salicylaldimine complexes.¹

2.2 Synthesis and Characterization of Silane functionalized Salicylaldimine Ligands.

2.2.1 Synthesis of Ligands.

The synthetic procedure of salicylaldimine ligands (**L1** and **L2**) was previously described in the literature.^{2, 5} The ligands were synthesized by condensation of 3-aminopropyl triethoxysilane with the salicylaldehyde in a 1:1 reaction ratio in the presence of dry ethanol as solvent. A yellow oil was obtained as the desired product. The yellow oil was stored under vacuum because if this ligand is left in air at room temperature, it hydrolyses after some time. The ligands were obtained as oils in high yields. The products were found to be soluble in organic solvents such as CHCl₃, CH₂Cl₂ and hexane. **L3** and **L4** were also synthesized in the same manner except instead of 3-aminopropyl triethoxysilane, propylamine was used. The general synthetic route for the ligands is schematically outlined in **Scheme 2.1**.

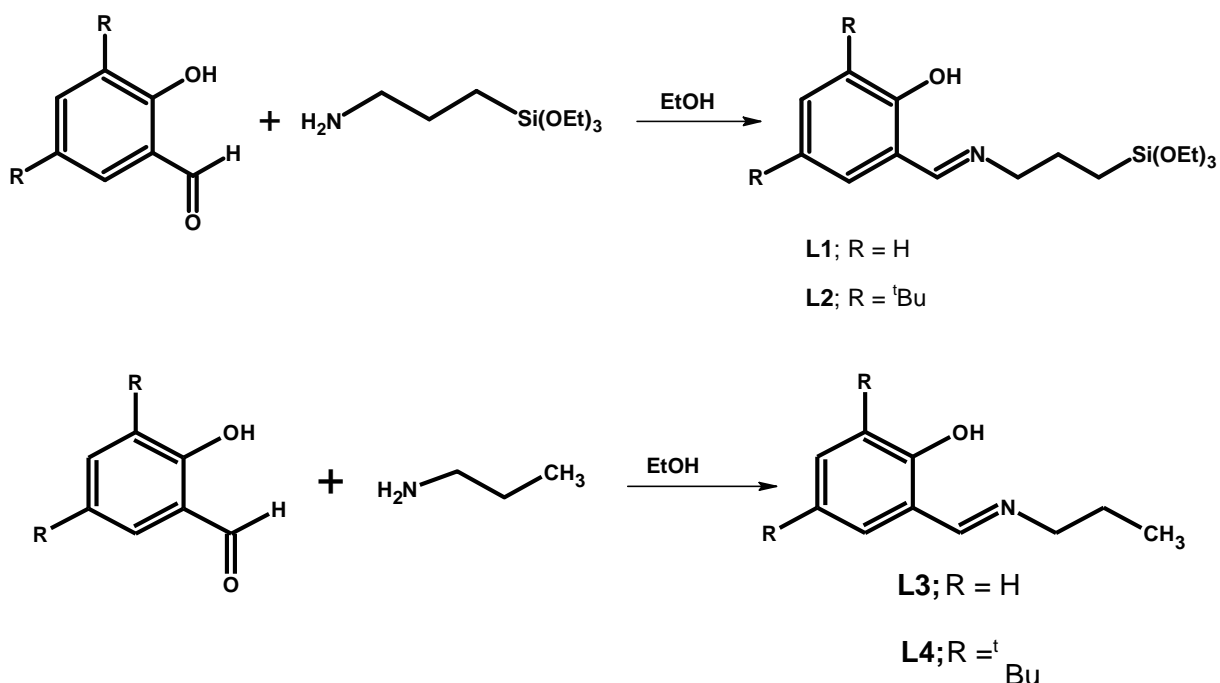


2.2.2 Characterization of the ligands

The ligands were characterized by ¹H NMR spectroscopy and infrared spectroscopy.

2.2.2.1 Characterization by means of ¹H NMR spectroscopy

The structures of the unsubstituted and the tertiary butyl substituted Ligands (**L1-L4**) their ¹H NMR data are shown in **Table 2.1**.



Scheme 2.1: Synthesis of Salicylaldimine ligands.

In general for ligand **L1**, a chemical shift in the aromatic region is observed around δ 6.95 ppm which is a multiplet due to the proton of C-3. Another multiplet is observed around δ 7.18 ppm which is due to protons of C-4, 5 and 6. The peak around δ 0.73 ppm which is a triplet is due to protons of $-\text{CH}_2$ that is next to $-\text{Si}(\text{OCH}_2\text{CH}_3)_3$. This peak is deshielded due to the oxygen of the $-\text{Si}(\text{OCH}_2\text{CH}_3)_3$. There is a triplet around δ 1.26 ppm which is due to nine protons of the $-\text{CH}_3$ of the ethoxy group. This peak is also deshielded due to the oxygen moiety. A multiplet is observed at δ 1.87 ppm, assigned to the protons of the central $-\text{CH}_2$ of the propyl chain. A multiplet is observed around δ 3.63 due to the two protons of the $-\text{CH}_2$ group that is next to the $\text{C}=\text{N}$. A quartet is observed around δ 3.88 ppm due to the six protons of the $-\text{CH}_2$ of the ethoxy group.

Lastly a singlet around δ 8.33 ppm is due to imine. Our results are similar to that obtained by Murphy *et.al.*⁵

Table 2.1: ¹H NMR data of the ligands prepared.

Ligand	δ (ppm)	Assignment
L1	0.73, t	Si-CH ₂
	1.27, t	Si-OCH ₂ CH ₃
	1.87, t	N-CH ₂
	3.63, m	N-CH ₂ CH ₂
	3.88, q	Si-OCH ₂
	6.95, m	Ar
	7.18, m	Ar
L2	8.36, s	N=CH
	0.78, t	Si-CH ₂
	1.26, t	Si-OCH ₂ CH ₃
	1.31, s	CH ₃ (^t Bu)
	1.44, s	CH ₃ (^t Bu)
	1.90, t	N-CH ₂
	3.61, m	N-CH ₂ CH ₂
	3.88, q	Si-OCH ₂
7.09, d	Ar	

Table 2.1. Continue

	7.37, d	Ar
	8.35, s	N= <u>CH</u>
L3	1.02, t	CH ₂ - <u>CH</u> ₃ (propyl)
	1,82, m	NCH ₂ <u>CH</u> ₂
	3.58, t	N- <u>CH</u> ₂
	6.08, m	Ar
	7.05, m	Ar
	8.32, s	N= <u>CH</u>
L4	1.02, t	CH ₂ - <u>CH</u> ₃ (propyl)
	1.31, s	<u>CH</u> ₃ (^t Bu)
	1.45, s	<u>CH</u> ₃ (^t Bu)
	1.74, m	NCH ₂ <u>CH</u> ₂
	3.36, t	N- <u>CH</u> ₂
	7.09, d	Ar
	7.26, s	Ar
	7.38, d	Ar
	8.24, s	N= <u>CH</u>

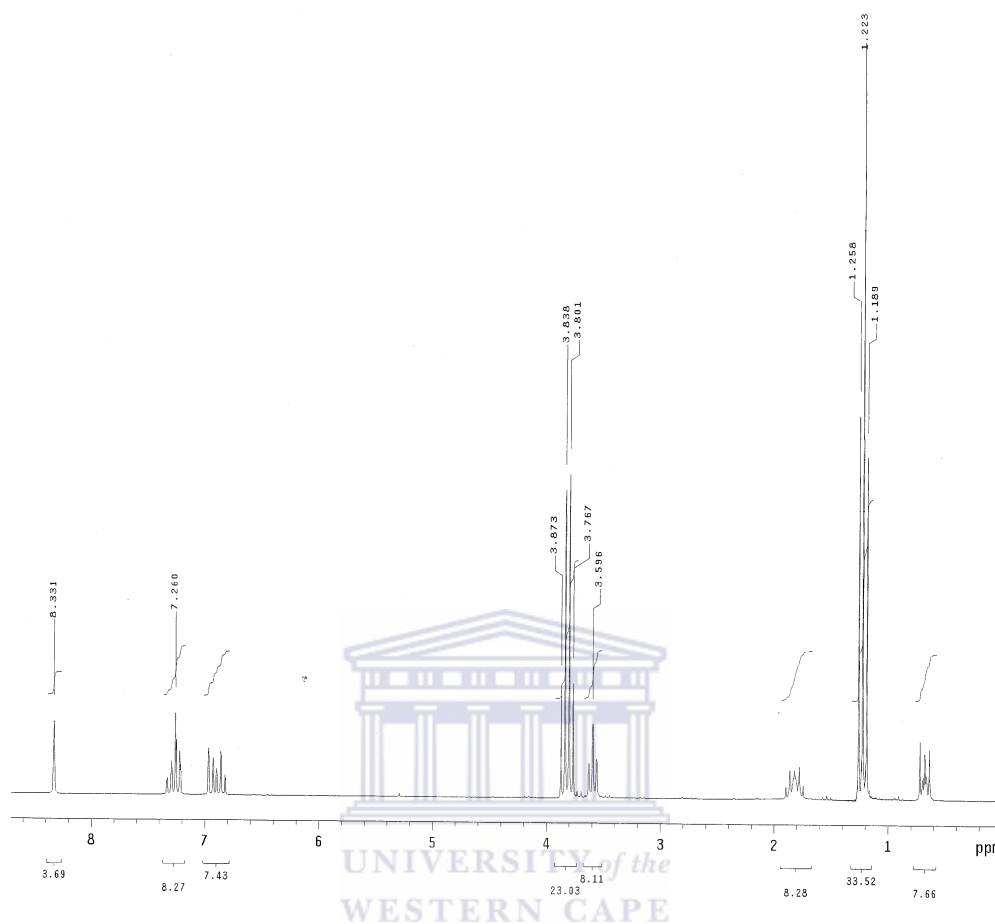


Figure 2.2: ^1H NMR of **L1**.

In the spectrum of **L2** the signals due to protons of the aromatic ring are found as a doublet at δ 7.09 ppm which is due to proton of C-6. A doublet at δ 7.37 ppm is due to C-4. The signals for the protons of the tertiary butyl group at position 5 of the ring is found at δ 1.31 ppm and the signal for the tertiary butyl group at position 1 which is a singlet, found at δ 1.44 ppm. The other signals for functional groups of the ligand are similar to those of the **L1**.

L3 has similar chemical shifts as **L1**, except that **L3** does not have the ethoxy functionality. The same applies for **L4**.

2.2.2.2 Characterization of ligands (L1-L4) by infrared spectroscopy.

For all ligands the infrared spectra have a characteristic band due to the stretching frequency of the C=N bond which is found between 1638 cm^{-1} and 1620 cm^{-1} . At 1280 cm^{-1} a sharp band that is assigned to the C-O bond. Another broad band is observed between 1100 cm^{-1} and 1000 cm^{-1} due to the stretching frequency of the Si-O bond of the siloxane functionality.

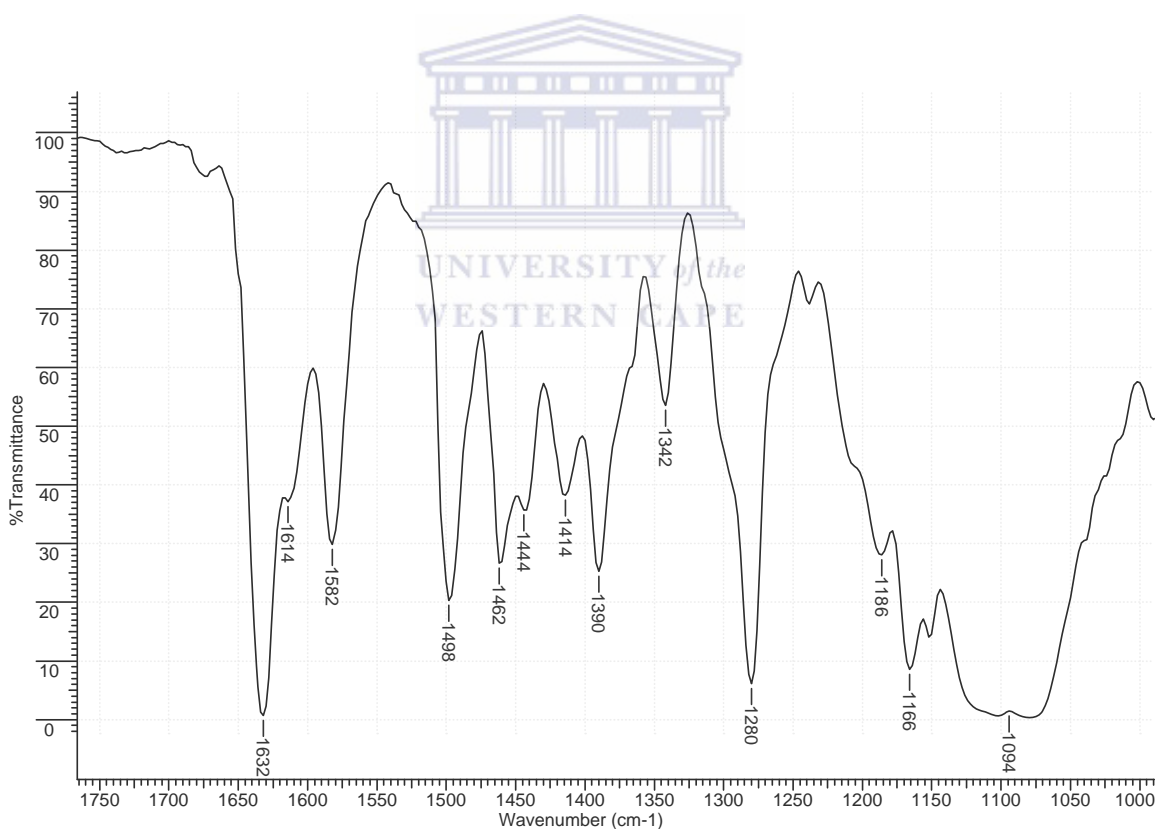


Figure 2.3: FTIR spectrum of **L1** recorded neat between NaCl plates.

In case of **L1** the IR spectrum shows an intense band at 1632 cm⁻¹ and a shoulder at 1614 cm⁻¹ which is due to the C=N bond. A band in the region 1582 cm⁻¹ to 1300 cm⁻¹ is due to the presence of the C=C bond of the aromatic ring. A big broad band is observed from 1119 cm⁻¹ to 1059 cm⁻¹ due to the Si-O bond of the siloxane functionality. Murphy *et.al.*⁵ found the same absorption bands and this confirmed that the ligand was successfully synthesized. Similar IR spectra were obtained for ligands **L2-L4**. The data is shown in **Table 2.2**.

Table 2.2: FTIR results of the Silane functionalized Salicylaldimine ligands.

Ligands	$\nu_{(C=N)} \text{ cm}^{-1}$	$\nu_{(C-O)} \text{ cm}^{-1}$	$\nu_{(C=C)} \text{ cm}^{-1}$	$\nu_{(Si-O)} \text{ cm}^{-1}$
L1	1632	1280	1582-1342	1186-1094
L2	1630	1250	1596-1342	1120-1078
L3	1632	1278	1582-1328	n/a
L4	1636	1202	1596-1316	n/a

2.3 Synthesis and Characterization of Salicylaldimine Copper(II) and Cobalt(II) Complexes.

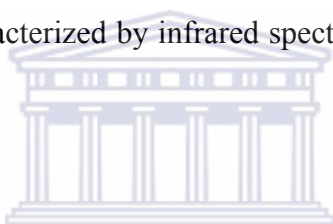
2.3.1 Complex formation

Generally the complex formation was done in a 2:1 reaction ratio of the ligand to metal salt. The synthesis of **Complexes 1** and **2** has been described previously in the literature.^{6, 7, 8} The ligands were reacted with either copper(II) acetate monohydrate or cobalt(II) acetate tetrahydrate using dry ethanol as the solvent to yield solid products. The

complexes were found to be soluble in dichloromethane and chloroform. The crude **Complex 2** was obtained as oil and was found to be soluble in hexane. The oil was purified by triturating it with acetonitrile at low temperature to obtain a solid product. **Complexes 1 and 2** were dark green solids; **Complex 3** a dark brown solid whereas **Complex 4** was isolated as a yellow orange solid. The products were stored in the glove box until further use. **Complexes 5 to 7** were obtained as dark green crystals. **Complex 8** was obtained as an orange powder.

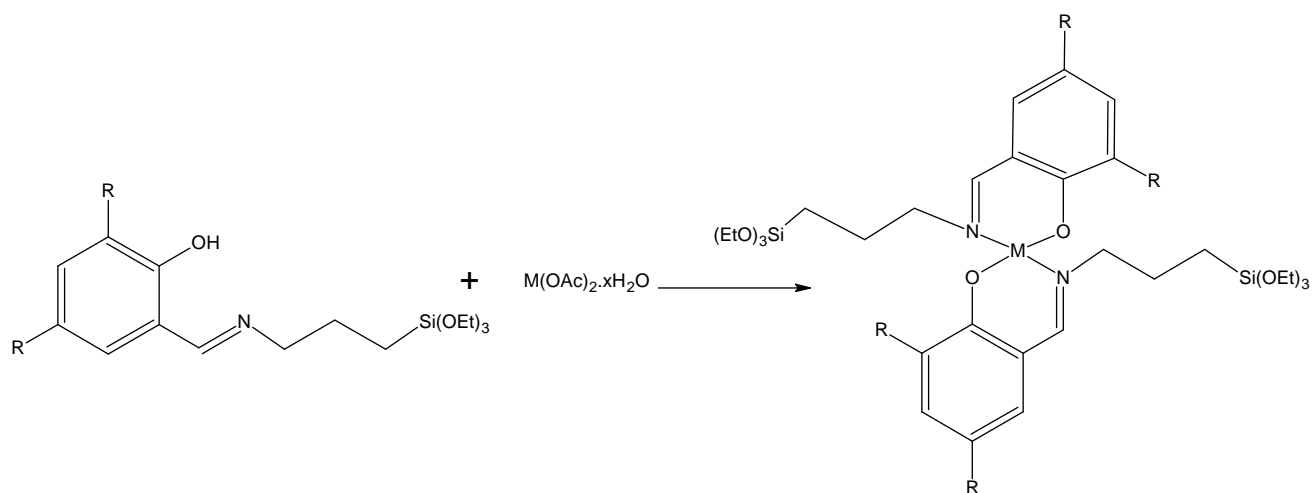
2.3.2 Characterization of Complexes

The **Complexes 1-8** were characterized by infrared spectroscopy, elemental analysis and mass spectrometry.

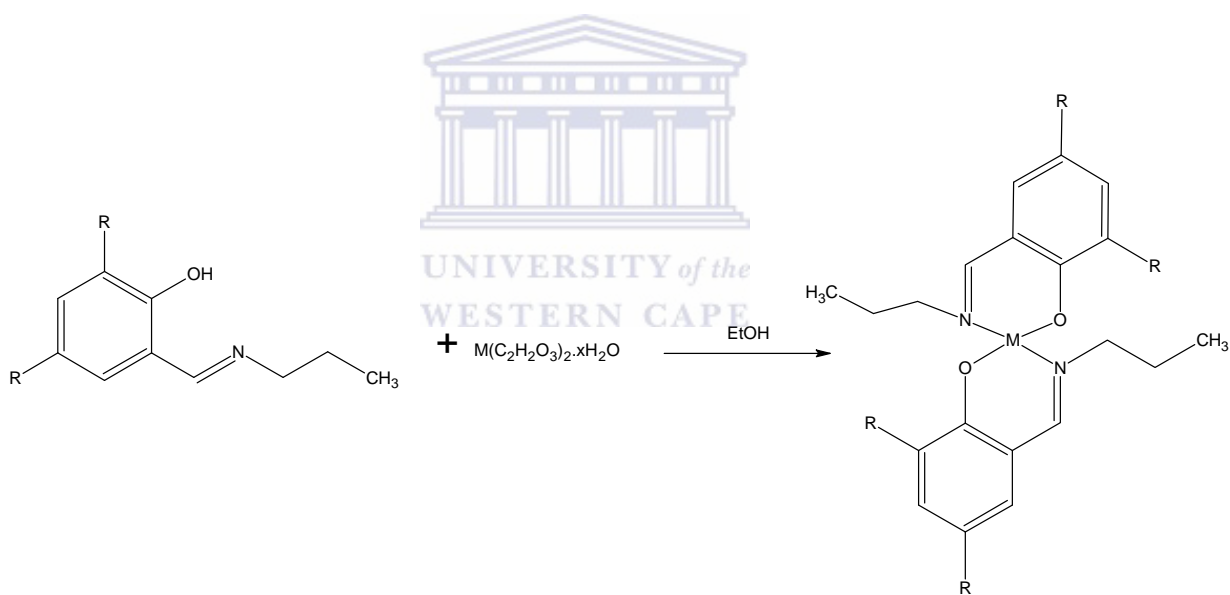


2.3.2.1 Characterization by infrared spectroscopy.

In the infrared spectra of the **Complexes 1-8** there is a shift of the C=N stretching frequency from 1632 cm^{-1} to a lower wavenumber around 1620 cm^{-1} . The stretching frequency of the C=C were observed from 1598 cm^{-1} to 1300 cm^{-1} (for ligand and complex). The C-O stretching frequency was observed at 1280 cm^{-1} for the ligand but shifted downwards to 1198 cm^{-1} for the complexes. The stretching frequency of the Si-O bond of the siloxane functionality is observed at higher wavenumber (1148 cm^{-1}) as compared to the ligand (1024 cm^{-1}). The shift of the stretching frequency of the functional groups confirms that the ligand was complexed to the metal salt.



Complex 1; M = Cu; R = H
Complex 2; M = Co; R = H
Complex 3; M = Cu; R = ^tBu
Complex 4; M = Co; R = ^tBu



Complex 5; M = Cu, R = H
Complex 6; M = Co, R = H
Complex 7; M = Cu, R = ^tBu
Complex 8; M = Co, R = ^tBu

Scheme 2.2: General schematic route for the complex formation.

Table 2.3: FTIR data for **Complexes 2 to 8^a**.

Complex	$\nu_{(\text{C}=\text{N})}\text{cm}^{-1}$	$\nu_{(\text{Si}-\text{O})}\text{cm}^{-1}$	$\nu_{(\text{C}-\text{O})}\text{cm}^{-1}$
2	1618	1134-1066	1172
3	1622	1124-1038	1194
4	1608	1132-1026	1192
5	1610	n/a	1198
6	1628	n/a	1148
7	1624	n/a	1168
8	1600	n/a	1170

^a = IR were recorded as KBr pellets.

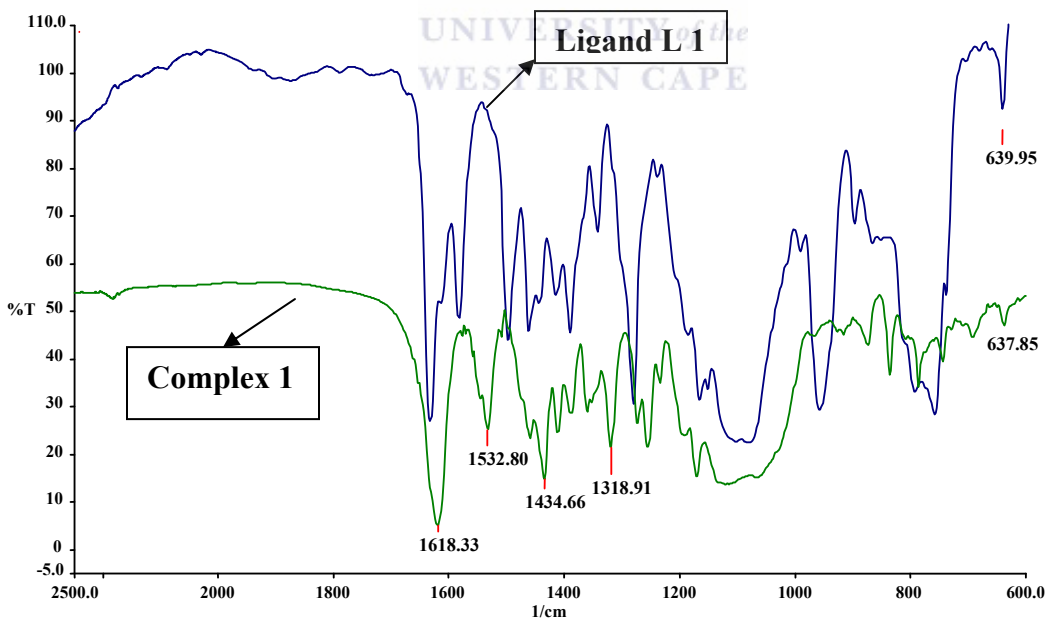


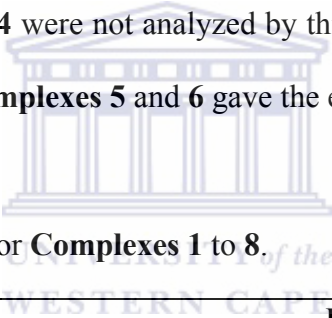
Figure 2.4: FTIR spectra showing change in bands after complexation, **Ligand L1** was recorded neat between NaCl plates and **Complex 1** was recorded as KBr pellets.

2.3.2.2 Characterization by elemental analysis.

Complexes were analyzed for percentage of carbon, hydrogen and nitrogen. The results are shown in **Table 2.3**.

Complexes 1 and **2** were found not to correlate with the expected findings due to acetate groups that were attached to the metal centers. Also for **Complex 2**, the ethoxy groups were also found to under gone hydrolysis. The above mentioned statement led to **Complex 1, 2** and **6** not giving the expected C:H:N percentages. Structures were proposed according to the found values of the complexes and these are presented in **Figure 2.5**. **Complexes 3** and **4** were not analyzed by this technique since **Complexes 1** and **2** gave unusual results. **Complexes 5** and **6** gave the expected results.

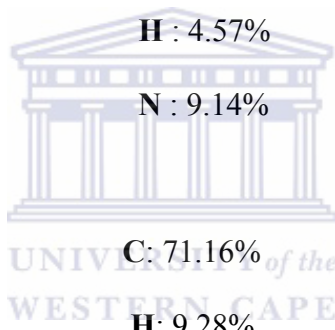
Table 2.4: Elemental analysis for **Complexes 1** to **8**.

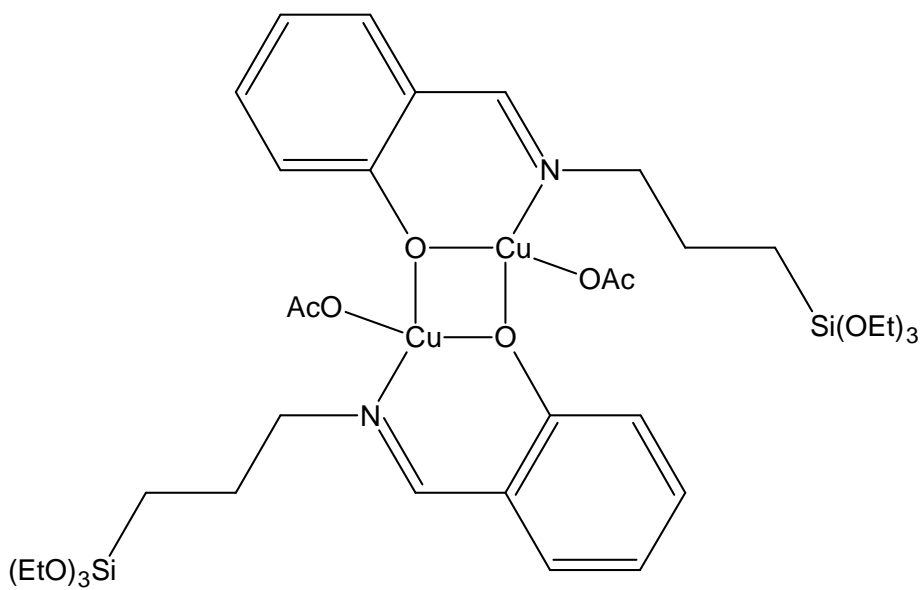


Complex	Results	
	Calculated	Found
1	C : 48.36 %	47.93 %
	H : 6.54 %	4.82 %
	N : 3.13 %	4.78 %
2	C : 43.52 %	42.98 %
	H : 5.48 %	5.16 %
	N : 3.63 %	4.65 %

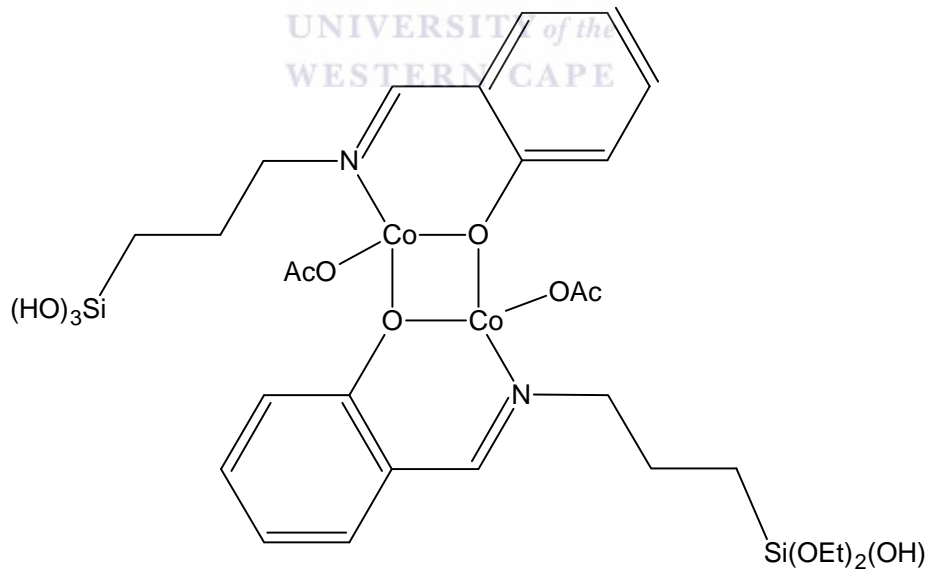
Table 2.4. Continue

	C : 61.86%	61.86%
5	H : 6.18%	6.29%
	N : 7.21%	7.02%
	C : 52.60%	53.21%
6	H : 5.62%	5.65%
	N : 5.58%	3.23%
	C : 70.05%	70.05%
7	H : 4.57%	3.38%
	N : 9.14%	9.31%
	C : 71.16%	71.30%
8	H : 9.28%	9.28%
	N : 4.61%	3.82%

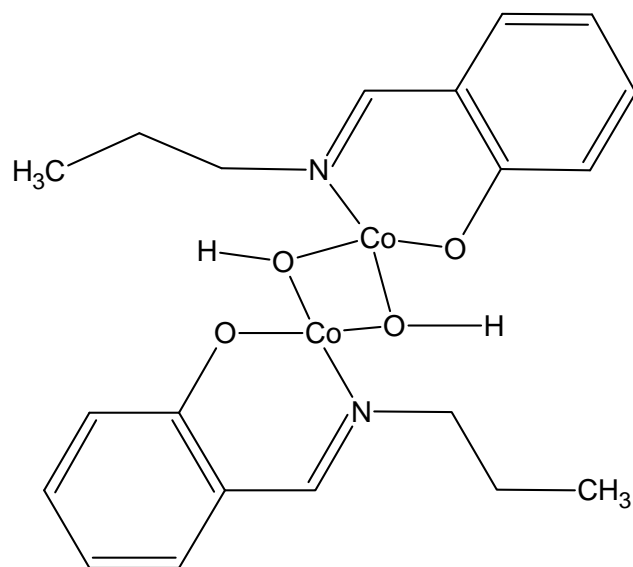




Proposed structure for complex 1



Proposed structure for Complex 2



Proposed structure for Complex 6



Figure 2.5: Proposed structures for Complexes 1, 2 and 6.

Figure 2.5 show that the **Complexes 1, 2 and 6** are binuclear complexes whereby the triethoxysilane complexes are bridged by phenolic groups of the ligand. **Complex 2** shows hydrolysis of some of the ethoxy groups, this is supported by the elemental analysis obtained for this complex.

2.3.2.3 Characterization by Mass Spectrometry.

Complex 1, 5, 6, and 7 were also characterized by ESI-Mass Spectrometry which gives a molecular weight and structural information about the complexes.

NM_74

NM_UWC_070910_1 11 (0.212) Cn (Top,4, Ht); Sm (Mn, 3x0.80); Sb (1,40.00); Cm (2:11-93:96)

1: Scan ES+
2.71e7

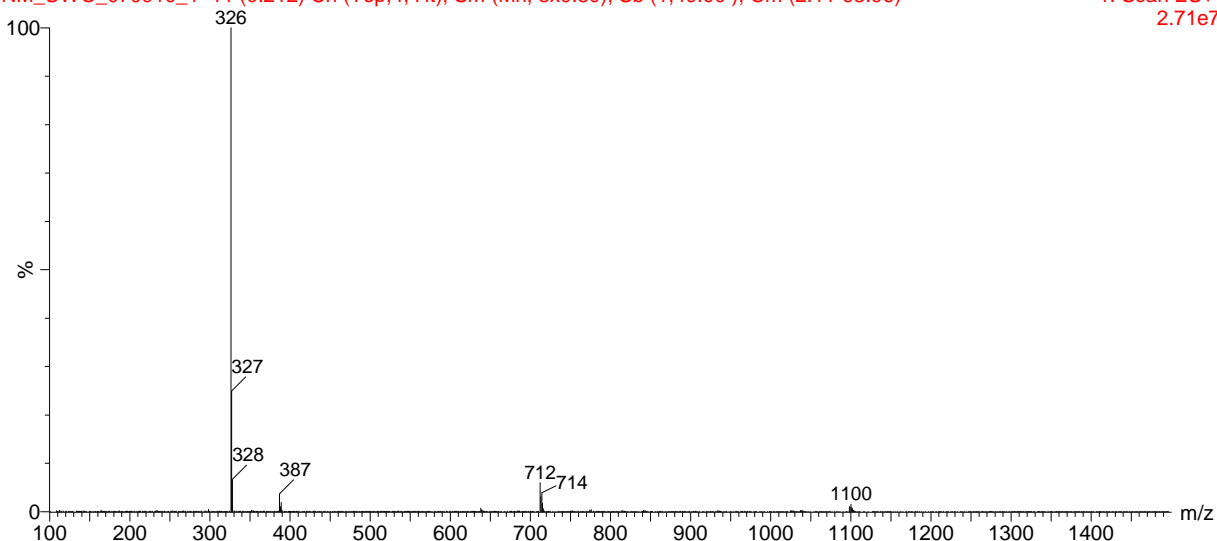


Figure 2.6: ESI-Mass spectrum for Complex 1.

Figure 2.6 shows a mass spectrum of **Complex 1**, where the base peak gave an $m/e = 712$ and this is the molecular weight of **Complex 1**. Mass spectrometry gave a base peak for **Complex 5** $m/e = 387$, $m/e = 383$ for **Complex 6** and for **Complex 7** $m/e = 612$ were obtained.

2.4 Synthesis and Characterization of Ordered Mesoporous supports.

The two most studied types of ordered mesoporous silica materials are MCM-41 and MCM-48. Both of these materials belong to M41S family, which was discovered by Mobil Scientists in 1992. In this study MCM-41 and SBA-15 are the ordered mesoporous silica materials that were utilized as inorganic silica supports. MCM-41 consists of a pore structure that has two dimensional, cylindrical pores which are organized in a hexagonal array. The pore structure of MCM-41 is highly ordered but

there is no crystallinity inside the pore walls resulting in thin walls. The pore structure of MCM-41 is completely amorphous which is due to the low thermal and chemical stability of these materials.⁹ MCM-41 is generally synthesized in alkaline media using a cationic surfactant as the structure directing agent. The synthetic approach to MCM-41 is an example of a liquid crystal templating mechanism which is represented in **Figure 2.7**.

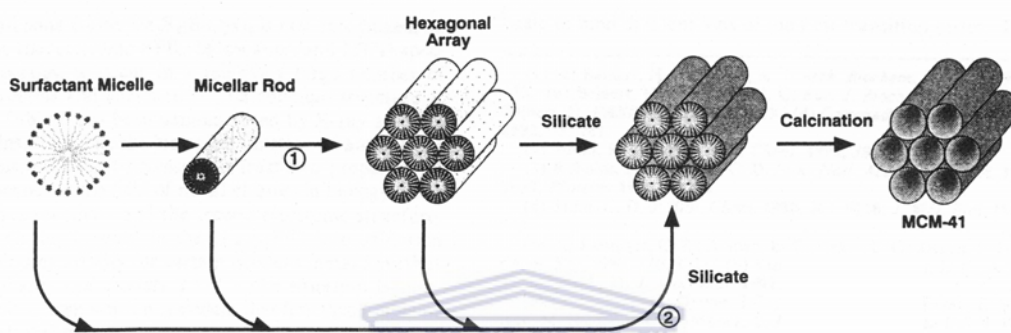


Figure 2.7: Proposed synthetic pathway for MCM-41, by the liquid crystal templating approach.^{10, 11}

Two possible synthetic pathways are suggested; pathway 1, in which the hexagonal liquid crystal surfactant phases exist in the solution before the silica precursors are added. The silica framework is precipitated around this template, forming a mesoporous structure. The surfactants are then removed by calcination, creating a porous structure with high surface area. In pathway 2; it is suggested that there is no ordered hexagonal structure in the solution before the silica is added. The silica precursors influence the arrangement of the surfactant aggregates and the hexagonal structure is formed when silica is added.

SBA-15 is synthesized with non-ionic surfactants in a highly acidic media, where the silica species are positively charged. It is synthesized using Pluronic surfactants as templates. The Pluronic surfactant is a polyethylene glycol such as P123, with the chemical formula $(\text{EtO})_{20}(\text{PO})_{70}(\text{EtO})_{20}$. SBA-15 has a hexagonal structure like MCM-41 with a pore size of 80-100 Å, depending on the reaction temperature.¹² Due to the non-ionic nature of the surfactant, the self assembly of the silica/surfactant mesophase in the gel is slower than for ionic surfactants, which creates thicker pore walls in these materials. Therefore SBA-15 is thermally and mechanically more stable than MCM-41.

2.4.1 Synthesis of MCM-41 and SBA-15.

MCM-41 was prepared using the method reported by Qiang Cai *et.al*¹², in which we have the hydrolysis of tetraethoxysilane in the presence of a templating agent such as cetyltrimethylammonium bromide (CTAB). Calcination of the product was done at 550°C.

SBA-15 was prepared using a method reported by Zhao *et.al*¹³, using the templating agent Pluronic 123, poly(ethyleneglycol)-block-poly(propyleneglycol)-block-poly(ethyleneglycol). For the synthesis of mesoporous materials, calcination should be properly done otherwise the template (surfactant) will still remain in the product.

Vartuli *et.al.* noted that the nature of the surfactant including its chain length, its aqueous concentration, surfactant/silicon ratio and reaction conditions e.g. aging temperature and time, are the critical factors that determines the nature of the material produced.¹⁰

2.4.2 Characterization of MCM-41 and SBA-15.

MCM-41 and SBA-15 were characterized by X-ray diffraction, infrared spectroscopy, scanning electron microscopy and BET surface analysis.

2.4.2.1 Characterization by means of X-ray diffraction.

X-ray diffraction analysis was performed on the samples, using scans for 2θ in the range of 0 to 10° . The samples were characterized at $\lambda = 1.54 \text{ \AA}$.

Figure 2.8 shows an X-ray diffraction pattern of MCM-41. It has four reflection peaks which are typical of this material. The main peak assigned to the $d(100)$ spacing corresponds to those in the walls in the cylindrical pore structure and has a θ value of 2.5° . The weak $d(110)$ peak has a 2θ value of 4.2° , the $d(200)$ peak has a 2θ value of 4.8° and lastly the $d(210)$ has a 2θ value of 6.6° . The 2θ values obtained for our samples matches well with those reported by Marler *et.al.*¹⁴ and which they claimed are due to the two dimensional hexagonal structure of MCM-41. The d spacing value (interplanar spacing in the crystals) for the reflection plane (100) was calculated using Bragg's equation, $n\lambda = 2d\sin\theta$, where $\lambda = 1.54039 \text{ \AA}$ and n for $d(100) = 1$. The calculated d spacing for the reflection plane $d(100)$ is 35.31 \AA .

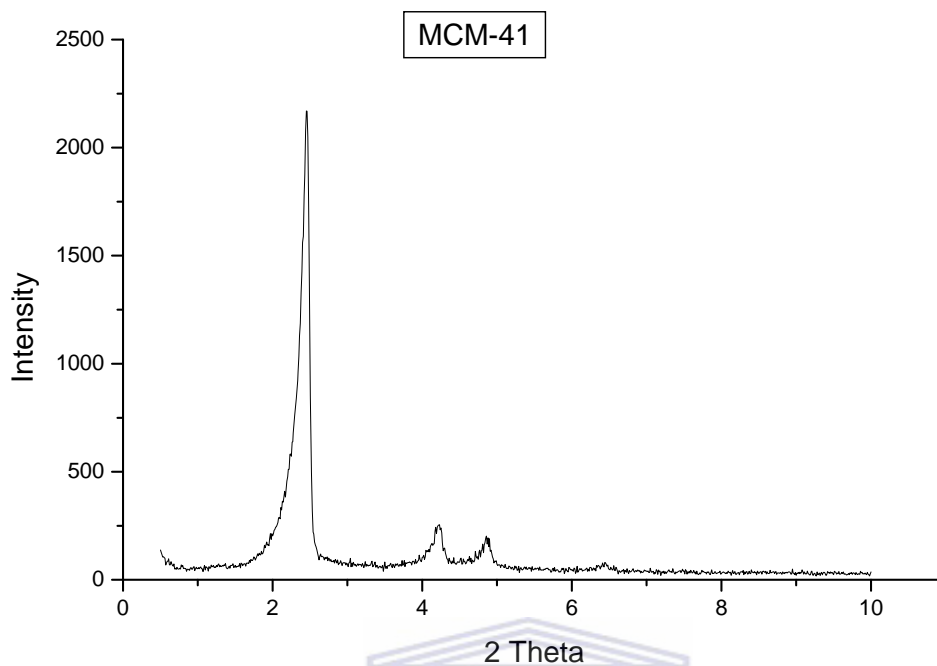


Figure 2.8: X-ray diffraction of MCM-41.

Figure 2.9 shows an X-ray diffraction pattern of the synthesized SBA-15 with three reflection peaks, at d(100), d(110) and d(200). The reflection angle of d(100) plane is 1° , for d (110) is 1.7° and for d (200) is 1.9° . The calculated d spacing value of reflection plane d (100) is 88.26 \AA .

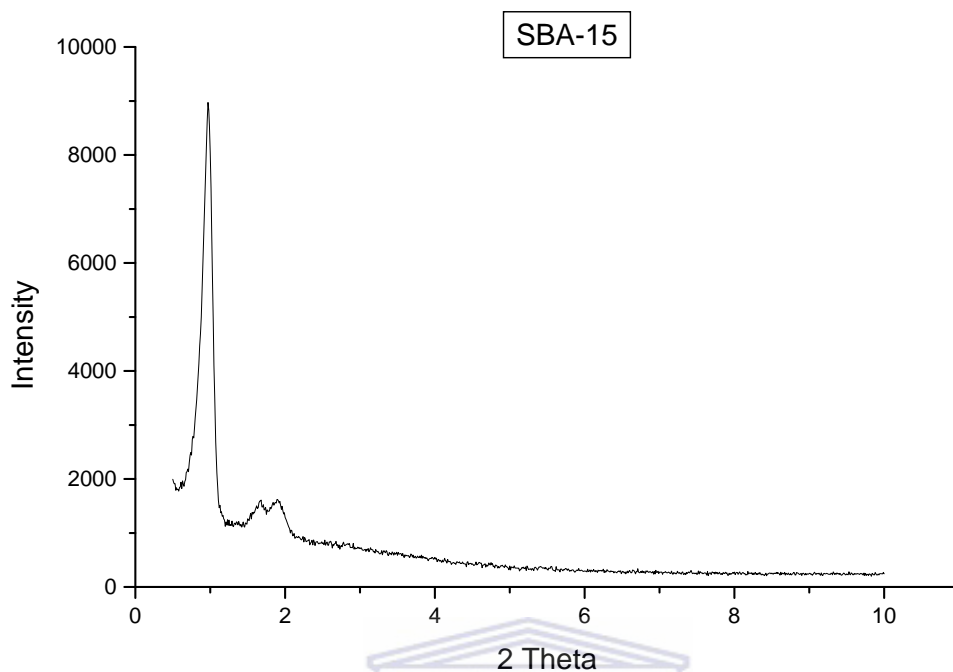


Figure 2.9: X-ray diffraction of SBA-15.

2.4.2.2 Characterization by means of infrared spectroscopy.

Generally the unmodified silica exhibits distinct bands for specific functional groups such as O-H (3800-3200), Si-O-Si (1090) and Si-OH (900 cm^{-1}). Characterization of MCM-41 and SBA-15 by infrared spectroscopy showed similar stretching frequencies around 1638 cm^{-1} , 1628 cm^{-1} , 804 cm^{-1} and 796 cm^{-1} which are due to the Si-OH groups that are on the surface of the support. A big broad band between 1250 cm^{-1} and 1012 cm^{-1} is due to Si-O-Si bond of the silica support.

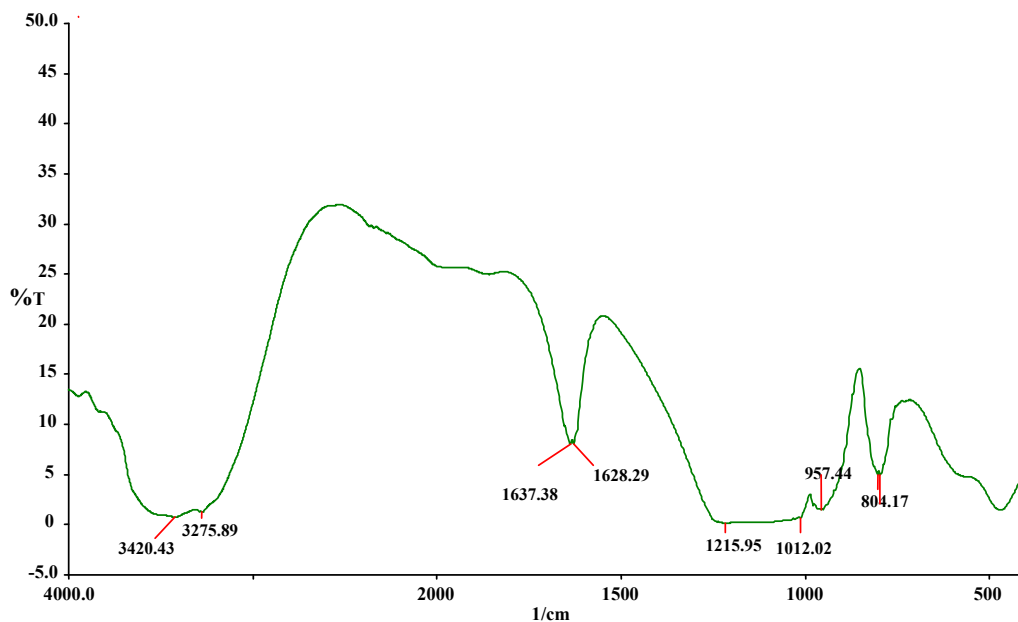


Figure 2.10: FTIR spectrum of MCM-41.

2.4.2.3 Characterization by means of Scanning Electron Microscopy.

Scanning electron microscopy gives a detailed indication of the morphology of the individual particles and it also determines the particle size of the material. Scanning electron microscopy analysis showed that the surface of MCM-41 has agglomerated spherical particles as shown in **Figure 2.11**.

Generally for SBA-15 the scanning electron microscopy image showed that the surface of SBA-15 has particles that are organized into rope-like structures, which are also elongated as shown in **Figure 2.12**, this is a typical morphology of SBA-15.

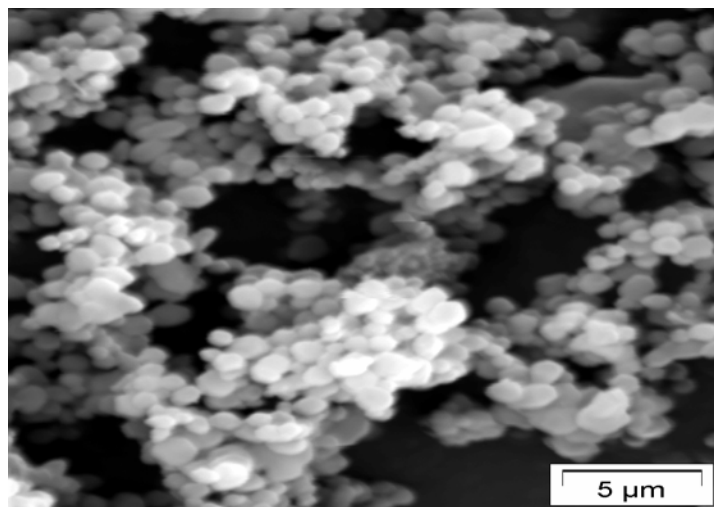


Figure 2.11: Scanning electron microscopy image of MCM-41.

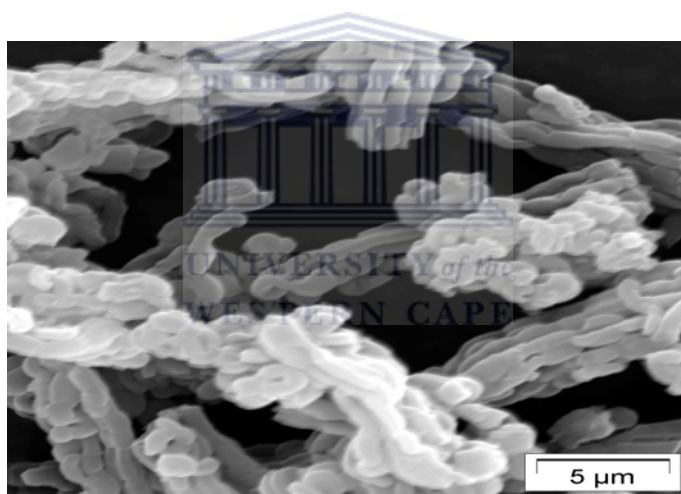


Figure 2.12: Scanning electron microscopy image of SBA-15.

2.4.2.4 Characterization by means of BET surface analysis.

This is a powerful technique to determine the physical structure of the inorganic silica supports. Nitrogen is adsorbed at 77 K over a relative pressure in a range of 0 to 1 which results in the nitrogen adsorption isotherm graph. BET analysis was used to get the surface area of the inorganic supports (MCM-41 and SBA-15) and the adsorption average pore diameter. Generally the surface area of MCM-41 should be greater than 1000 m²/g and for SBA-15 it should be greater than 500 m²/g. At low relative pressures (0.05 to 0.3) a monolayer of nitrogen is formed and at higher relative pressures (p/p_0 greater than 0.4) capillary condensation occurs in the smaller pores. As the relative pressures increase, the size of the pores filled with adsorbate increases with the entire pore being filled at saturation ($p/p_0 = 1$). From this information an adsorption isotherm graph can be plotted, the shape of the graph provides information of the pore structure.^{15, 16}

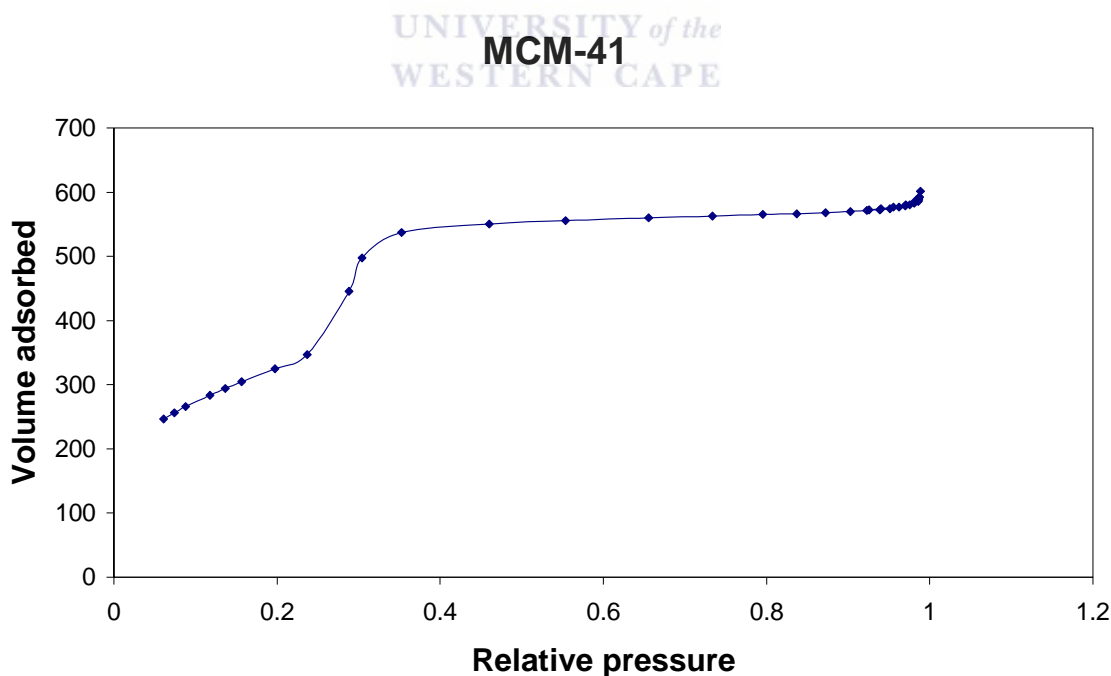


Figure 2.13: Nitrogen adsorption isotherm graph of MCM-41.

The BET surface area of MCM-41 prepared was found to be 1191.09 m²/g and the adsorptive pore diameter is 31.2 Å. The nitrogen adsorption isotherm graph obtained was a Type IV graph, as shown in **Figure 2.13** which is characteristic of mesoporous materials.

The BET surface area obtained for SBA-15 is 943.3 m²/g and the average pore diameter is 43.4 Å. Nitrogen adsorption isotherm graph shown in **Figure 2.14** is a typical Type IV graph which resembles mesoporosity of the material.

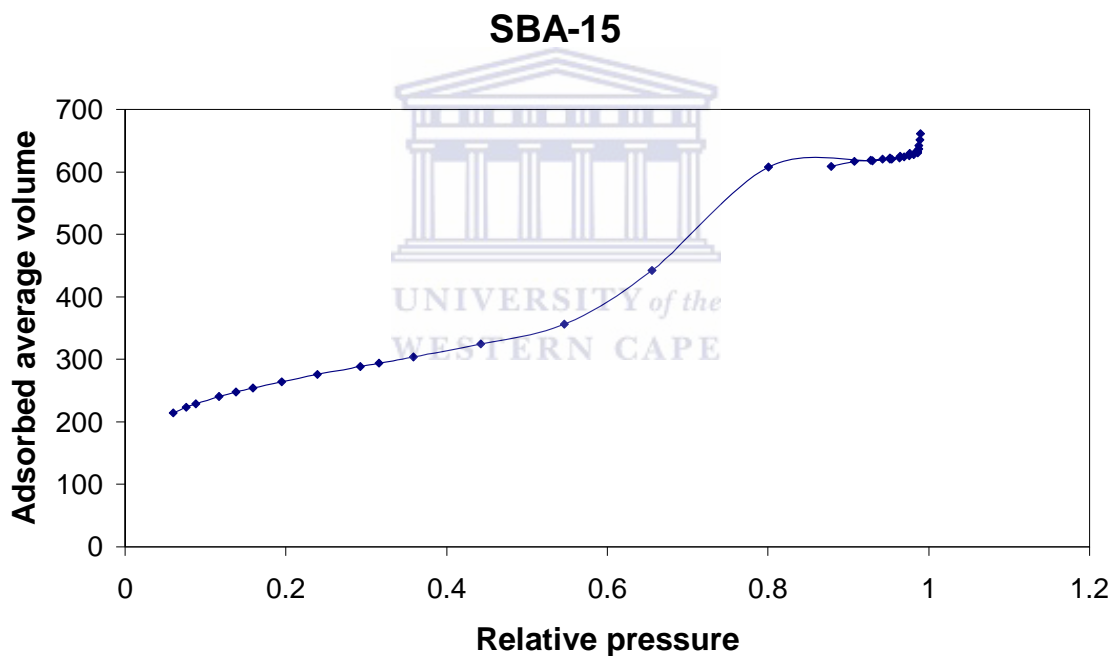
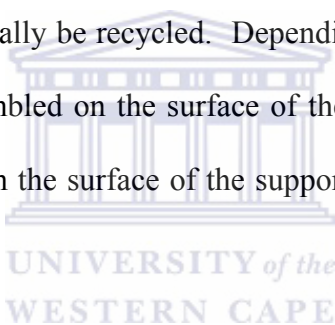


Figure 2.14: Nitrogen adsorption isotherm graph of SBA-15.

2.5 Synthesis and Characterization of the immobilized Copper(II) and Cobalt(II) complexes.

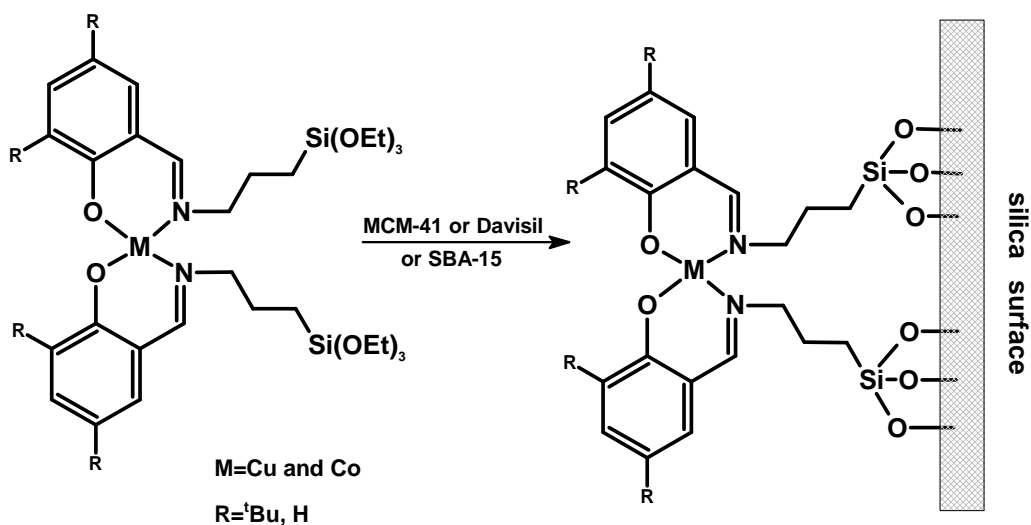
2.5.1 Immobilization of Complexes 1 to 4 onto different silica supports.

The method used for the immobilization process is the covalent tethering of the metal complex. In this case the metal complex or the ligand contains appropriate functional groups that allow it to be immobilized onto the support. If such groups are absent then the ligand is modified to include these functional groups e.g. Si(OR)₃ moieties. Also the supporting material can be chemically modified using the Si(OR)₃ moieties so that the immobilization can be achieved. This method was chosen due to the fact that it forms stable catalysts that can potentially be recycled. Depending on the type of support (pore size), the catalyst can be assembled on the surface of the support which means that the catalyst will be suspended from the surface of the support or it can be assembled within the pores of the support.



2.5.1.1 Immobilization of metal complexes onto silica supports.

In the immobilization process, **Complexes 1 to 4** were reacted with different support materials such as amorphous Davisil silica gel, MCM-41 and SBA-15 in the presence of dry toluene as the solvent. The reason for the use of different supporting materials is that they differ in pore sizes with SBA-15 having a larger pore size than MCM-41, which in turn has a larger pore size than Davisil silica gel. The immobilized catalysts were obtained as powders in high yields.



Catalyst 1; M = Cu; R = H; Davisil silica gel

Catalyst 2; M = Co; R = H; Davisil silica gel

Catalyst 3; M = Cu; R = ^tBu; Davisil silica gel

Catalyst 4; M = Co; R = ^tBu; Davisil silica gel

Catalyst 5; M = Cu; R = H; MCM-41

Catalyst 6; M = Co; R = H; MCM-41

Catalyst 7; M = Cu; R = ^tBu; MCM-41

Catalyst 8; M = Co; R = ^tBu; MCM-41

Catalyst 9; M = Cu; R = H; SBA-15

Catalyst 10; M = Co; R = H; SBA-15

Catalyst 11; M = Cu; R = ^tBu; SBA-15

Catalyst 12; M = Co; R = ^tBu; SBA-15

Scheme 2.3: Schematic representation of the immobilization of metal complexes onto silica supports.

2.5.2 Characterization of the immobilized metal complexes.

Catalysts 1 to 12 were characterized by atomic absorption spectroscopy and infrared spectroscopy. **Catalysts 5 to 12** were also characterized by X-ray diffraction to analyze the crystallinity because these catalysts are supported on mesoporous materials.

Scanning electron microscopy was also employed (**Catalyst 5 to 12**) to look at the morphology of the mesoporous materials. Finally **Catalysts 5 to 12** were analyzed by BET surface analysis.

2.5.2.1 Characterization by X-ray diffraction.

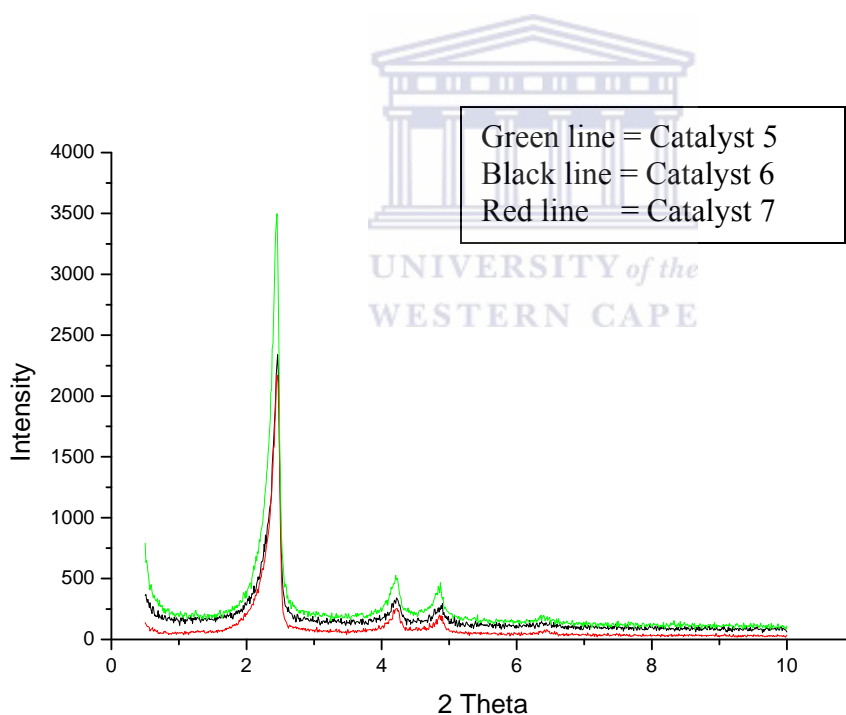


Figure 2.15: X-ray diffraction of *Catalysts 5-7*.

Figure 2.15 shows **Catalysts 5 to 7** and **Figure 2.16** shows **Catalysts 9 to 12**. X-ray diffraction patterns of **Catalyst 1 to Catalyst 12** are shown. X-ray diffraction plots of **Catalyst 5 to Catalyst 7 (Figure 2.15)** show four reflections peaks that are common for MCM-41. The main reflection peak being d(100) which is seen at a 2θ value of 2.5° followed by d(110) that has 2θ equal to 4.2° , third reflection peak is d(200) that is observed at 2θ of 4.8° and the last reflection peak d(210) is observed at 2θ equal to 6.6° . The d spacing for the reflection plane (100) is 35.31 \AA which is the same as for the unmodified MCM-41.

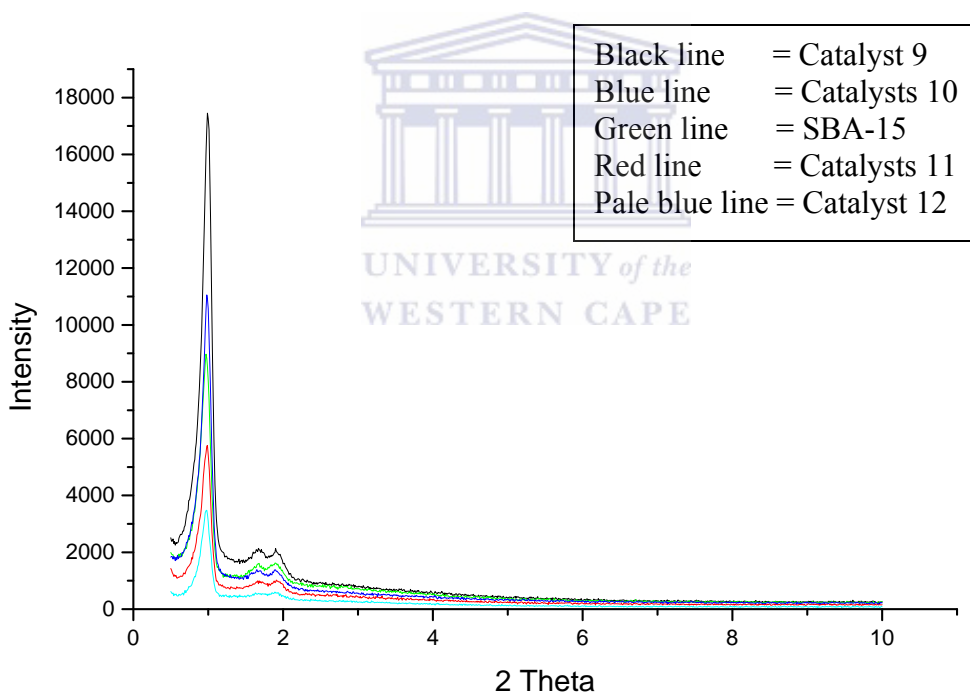


Figure 2.16: X-ray diffraction of **Catalysts 9-12**.

For SBA-15 supported catalysts, **Catalysts 9 to Catalyst 12 (Figure 2.16)**, three reflection peaks are observed. These are also observed in unmodified SBA-15. The main reflection peak is d(100) that appears at $2\theta = 1^\circ$, the second peak is d(110) appears at $2\theta = 1.7^\circ$ and the last one is d(200) which is appears at $2\theta = 1.9^\circ$. The d spacing value for the reflection plane (100) is 88.26 Å. It is known that SBA-15 has three reflection peaks and MCM-41 has four reflection peaks due to the fact that SBA-15 has larger pores than MCM-41.¹⁷

2.5.2.2 Characterization by infrared spectroscopy.

After immobilization, the stretching frequencies of the functional groups shifted to higher wavenumbers which confirms that the complexes were immobilized onto the inorganic silica supports. The FTIR spectra of the immobilized complexes show stretching frequencies for the Si-O and C=N bonds of the complex. These are observed in **Figure 2.17** in the region 1650 cm^{-1} to 1600 cm^{-1} . The Si-O stretching frequency of the silanol groups overlaps that of the C=N bond. The Si-O bond of the siloxane groups is observed in the region 1300 cm^{-1} to 800 cm^{-1} . It consists of a very broad band around the region of 1300 cm^{-1} to 1000 cm^{-1} and a sharp band at 900 to 800 cm^{-1} .

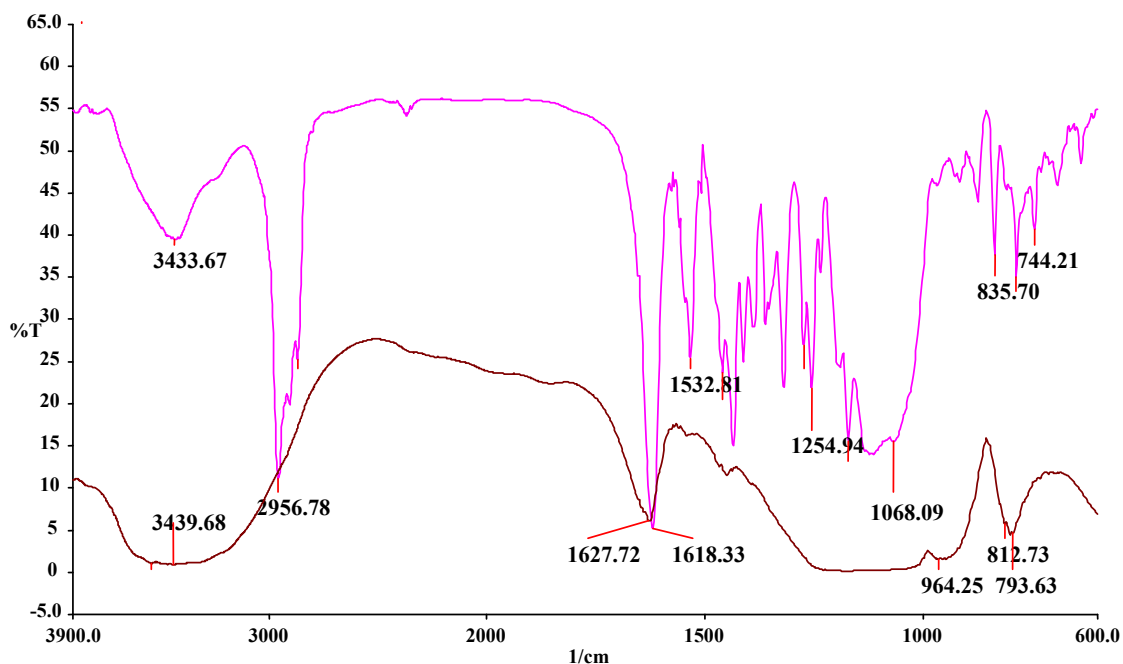


Figure 2.17: FTIR spectra of immobilized catalyst (red line) against metal complex (pink line).

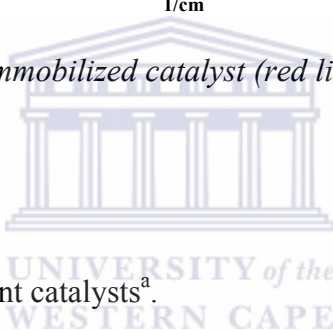


Table 2.5: FTIR data of different catalysts^a.

Catalysts	$\nu_{(\text{Si-OH})}\text{cm}^{-1}$	$\nu_{(\text{Si-O-Si})}\text{cm}^{-1}$	$\nu_{(\text{OH})}\text{cm}^{-1}$
1	1627, 790	1225-964	3600-3200
2	1636, 790	1226-970	3690-3342
3	1632, 804	1242-1010	3600-3200
4	1632, 804	1212-966	3662-3280
5	1624, 800	1224-964	3600-3250
6	1620,800	1222-940	3600-32000
7	1632, 800	1234-954	3546-3220

Table 2.5: Continue

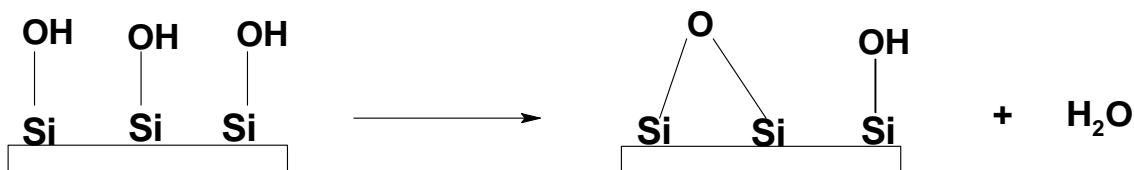
8	1624,805	1178-954	3612-3225
9	1628, 798	1126-956	3618-3226
10	1618, 806	1228-960	3602-3264
11	1628, 804	1214-954	3578-3240
12	1636, 808	1222-954	3652-3232

a = FTIR was recorded as KBr pellets.

2.5.2.3 Characterization by Atomic Absorption Spectroscopy.

Atomic absorption spectroscopy analysis was used to determine the amount of metal loading on the support. It is observed that the metal content of the catalysts varies in respect to the type of metal used, the type of the inorganic support used and also the type of ligand used. Comparing the type of inorganic support used, there is a higher metal loading in the case of Davisil silica gel, followed by SBA-15 and lastly by the MCM-41, as illustrated in **Table 2.6**.

Difference in metal loading between Davisil silica gel and mesoporous silicas could be due to the fact that the latter was subjected to calcination before supporting of the metal. Calcination could result in the condensation of adjacent silanol groups (shown in **Scheme 2.4**) on the surface of the silica. This would reduce the amount of silanol groups available to condense with the siloxane functionalities of the metal complexes. The result is the lowering of metal loading.



Scheme 2.4: Condensation of adjacent silanol groups.

The difference in the metal loading of SBA-15 and MCM-41 could be due to the difference in pore sizes. In case of SBA-15 there would be higher possibility of metal complexes being anchored to the internal pores as well as on the surface. In the case of MCM-41 because of its smaller pores it might favour anchoring largely on the surface.

Comparing the type of complex that is used, it is seen that when using unsubstituted immobilized metal complexes, higher metal loading is obtained as compared to when tertiary butyl substituted immobilized complexes are used, as illustrated in **Table 2.6**. The reason behind these observations is that tertiary butyl substituted complexes have higher steric crowding so it is not easy for these complexes to be supported on the silica surface in close proximity to each other.

Table 2.6: Metal content of immobilized catalysts.

Catalysts	Metal	Support	Metal loading (%wt)
1	Cu	Davisil	0.96
2	Co	Davisil	0.63
5	Cu	MCM-41	0.94
6	Co	MCM-41	0.55

Table 2.6: Continue

9	Cu	SBA-15	0.80
10	Co	SBA-15	0.61
3	^t Cu	Davisil	0.60
4	^t Co	Davisil	0.51
7	^t Cu	MCM-41	0.18
8	^t Co	MCM-41	0.22
11	^t Cu	SBA-15	0.42
12	^t Co	SBA-15	0.50

2.5.2.4 Characterization of immobilized catalysts by scanning electron microscopy.

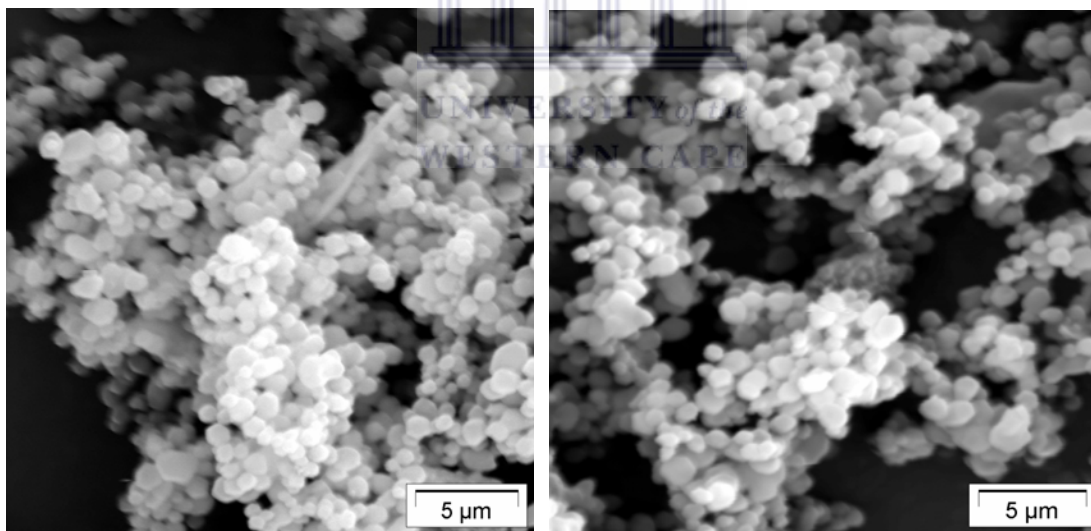


Figure 2.18: Scanning electron microscopy images of pure MCM-41 (right), immobilized catalyst on MCM-41 (left).

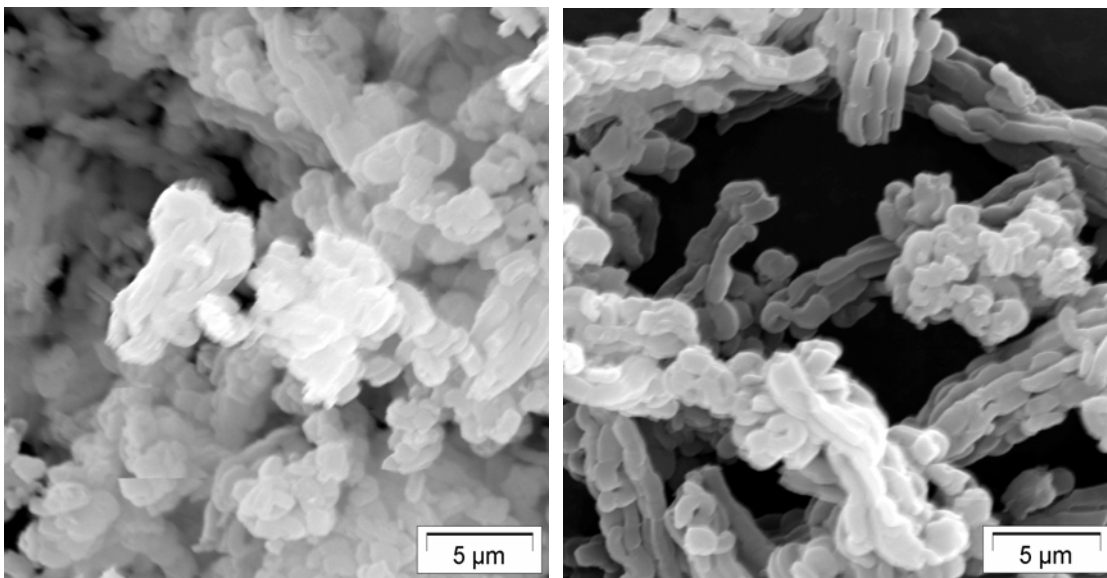


Figure 2.19: Scanning electron microscopy images of pure SBA-15 (right) and immobilized catalyst on SBA-15 (left).

The morphology of SBA-15 and MCM-41 depends on the type of surfactant used. Scanning electron microscopy images shows that the surface morphology of MCM-41 and SBA-15 did not change dramatically even after the immobilization of the metal complexes on the supporting materials. This is independent of the metal as well as the nature of the ligand employed.

2.5.2.5 Characterization by BET surface analysis.

BET surface analysis was used to analyze the surface area of the neat mesoporous silica supports and the immobilized systems. BET surface area analysis also gives a nitrogen adsorption isotherm graph, typical graph for mesoporous materials is a Type IV graph.

Nitrogen adsorption isotherms of MCM-41 immobilized catalysts

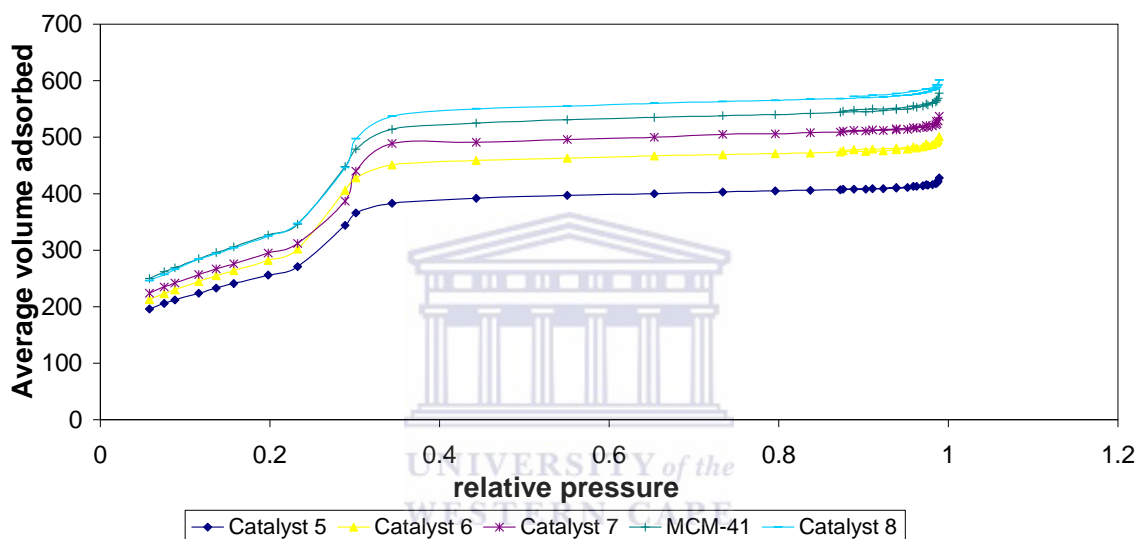


Figure 2.20: Nitrogen adsorption isotherm graph (Type IV graph) of Catalyst 5-8.

As observed in **Figures 2.20 and 2.21** above, the nitrogen adsorption isotherm graphs of the immobilized catalysts suggests that the SBA-15 immobilized catalysts have larger pores than the MCM-41 immobilized catalysts because the capillary condensation in SBA-15 immobilized catalysts occurs at high relative pressures ($P/P_0 = 0.6$ to 0.85) than MCM-41 immobilized catalysts ($P/P_0 = 0.25$ to 0.6). The BET average pore volume of the SBA-15 and MCM-41 immobilized catalysts also differs, average pore volume of SBA-15 immobilized catalysts ranges from 43.4 \AA to 44.40 \AA where as for MCM-41

immobilized catalysts, average pore volume by BET ranges from 28.53 Å to 30.90 Å. It is noted that even after the immobilization, the mesoporosity of the support is maintained because a type IV graph is observed during the BET analysis.

Nitrogen adsorption isotherm of SBA-15 immobilized catalysts

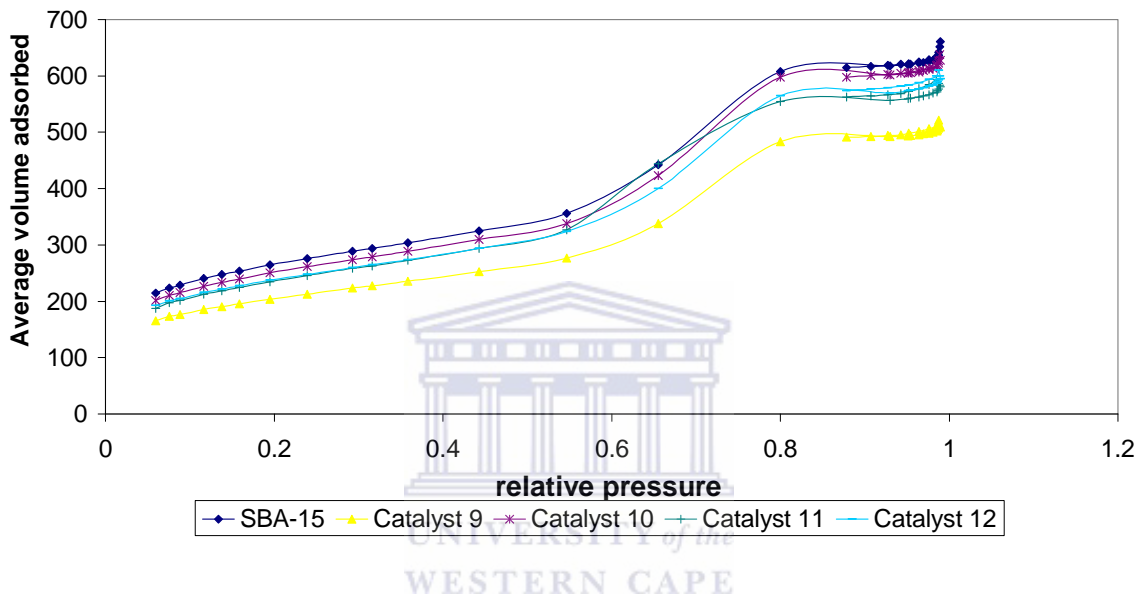


Figure 2.21: Nitrogen adsorption isotherm graph (Type IV graph) of Catalysts 9-12.

The BET surface area of the MCM-41 immobilized catalysts (Catalyst 5 to 8) ranges from 1190.10 m²/g to 928.35 m²/g and for SBA-15 the BET surface area ranges from 943.30 m²/g to 842.93 m²/g, Thommes *et.al.* suggested that if SBA-15 has a surface area of about 700 m²/g to 950 m²/g, then that means this material was synthesized at a temperature between 35 to 60 °C.¹⁹ The neat supports were observed to have higher surface area but after immobilization it was noted that the surface area decreased. It was

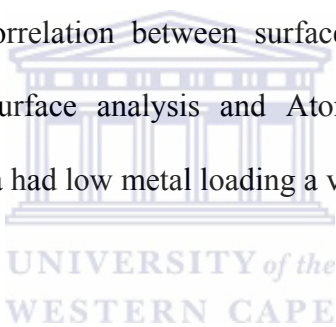
noticed that the catalysts having lower BET surface area values have higher metal loading and those with higher BET surface area have lower metal loading.

Table 2.7: Physical properties of the immobilized catalysts.

Catalysts	Support	Metal	Adsorption properties of supports	
			BET Surface area (m ² /g ⁻¹)	Average pore diameter(Å)
Cat 5	MCM-41	Cu	928.35	28.53
Cat 6	MCM-41	Co	1033.43	30.00
Cat 7	MCM-41	^t Cu	1077.22	30.90
Cat 8	MCM-41	^t Co	1190.10	30.04
Cat 9	SBA-15	Cu	943.30	43.40
Cat 10	SBA-15	Co	894.44	44.13
Cat 11	SBA-15	^t Cu	842.93	43.60
Cat 12	SBA-15	Co	850.52	44.40

2.6 Conclusion

All the ligands were successfully synthesized but it was noted that these ligands tend to hydrolyze (ethoxy groups) after being left in air for few days at room temperature. Precautions were taken that these ligands should be stored under vacuum. The complexes were successfully synthesized and characterized but in the case of triethoxysilane complexes we tend to form a binuclear species bridged by phenolic group of the ligand as this was observed on elemental analysis results of **Complex 1** and **2**. The silica supports (MCM-41 and SBA-15) were synthesized and successfully characterized. Immobilization of the metal complexes and characterization of the immobilized catalysts was successfully done. A correlation between surface area and metal loading was observed as seen by BET surface analysis and Atomic Absorption Spectroscopy. Catalysts with high surface area had low metal loading a vice versa.



2.7 Experimental Method

2.7.1 Reagents

All experiments were carried out under nitrogen. The highest grades of commercially available reagents were used throughout this study. The following reagents were obtained from Aldrich Chemicals: salicylaldehyde, 3-aminopropyltriethoxysilane, copper(II) acetate monohydrate, cobalt(II) acetate tetrahydrate, Davisil 710 silica gel 4-20 μ 99%, cetyl-trimethyl-ammonium bromine (CTAB), tetraethylorthosilicate 98% (TEOS), poly-(ethyleneglycol)-*block*-poly(propyleneglycol)-*block*-poly(ethyleneglycol) average M_n ca. 5800, ethylene glycol (triblock copolymer, EtO₂₀PO₇₀EtO₂₀) and atomic absorption 1000 ppm standards.

The solvents used were dried before use; ethanol was dried by distillation over magnesium turnings and iodine. Toluene was dried by distillation over sodium wire and benzophenone. Acetonitrile and the above mentioned solvents were purchased from Saarchem uniVAR. Distilled water and ultra pure water were used for preparation of aqueous solutions.

2.7.2 Apparatus

¹H-NMR spectra were recorded using a Varian Gemini 2000 instrument at 200 MHz. ¹H-NMR was used for analysis of the ligands. IR spectra were recorded as nujol mulls or as KBr pellets on a Perkin Elmer, Paragon 1000 PC spectrometer. Elemental analysis was performed at the Microanalytical Laboratory at the University of Cape Town.

Electrospray ionization mass spectra were recorded using a Waters API Q-TOF ultima and was performed at the University of Stellenbosch. X-ray diffraction (XRD) was performed at iThemba Labs. Scanning electron microscopy (SEM) was performed using a HITACHI Scanning Electron Analyzer, model X-650 at the University of the Western Cape, Physics Department.

2.7.3 Synthesis of Ligands

Synthesis of L1^{2,5}

3-Aminopropyltriethoxysilane (2.20 g, 10 mmol) was added to dry ethanol (5 ml). Whilst this solution was stirred, salicylaldehyde (1.107 g, 10 mmol) was added to the solution which immediately turned yellow. This yellow solution was refluxed for 2 hrs under a nitrogen atmosphere after which the solvent was removed by rotatory

evaporation, yielding a bright yellow oil. The sample was dried under vacuum. The yield of the propyl triethoxysalicyaldimine ligand, **L1** was 2.43 g (75%).

Synthesis of L2.

For the propyltriethoxy-3,5-ditertiarybutyl-salicyaldimine ligand, a 1:1 stoichiometric reaction ratio was used. 3-aminopropyltriethoxysilane (1.11 g, 5 mmol) was added to dry ethanol (5 ml). While this solution was stirred, 3,5-ditertiarybutyl-2-aldehyde (1.18 g, 5 mmol) was added to the amine solution. The solution turned yellow immediately. The yellow solution was stirred for 2 hrs under a nitrogen atmosphere at 75 °C.

The solvent was removed by rotatory evaporation. The yellow oil was dried under vacuum for 24 hrs to remove excess solvent. The yield obtained for ligand **L2** was 2.43 g (56%).

L3 and **L4** were synthesized in the same manner except instead of 3-aminopropyltriethoxysilane, propylamine was used. **L3** was obtained in yields of 0.59 g (72%) and **L4** in yields of 0.88 g (64%).

2.7.4 Complex formation

Formation of Complex 1.

This reaction was carried in a 2:1 stoichiometric ratio of a ligand to metal. Propyltriethoxysalicyaldimine ligand **L1** (0.49 g, 1.53 mmoles) was dissolved in dry ethanol (5 ml) which was stirred under nitrogen atmosphere. Copper acetate monohydrate (0.15 g, 0.77 mmoles) was added to the salicyaldimine solution which

immediately turned dark green. The dark green solution was refluxed under nitrogen for 5 hrs at 75⁰ C. The dark green solution was filtered and the green solid was washed with ethanol (20 ml) followed by washing with hexane.

The dark green solid was left on the bench top to dry then the solid was further dried under vacuum for 24 hrs, giving a yield of 0.11 g (16%).

Formation of Complex 2.

For cobalt; the reaction was also carried in a 2:1 stoichiometric ratio of a ligand to metal. Propyltriethoxysalicyaldimine ligand, **L1** (0.49 g, 1.53 mmoles) was dissolved in dry ethanol (5 ml). This solution was stirred under nitrogen, and cobalt acetate tetrahydrate (0.19 g, 0.77 mmoles) was added to the salicyaldimine solution. The reaction mixture immediately turned reddish/pink but after few minutes of stirring the solution became black/green. This solution was refluxed for 5 hrs under a nitrogen atmosphere at 75⁰C. During this time the solution became dark green in color. The solution was filtered, washed with ethanol (20 ml) followed by hexane (20 ml). The dark green solid was dried under vacuum for 24 hrs. The yield obtained was 0.36 g (53%).

Complexes 3 to 8 were synthesized in a similar manner except for **Complex 6** and **8** where NaOH was used as a base to abstract the phenolic proton on the ligand. **Complex 3** was isolated as a dark brown solid (48% yield) while **Complex 4** was obtained as a yellow/orange solid, 48%. **Complexes 5-7** were isolated as dark green crystals, with **Complex 5** obtained in a yield of 0.31 g (40%), **Complex 6** in a yield of 0.33 g (43%),

Complex 7 in a yield of 0.54 g (44%) and **Complex 8** was isolated as an orange solid in a yield of 0.64 (55%).

For **Complexes 5** to **7**, single crystals were obtained by recrystallization from ethanol/hexane.

2.7.5 Synthesis of inorganic silica supports.

Synthesis of MCM-41.

The method used was previously reported by Qiang Cai *et.al.*¹² Ammonium solution (205 ml, 25% wt) was mixed with distilled water (270 ml), surfactant (cetyltrimethylammonium bromide, 2 g) was added into the solution with stirring and heating at 50 °C and pH 12.5. When the solution became homogeneous, TEOS (10 ml) was introduced, giving a white slurry. After 2 hrs the solution was filtered washed with distilled water (700 ml) and then dried at room temperature. The white solid was calcined at 550 °C. The temperature was slowly increased from 100°C to 450 °C and then increased to 550 °C. The temperature was maintained at this temperature for 4 hrs. 2.109 g of MCM-41 was obtained.

Synthesis of SBA-15.

Method used for the synthesis of SBA-15 was that reported by Zhao *et.al.* The surfactant (poly(ethyleneglycol)-*block*-poly(propyleneglycol)-*block*-poly(ethyleneglycol), 8 g) was dissolved in a mixture of distilled water (60 ml) and 2 M HCl solution (360 ml) with

stirring at 35 °C. Then TEOS (18.2 ml) was added into the solution with stirring at 35 °C for 20 hrs.

The mixture was aged at 80 °C for 24 hrs without stirring. The solid product was filtered and washed with 1000 ml of distilled water and air dried at room temperature. The white solid was calcined by slowly increasing the temperature to 450 °C and then to 500 °C. The temperature was kept at 500 °C for 8 hrs.

2.7.6 Immobilization of complexes onto inorganic silica supports.

Preparation of Catalyst 1

0.10 g of *bis*-(propyltriethoxysalicylaldehyde) copper(II) complex was added to a slurry 1.0 g of commercial silica gel Davisil 710 in 10 ml of dry toluene in a 100 ml round bottom flask. The mixture was refluxed under a nitrogen atmosphere at 110 °C for 24 hrs resulting in a dark green mixture. The solution was filtered using gravity filtration, washed with 20 ml of toluene and with 20 ml of dichloromethane to remove any unreacted *bis*-(propyltriethoxysalicylaldehyde) copper(II) complex. The dark green powder was dried under vacuum for 24 hrs. The products were stored in the glove box until further use.

Catalysts 2 to 12 were synthesized in the same manner.

2.8 References

1. Progress in Inorganic Chemistry, A. Chahravorty, G. W. Everett, Jr, R. D. Gillard, H. Tracy Hall, R. H. Hall, B. F. G. Johnson, J. A. McCleverty, S. M. Williamson, Volume 7, 87.
2. P. G. Cozzi, *Chem. Soc. Rev.*, **33** (2004) 410.
3. E. Sinn, C. M. Harris, *Coord. Chem. Rev.*, **4** (1969) 391.
4. S. J. Gruber, C. M. Harris, E. Sinn, *Inorg. Chem.*, **7** (1968) 268.
5. E. F. Murphy, D. F., A. Baiker, *Inorg. Chem.*, **42** (2003) 2559.
6. E. F. Murphy, L. Schmid, T. Burgi, M. Maciejewski, A. Baiker, D. Gunther, M. Schneider, *Chem. Mater.*, **13** (2001) 1296.
7. U. G. Sigh, R. T. Williams, K. R. Hallam, G. C. Allen, *J. Sol. Chem.*, **178** (2005) 3405.
8. S. Ray, S. F. Mapolie, J. Darkwa, *J. Mol. Cat. A: Chemical*, **267** (2007) 143.
9. B. Marler, U. Oberhagemann, S. Vortmann and H. Gies, *Micro. Mat.*, **6** (1996) 375.
10. J. S. Beck, J. C. Vartuli, W. J. Roth, M. E. Leonowicz, C. T. Kresge, K.D. Schmitt, C. T.-W. Chu, D. H. Olson, E. W. Sheppard, S. B. McCullen, J. B. Higgins, J. L. Schlenker, *J. Am. Chem. Soc.*, **114** (1992) 10834
11. J. Y. Ying, C. P. Mehnert, M. S. Wong, *Angew. Chem. Int. Ed.*, **38** (1999) 56.
12. Q. Chai, W. Y. Lin, F. Xiao, W. Pang, B. Zhou, X. Chen, *Micropor. Mesopor. Mater.*, **32** (1999) 1.
13. D. Zhao, Q. Huo, J. Feng, B. F. Chmelka, G. D. Stucky, *J. Am. Chem. Soc.*, **120** (1998) 6024.

-
14. B. Marler, U. Oberhagemann, S. Vortmann, H. Gies, *Micropor. Mater.*, **6** (1996) 375.
 15. S. Brunauer, P. H. Emmett, E. Teller, *J. Am. Chem. Soc.*, **60** (1938), 309.
 16. P. M. Price, J. M. Clark, D. J. Macquarrie, *J. Chem. Soc., Dalton Trans*, 2000, 101.
 17. K. Morishige, M. Tateishi, *Langmuir*, **22** (2006) 4165.
 18. K. Cassiers, T. Linsen, M. Mathieu, M. Benjelloun, K. Schrijnemakers, P. Van Der Voort, P. Cool, E. F. Vansant, *Chem. Mater.*, **14** (2002) 2317.
 19. M. Thommes, R. Kohn, M. Froba, *Appl. Surf. Sc.*, **196** (2002) 239.



CHAPTER 3

Oxidation of Cyclohexene



UNIVERSITY *of the*
WESTERN CAPE

3.1 Introduction

3.1.1 Salicylaldimine complexes as catalysts for alkene oxidation.

Salicylaldimine complexes are known to contain N,O donor atoms, these complexes were proven to be very effective catalysts in a range of catalytic reactions. Immobilizing these complexes onto amorphous and mesoporous silica supports makes salicylaldimines even much more effective catalysts than their homogeneous counterparts. These compounds are very attractive as oxidation catalysts due to their structural flexibility as well as their stability.

Cyclohexene oxidation using hydrogen peroxide as co-oxidant is found to be environmentally more friendly than using peracids. In addition hydrogen peroxide tends to be more stable in the reaction mixture as compared to peracids. Peracids are also very expensive, hazardous to handle and are non-selective in alkene oxidation which leads to formation of undesirable products, creating lots of waste.¹ Oxygen can also be used as co-oxidant, since the radical intermediates can capture oxygen from the atmosphere, even to the extent where hydrogen peroxide is acting more as a radical initiator than a stoichiometric oxidant.² Alkene oxidation leads to very useful organic intermediates (alcohols, ketones, acids, aldehydes *etc.*) which are commonly used for the synthesis of many chemical materials especially for the production of fine chemicals.

Some work on alkene oxidation has been done using various immobilized transition metals including copper(II) and cobalt(II) salicylaldimine complexes. Some copper(II) salicylaldimines have previously been immobilized on a MCM-41 matrix and tested for epoxidation of styrene and cyclohexene using tertiary butyl hydroperoxide as the oxidant. The catalysts showed excellent cyclohexene conversion of up to 94% with the selectivity of 78% to cyclohexene oxide and 16% to 2-cyclohexen-1-ol. Styrene conversion of 97% and a selectivity of 86% to the epoxide and 11% to benzaldehyde were obtained.³ Co and Cu salen complexes immobilized on MCM-41 were also found to be very effective catalysts for styrene, cyclohexene and 1-decene oxidation using tertiary butyl hydrogen peroxide as oxidant, giving higher % conversion for the immobilized Cu and Co salen catalysts as compared to the homogeneous Cu and Co salen catalysts.⁴



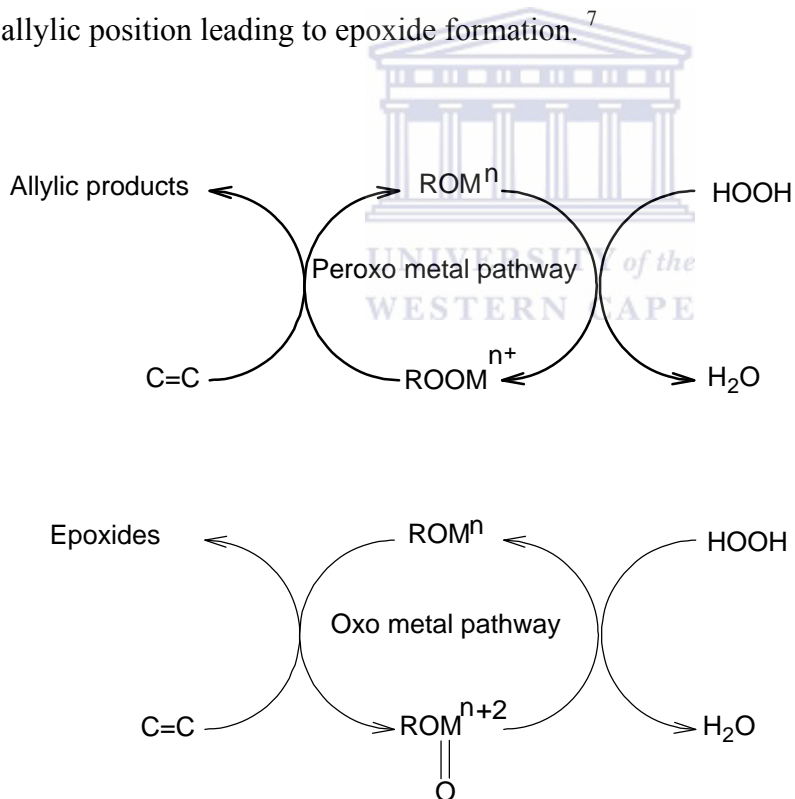
3.1.2 Mechanism of alkene oxidation

The mechanism of alkene oxidation involves hydrogen-atom abstraction from the substrates (alkene) which mostly occurs at alpha positions to unsaturated groups, particularly at the allylic positions, because of the resonance stabilization of the resulting radical.

Basically there are two competing reaction mechanisms that are possible in alkene oxidation. The first is the so-called free radical mechanism in which hydrogen peroxide undergoes homolytic decomposition forming the allylic hydroperoxide radical intermediate which reacts with the catalyst to form allylic products, as shown in **Scheme 3.1**.⁵ In most oxidation reactions involving molecular oxygen, the peroxide acts as an

initiator of the radicals. Such radicals are produced by thermal decomposition of the peroxide.² Direct thermal initiation by hydrogen-abstraction by molecular oxygen may sometimes occur but it is difficult to detect because traces of the peroxidic impurity are always present in the reaction mixture.⁶

The second possible mechanism is where the hydrogen peroxide is cleaved heterolytically, a process catalyzed by metal ion centres (e.g. Mo, V, W, Ti *etc.*) to yield epoxides. Thus hydrogen peroxide reacts with the metal ions to produce a metal oxo intermediate. The latter further reacts with cyclohexene, by abstraction of hydrogen from the allylic position leading to epoxide formation.⁷

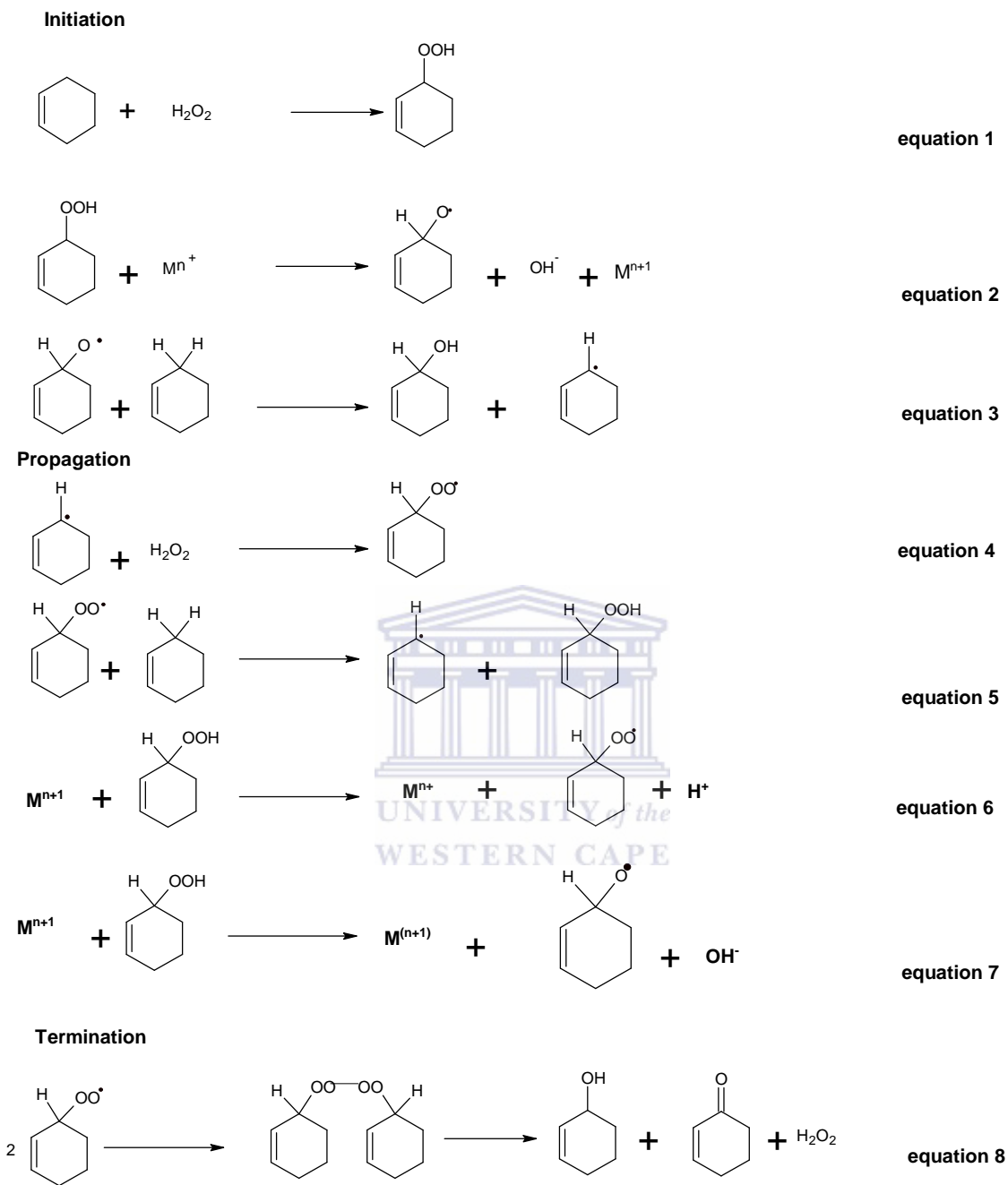


Scheme 3.1: Peroxo metal and oxo-metal pathways.

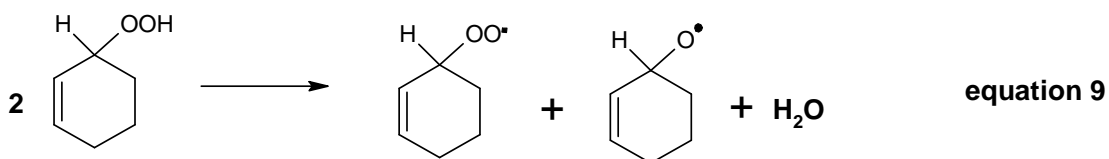
3.1.2.1 Homolytic oxidation

Homolytic systems are those involving free radicals as intermediates and the catalysis mechanism involves the metal in a series of one electron oxidation or reduction steps. This may be discussed in terms of three steps: initiation, propagation and termination (**Scheme 3.2**). The metal may intervene in any of these basic steps influencing the rate of reaction. The key role of the metal complexes added to these systems is to catalyze the decomposition of the hydroperoxide species RO_2H or to a lesser extent, peroxy species of the type RO_2R . Addition of the metal complex can induce the reaction rate of these systems thus reducing the reaction period.

Two basic steps in metal catalyzed hydroperoxide decomposition first proposed to explain Fe(II) catalyzed decomposition of hydrogen peroxide (as found in the Fenton reagent) are shown in **Equations 6** and **7**. If a metal ion is capable of effecting only one of these reactions, then stoichiometric rather than catalytic decomposition of hydroperoxide occurs unless a catalytic means is devised for returning the metal ion to its original oxidation state. In general when the metal is a strong reducing agent e.g. Cu^{I} or Cr^{II} , hydroperoxide decomposition occurs via **Equation 6**, while with strong oxidants, e.g. Pb^{IV} , Ce^{IV} **Equation 7** predominates. When the metal is equally satisfied in either the n or the $n+1$ oxidation states, then the two states are of comparable stability. Both reactions can occur concurrently, resulting in a combination of **Equations 6** and **7** which then represents catalytic decomposition of the hydroperoxide into alkoxy and alkylperoxy radicals as shown in **Equation 9, Scheme 3.3**.⁸



Scheme 3.2: Homolytic decomposition of hydrogen peroxide, the free radical mechanism of alkene oxidation.



Scheme 3.3: Combination of equation 6 and 7.

3.1.2.2 Heterolytic oxidation

The essential step in the epoxidation reaction is thought to be the non-dissociative coordination of the hydroperoxide molecule to the metal center via the R bonded oxygen to give the structure shown in **Figure 3.1**.

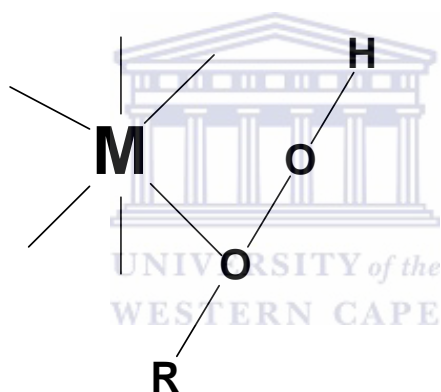


Figure 3.1: Coordination of hydroperoxide molecule to the metal center.

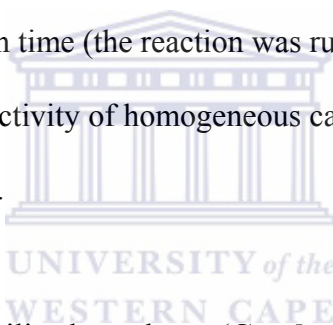
The hydroperoxide is activated by coordination in that the metal center reduces the electron density at the peroxide oxygen thus rendering it more susceptible to nucleophilic attack by the substrate. Once the activated catalyst-peroxide adduct has been formed, efficient transfer of oxygen to the substrate is important. Oxygen transfer from a metal can be achieved directly in order to minimize reaction byproducts.⁹ Suitable catalysts involve early transition metals in high oxidation states.

3.2 Evaluation of Catalytic Activity using Immobilized Catalysts

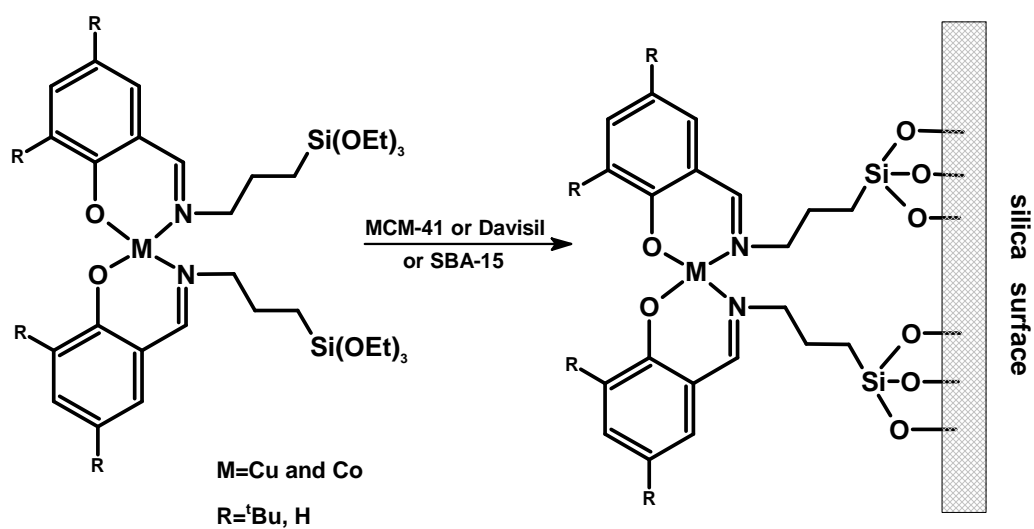
In this study, cyclohexene oxidation was investigated using silica immobilized salicylaldehyde Cu(II) and Co(II) catalysts (**Scheme 3.4**) and their homogeneous analogues. The following aspects were investigated:

- The effect of the metal (Cu versus Co),
- Effect of substituents on the ligands (tertiary butyl was used as substituent which is known to be a very good electron donating group),
- Effect of the type of support used (Davisil silica gel, MCM-41 and SBA-15 were used as supporting materials with different pore sizes),
- Effect of reaction time (the reaction was run for 5 hours and 24 hours).

In addition the activity and selectivity of homogeneous catalysts were compared with that of the heterogeneous analogues.



The Cu(II) and Co(II) immobilized catalysts (**Catalysts 1 to 12**) were evaluated in cyclohexene oxidation. Reactions were carried out for 5 hrs and 24 hrs using a 1:1000:1000 and 1:500:500 ratio of metal: cyclohexene: hydrogen peroxide, 0.01 mmoles of metal, 30% of hydrogen peroxide and acetonitrile as a choice of solvent. The variables used for substrate and oxidant concentration varied according to the ratio of metal: cyclohexene: hydrogen peroxide used. Irrespective of the ratio used, the total volume of the overall reaction remained 5 ml. The reactions were carried out at 60 °C. The products were characterized by Gas Chromatography.



Catalyst 1; M = Cu; R = H; Davisil silica gel

Catalyst 2; M = Co; R = H; Davisil silica gel

Catalyst 3; M = Cu; R = 'Bu; Davisil silica gel

Catalyst 4; M = Co; R = 'Bu; Davisil silica gel

Catalyst 5; M = Cu; R = H; MCM-41

Catalyst 6; M = Co; R = H; MCM-41

Catalyst 7; M = Cu; R = 'Bu; MCM-41

Catalyst 8; M = Co; R = 'Bu; MCM-41

Catalyst 9; M = Cu; R = H; SBA-15

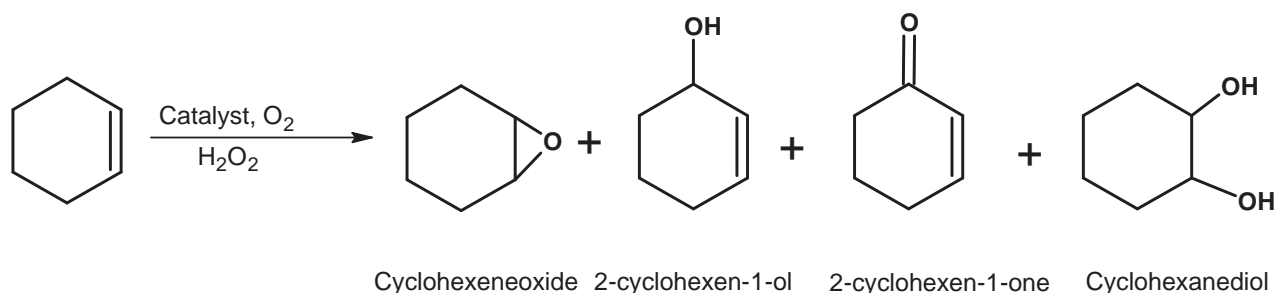
Catalyst 10; M = Co; R = H; SBA-15

Catalyst 11; M = Cu; R = 'Bu; SBA-15

Catalyst 12; M = Co; R = 'Bu; SBA-15

Scheme 3.4: Schematic view of the preparation of immobilized catalysts.

Cyclohexene oxidation normally gives four possible products viz. cyclohexene oxide, 2-cyclohexen-1-ol, 2-cyclohexen-1-one and 1,2-cyclohexanediol (**Scheme 3.5**).



Scheme 3.5: Possible products of cyclohexene oxidation.

In this investigation allylic products were obtained in most cases and the homogeneous catalysts gave poor conversion but good selectivity to allylic products as compared to the heterogeneous catalysts, the following results illustrates some of the findings of this study.

3.2.1 The effect of metal.

The effect of metal was investigated using immobilized Cu and Co catalysts.

Chart 3.1 shows that there is no significant difference in conversion when the different metals are utilized except in the case where the complexes are immobilized on Davisil silica gel. In this case slightly higher conversions are obtained. Also in the case of the Davisil silica gel supported catalysts, the Co based system is slightly more active. In

general immobilized Co catalysts show better conversion than the immobilized Cu catalysts.

Chart 3.2 shows that there is also no significant difference in product distribution when the two metals were used. 2-cyclohexen-1-one and 2-cyclohexen-1-ol are the major products that are observed in the reaction. This shows that these catalysts favour the formation of allylic products. Karandikar *et.al.* used Cu and Co-Salen immobilized on MCM-41 for cyclohexene oxidation using tertiary butyl hydroperoxide as oxidant. Their results showed that these immobilized Cu and Co-Salen catalysts favoured the formation of 2-cyclohexen-1-one as the major product. They claimed that this is due to the fact that allylic hydrogen is more active than the C=C bond towards the tertiary butyl peroxy radical which leads to formation of allylic products. Our results are similar to that of the above mentioned researchers as can be seen in the similarity in the product distribution using the different metals (Cu and Co).⁴ **Cat 6** however behaves slightly different to the other systems in that it produces only the ketone.

Effect of metals on conversion using immobilized catalysts

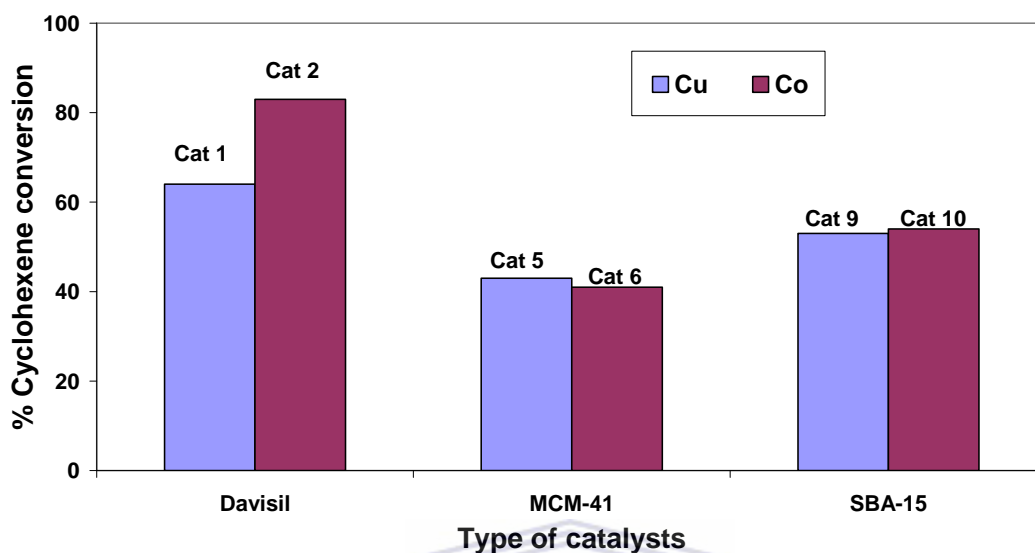


Chart 3.1: Effect of metal on cyclohexene conversion using unsubstituted immobilized catalysts.

Effect of metal on product selectivity using Cu and Co catalysts

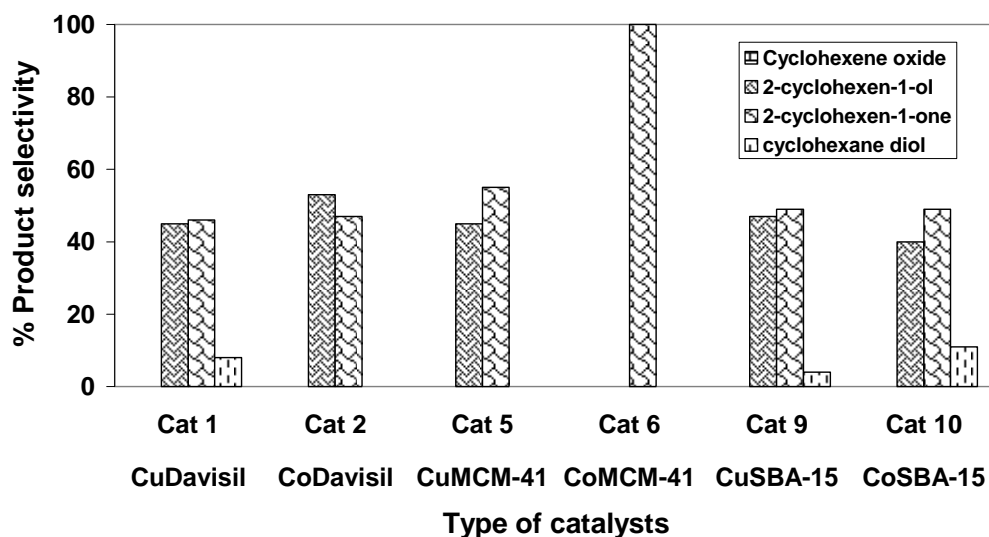


Chart 3.2: Effect of metal on product distribution using unsubstituted immobilized Cu and Co catalysts.

3.2.2 The effect of substituents.

The catalysts employed consisted of two types of salicylaldimine ligands viz a system with no substituents on the aryl ring and another in which positions 3 and 5 are substituted with tertiary butyl groups. The effect of the substituents on the cyclohexene conversion and selectivity of the catalysts were evaluated using a reaction ratio of 1:1000:1000 (metal: cyclohexene: oxidant). It is known that tertiary butyl substituents are good electron donating groups. These substituents are also expected to have a steric influence and they are known to often enhance the rate of reaction as compared to unsubstituted ligands.

Chart 3.3 shows the cyclohexene conversion of Cu and Co unsubstituted and tertiary butyl substituted immobilized catalysts. These immobilized systems generally show high cyclohexene conversion. It is observed that in most cases the immobilized tertiary butyl substituted Cu(II) catalysts show slightly higher conversions than the unsubstituted immobilized catalysts, except for the Davisil silica gel immobilized tertiary butyl substituted Cu(II) catalysts, which have a lower cyclohexene conversion than the unsubstituted Davisil silica gel immobilized catalyst. Thus for example in the case of both MCM-41 and SBA-15 supported catalysts, the tertiary butyl substituted analogues show higher conversions. A similar trend is observed for the Co systems however the difference in activity between the tertiary butyl substituted and unsubstituted catalysts is not as great in the latter case. This proves that the tertiary butyl groups enhance the reaction rate thus converting cyclohexene to a greater extent than when the systems are unsubstituted. The presence of tertiary butyl groups might influence the electronic

properties of the catalysts making it more electron rich. Electron rich metal centres are known to facilitate the decomposition of hydrogen peroxide enhancing the reaction rate of oxidation of alkenes.

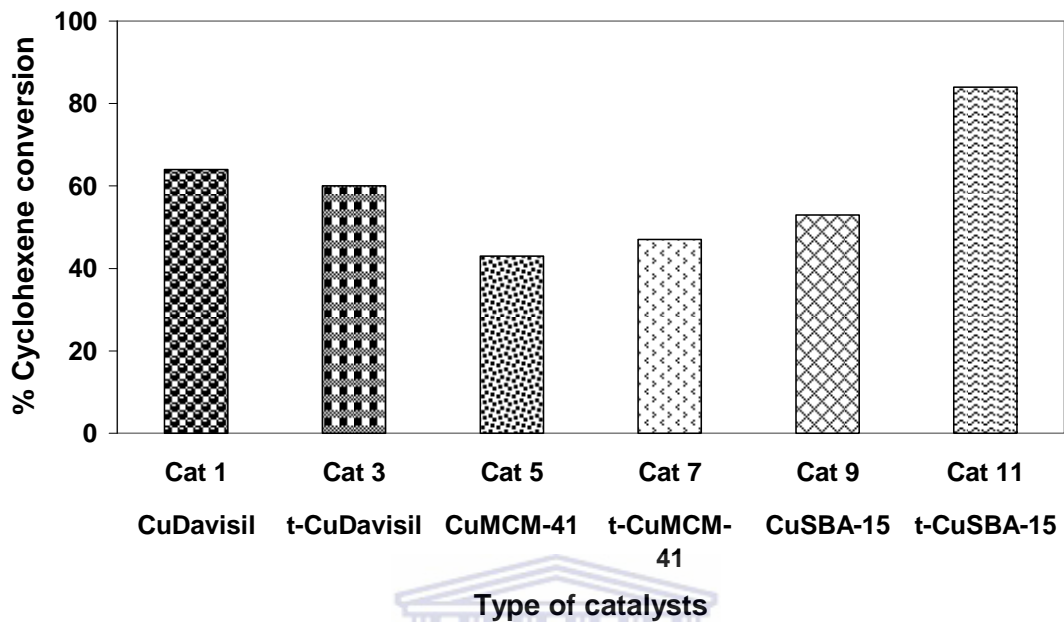
Chart 3.4 shows that **Cat 1 to 11** has almost the same product distribution in that 2-cyclohexen-1-one is observed to be the major product followed by 2-cyclohexen-1-ol in fairly similar percentages followed in turn by cyclohexane diol. In the case of immobilized Cu systems, the nature of the ligand has very little effect on the product distribution. This can be seen by the fact that catalysts on the same support have very similar levels of 2-cyclohexen-1-one and 2-cyclohexen-1-ol. As far as the Co systems are concerned, the immobilized tertiary butyl substituted catalysts produce higher levels of the 2-cyclohexen-1-ol. **Chart 3.4** also shows that **Cat 6** is very selective for 2-cyclohexen-1-one. **Cat 2, 4** and **12** have also similar product distributions where 2-cyclohexen-1-ol is the major product followed by 2-cyclohexen-1-one with cyclohexene oxide produced in small amounts for **Cat 4**. **Cat 10** favours the formation of 2-cyclohexen-1-one as the major product followed by 2-cyclohexen-1-ol and cyclohexane diol in small amounts.

In conclusion most of the tertiary butyl substituted Co(II) immobilized catalysts seem to favour the formation allylic products, with 2-cyclohexen-1-ol as the major product. The unsubstituted Co(II) immobilized catalysts favours the formation of 2-cyclohexen-1-one and 2-cyclohexen-1-ol in almost equal amounts. In our observation the electron donating group substituents leads to an electron rich catalyst species which facilitates hydrogen

peroxide decomposition and leads to homolytic cleavage which in turn favours formation of allylic products. It has been proven by Nam *et.al.* that electron poor catalysts such as iron(IV) porphyrin facilitates heterolytic O-O bond cleavage which leads to epoxidation products.⁷ Similar to our allylic products observations, Savalati-Niasari *et.al.* noted that one electron oxidants such as Co(II), Mn(II), Cu(II) and Ni(II) catalyze free radical oxidation processes by promoting the decomposition of TBHP into chain initiating alkoxy and alkyl peroxy radicals in one electron transfer process (as shown in **Scheme 3.4**). They also claimed that the metal ion acts as an initiator of free radical oxidation rather than a catalyst.¹¹



Effect of substituents on conversion using Cu catalysts



Effect of substituents on conversion using Co catalysts

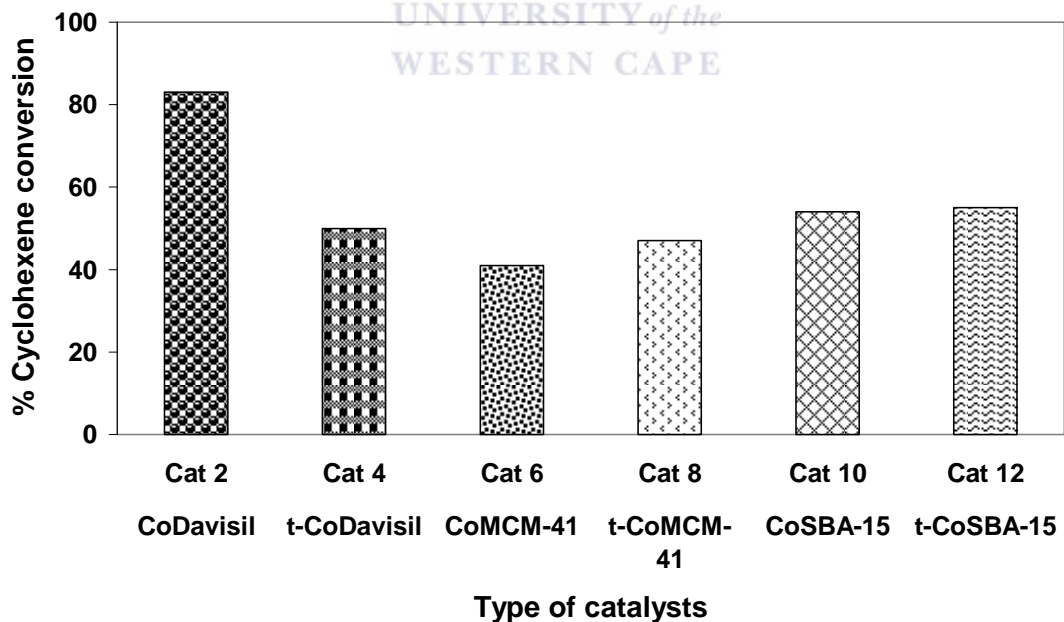
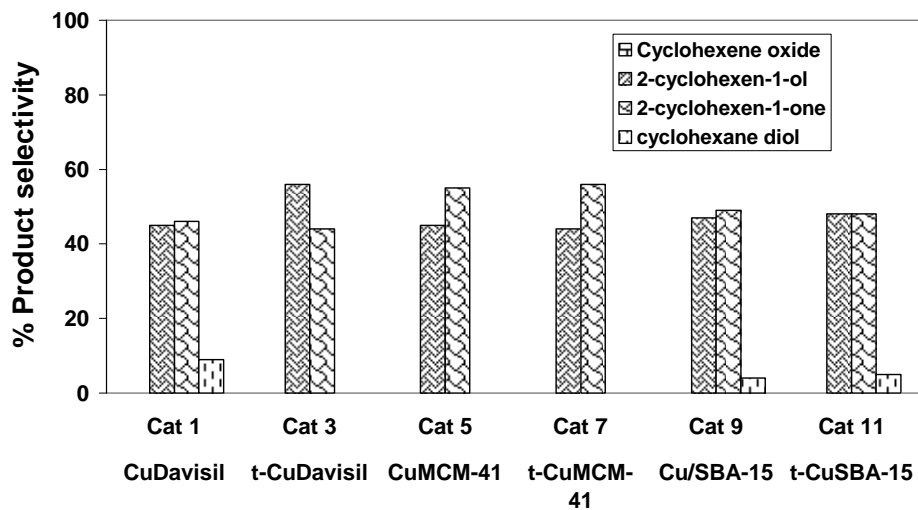


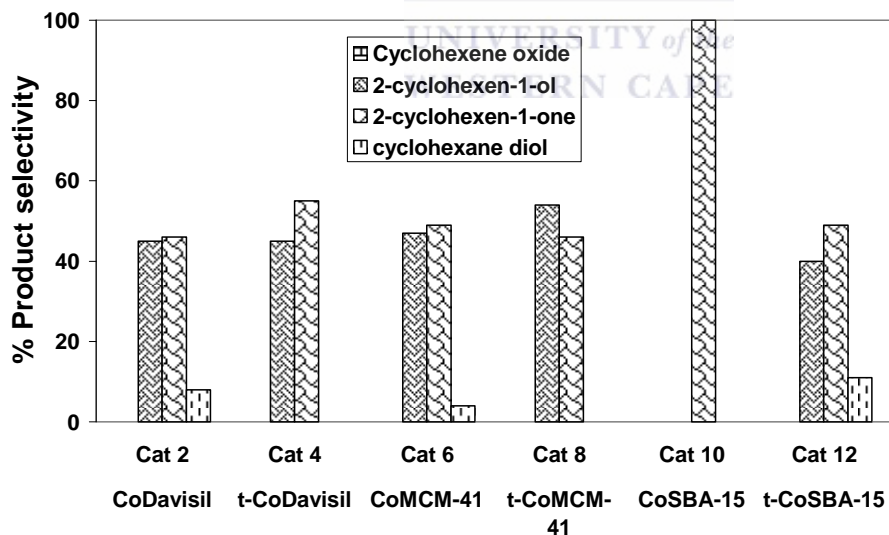
Chart 3.3: Cyclohexene conversion using immobilized Cu and Co unsubstituted and tertiary butyl substituted catalysts.

Effect of substituents on product selectivity using Cu catalysts



Type of catalysts

Effect of substituents on product selectivity using Co catalysts



Type of catalysts

Chart 3.4: Product distribution using immobilized unsubstituted and tertiary butyl Cu(II) and Co(II) catalysts.

3.2.3 The effect of support

Different types of amorphous and mesoporous silica carriers were used to support the catalysts. A reaction ratio of 1:1000:1000 (metal: cyclohexene: hydrogen peroxide) was used. The silica supports differ in pore sizes and have different well-defined surface areas. The reason for the use of silica supports with different pore sizes is that the catalysts can either be anchored on the surface of the support or in the pores of the support depending on the size of the pores. This allows for the probing of the effect of locations of catalytic sites. SBA-15, MCM-41 and Davisil silica gel were used. SBA-15 has larger pore sizes than MCM-41, while the latter have larger pore sizes than Davisil silica gel. It is suspected that the catalysts will either bind on the surface or inside the pores in case of SBA-15 and MCM-41. While in the case of Davisil silica gel, catalysts will bind only on the surface. Also the surface area of these supports differ, with Davisil silica gel having a surface area of 480 m²/g, MCM-41 a surface area of 1191.1 m²/g and SBA-15 with surface area of 943.3 m²/g. Due to these differences of the supporting materials, the immobilized catalysts are expected to behave differently in cyclohexene oxidation.

Chart 3.5 shows that the Davisil silica gel immobilized catalysts exhibited the highest cyclohexene conversion followed by SBA-15 immobilized catalysts. Lastly MCM-41 immobilized catalysts gave the lowest conversion.

Effect of support on conversion using immobilized unsubstituted Cu(II) and Co(II) catalysts

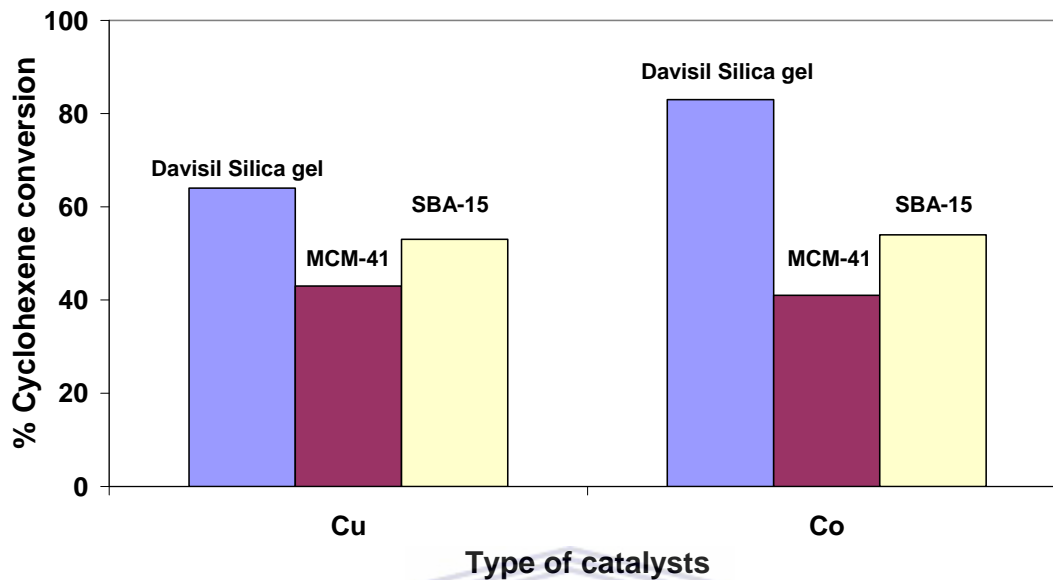
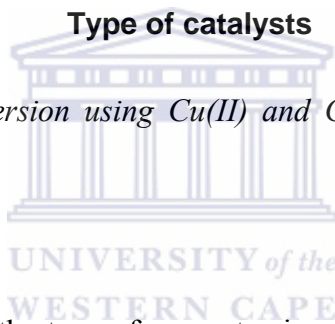


Chart 3.5: Cyclohexene conversion using Cu(II) and Co(II) catalysts immobilized on different supports.



When comparing the effect of the type of support using the Cu(II) catalysts, the product selectivity favours the formation of 2-cyclohexen-1-one and 2-cyclohexen-1-ol as the major products while the 1,2-diol is formed in small amounts as shown in **Chart 3.6**. SBA-15 and Davisil silica gel immobilized catalysts show similar product distributions.

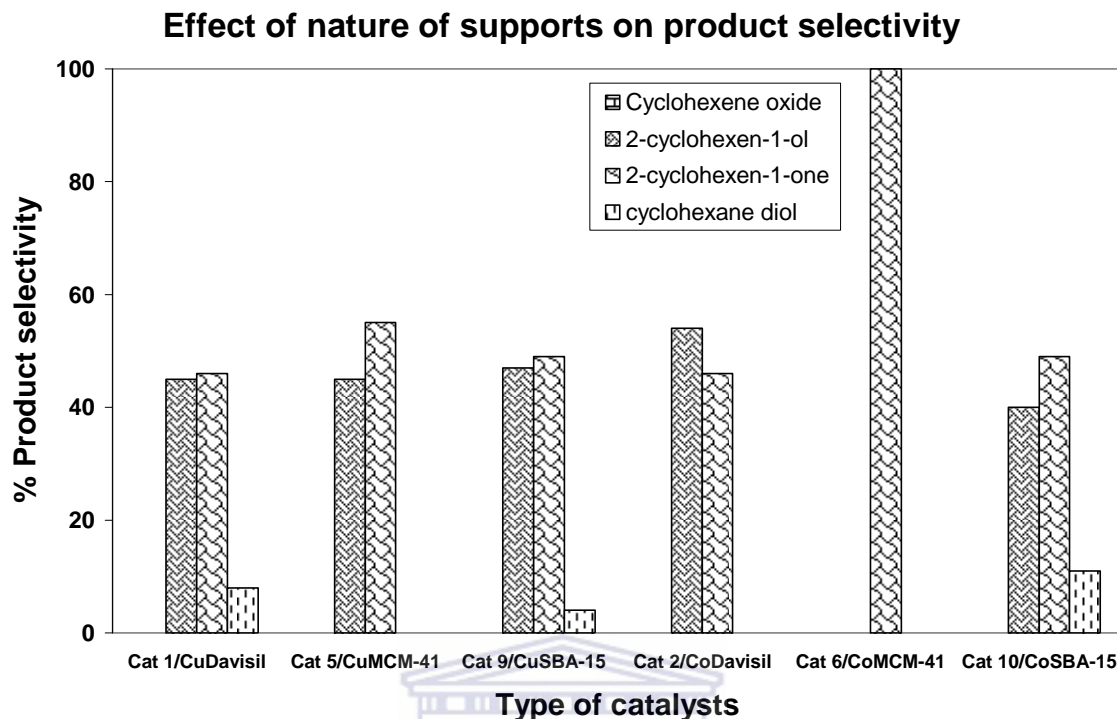


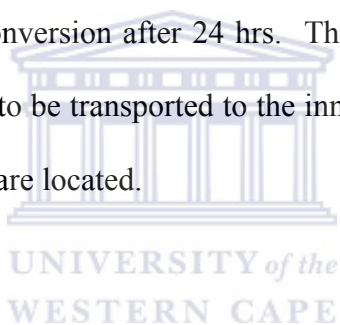
Chart 3.6: Effect of nature of support on product selectivity using unsubstituted Cu(II) and Co(II) immobilized catalysts.

This would suggest that these catalysts sites are in a similar environment. The only situation where this is possible for both Davisil silica gel and SBA-15 is if the catalysts sites are on the external surfaces of the support. In the case of SBA-15 there are two possible environments, viz external surface and the inside of the pores. In the case of Co(II) catalysts, the SBA-15 immobilized systems shows a similar trend to that of SBA-15 immobilized Cu(II) catalysts. The Davisil silica gel immobilized Co(II) catalysts were found to be selective to both 2-cyclohexen-1-ol and 2-cyclohexen-1-one. Lastly MCM-41 immobilized Co(II) catalyst shows 100% selectivity to 2-cyclohexen-1-one.

3.2.4 The effect of time.

The effect of time was evaluated to check the life time of the catalysts. The reaction ratio used is 1:1000:1000 (metal: cyclohexene: hydrogen peroxide). Samples were taken from the reaction mixture after 5 hrs and after 24 hrs.

Chart 3.7 shows the effect of time on cyclohexene conversion using immobilized Cu(II) and Co(II) catalysts. As expected the conversion after 24 hrs is higher than after 5 hrs. However the increase in conversion after 24 hrs is not significant in the case of Davisil silica gel and SBA-15 supported catalysts. MCM-41 based catalysts on the other hand show significant increase in conversion after 24 hrs. This might be due to the fact that the substrate takes longer time to be transported to the inner pores where it is suspected a large proportion of active sites are located.



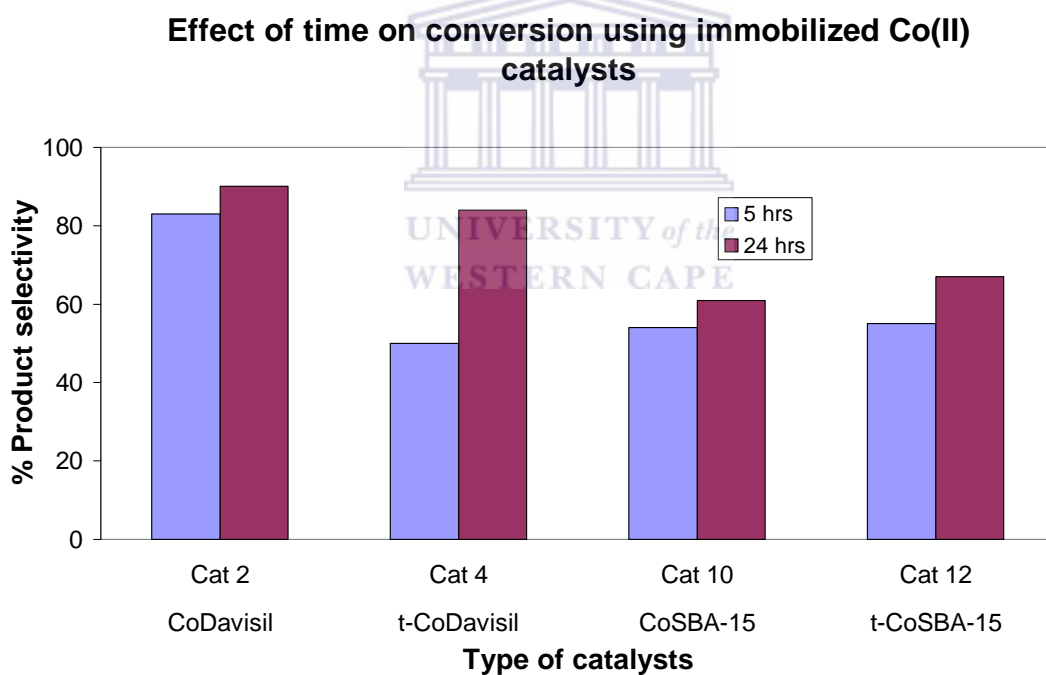
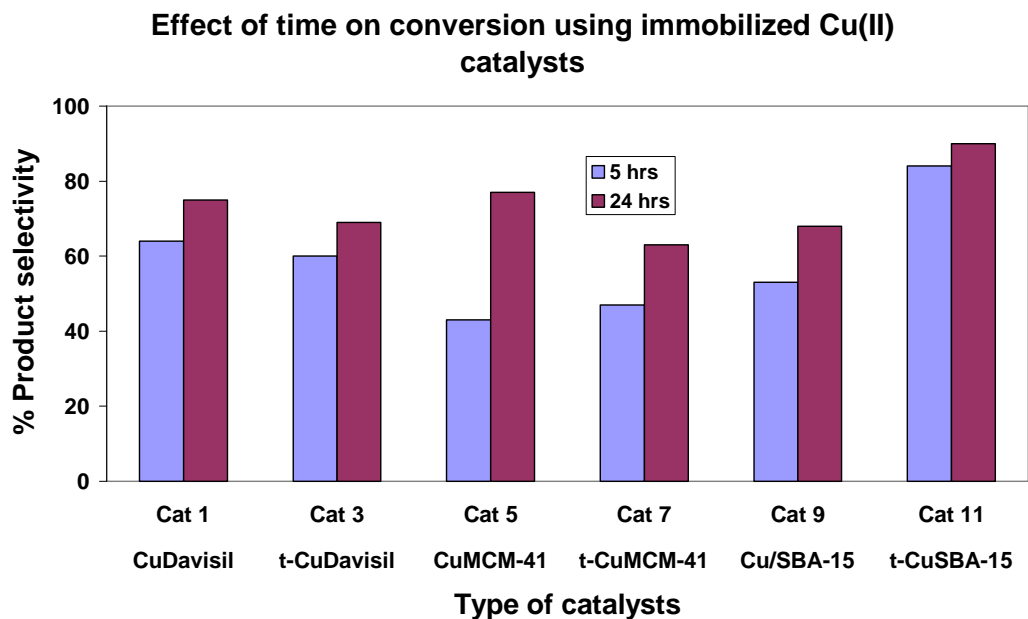
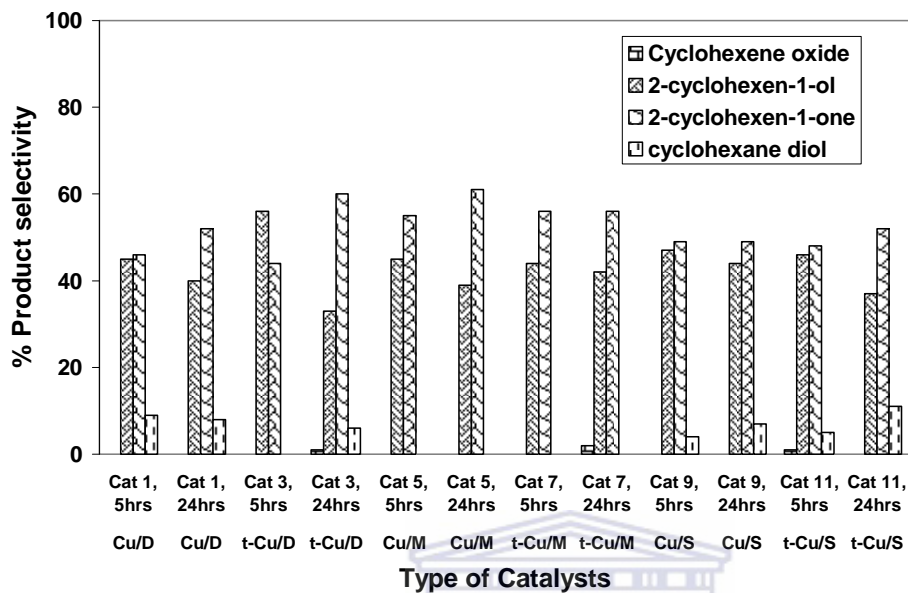


Chart 3.7: The effect of time on cyclohexene conversion using immobilized Cu(II) and Co(II) catalysts.

Effect of reaction time on product selectivity using immobilized Cu catalysts



Effect of reaction time on product selectivity using immobilized Co catalysts

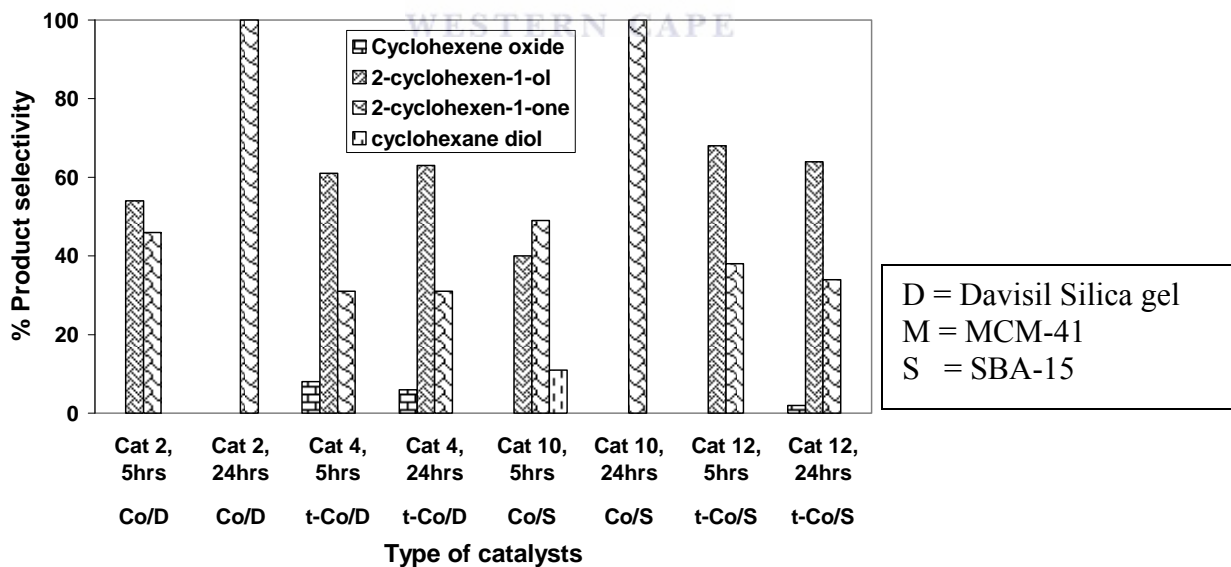


Chart 3.8: Product distribution of immobilized Cu(II) and Co(II) catalysts after 5 hrs and 24 hrs.

It is also observed that after 24 hrs, immobilized Co catalysts shows higher cyclohexene conversion (> 80%) as compared to the immobilized Cu catalysts.

In **chart 3.8**, it is observed that when using immobilized Cu catalysts after 5 hrs the product selectivity shows almost equal amounts of 2-cyclohexen-1-ol and 2-cyclohexen-1-one formation. While after 24 hrs the major product is the 2-cyclohexen-1-one. In some cases there is formation of cyclohexene oxide and cyclohexane diol in small amounts. Using tertiary butyl substituted Cu immobilized on Davisil silica gel (**Cat 3**) as catalyst gave 2-cyclohexen-1-ol as the major product after 5 hrs. Homolytic cleavage seems to be the most dominating mechanism for these reactions, forming the most stable product (2-cyclohexen-1-one) after 24 hrs. When using immobilized Co catalysts, the major product is the 2-cyclohexen-1-ol in most cases especially in the case of the immobilized tertiary butyl substituted Co catalysts after 5 hrs. **Cat 6** was found to be the most selective for 2-cyclohexen-1-one.

After 24 hrs, the immobilized tertiary butyl substituted Co catalysts favours 2-cyclohexen-1-ol as the major product, while Co/SBA-15 (**Cat 10**) and Co/Davisil (**Cat 2**) are more selective for 2-cyclohexen-1-one. The Co/MCM-41 (**Cat 6**) favours almost equal amounts of 2-cyclohexen-1-ol and 2-cyclohexen-1-one while cyclohexeneoxide is formed in small amounts.

In conclusion, there was no significant change in product selectivity after 5 hrs and 24 hrs. The immobilized Cu and Co catalysts were found to be selective to 2-cyclohexen-1-ol and 2-cyclohexen-1-one. Shakhivel *et.al.* noted that at first the 2-cyclohexen-1-one was the major product. The selectivity of 2-cyclohexen-1-one decreased due to time, side products such as cyclohexeneoxide and cyclohexanediol were observed.¹¹

3.2.5 The effect of substrate concentration

Cyclohexene oxidation was also evaluated using 1:500:500 mol ratio (metal: cyclohexene: hydrogen peroxide) at 60 °C, using 0.01mmoles of catalysts, 30% of hydrogen peroxide as oxidant, molecular oxygen as co-oxidant and acetonitrile as solvent. The reaction was run for 5 hrs and 24 hrs.

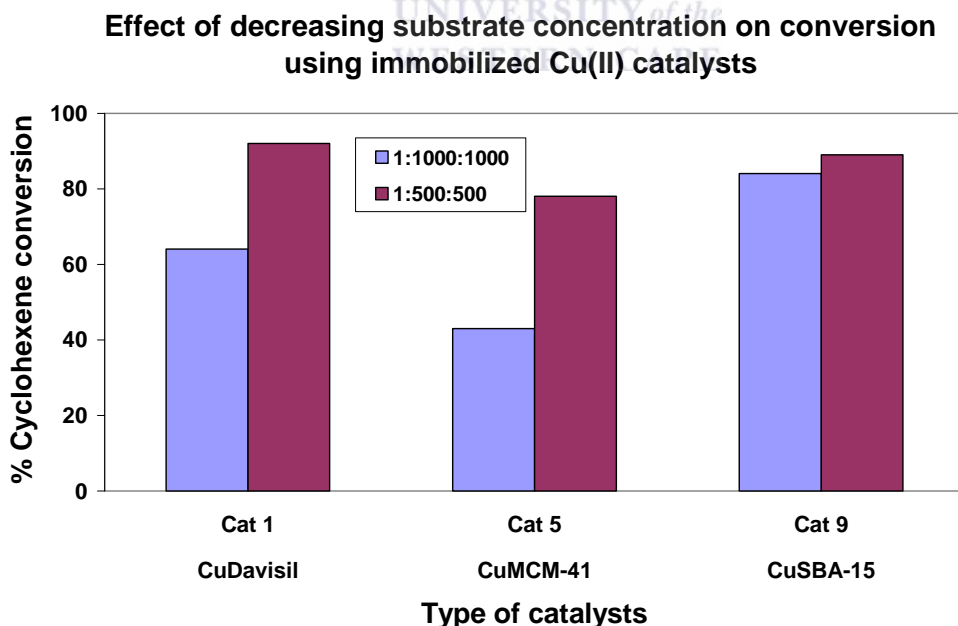
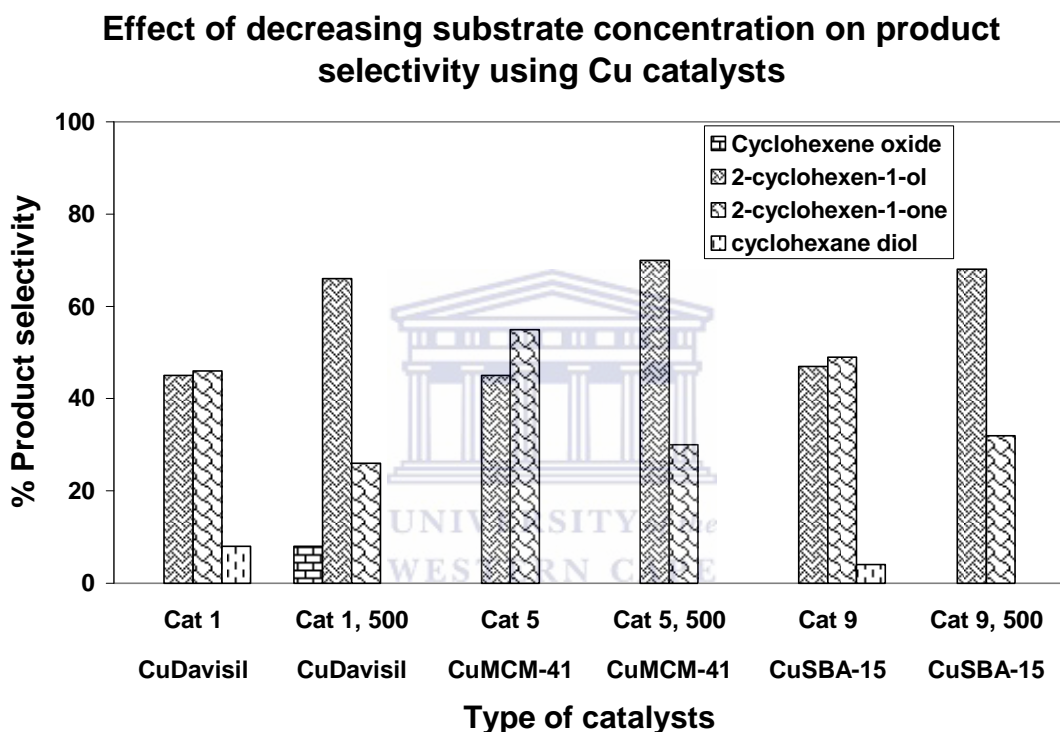


Chart 3.9: Effect of decreasing substrate on cyclohexene conversion using immobilized unsubstituted Cu(II) catalysts.

Chart 3.9 shows the comparison of 1:1000:1000 with 1:500:500 (metal: cyclohexene: hydrogen peroxide) reaction ratio using immobilized unsubstituted Cu(II) catalysts. This chart shows that when decreasing the concentration of substrate by 50%, the immobilized Cu(II) catalysts tends to convert cyclohexene in higher amounts as compared to when using a 1:1000:1000 (metal: cyclohexene: hydrogen peroxide) reaction ratio.



500 = 1:500:500 (metal: cyclohexene: hydrogen peroxide)

Chart 3.10: Effect of decreasing substrate on product distribution using Cu(II) immobilized catalysts.

Chart 3.10 shows the effect on selectivity when comparing reaction ratio of 1:1000:1000 with 1:500:500 reaction ratio using immobilized unsubstituted Cu catalysts. When decreasing the substrate concentration by 50% using immobilized unsubstituted Cu

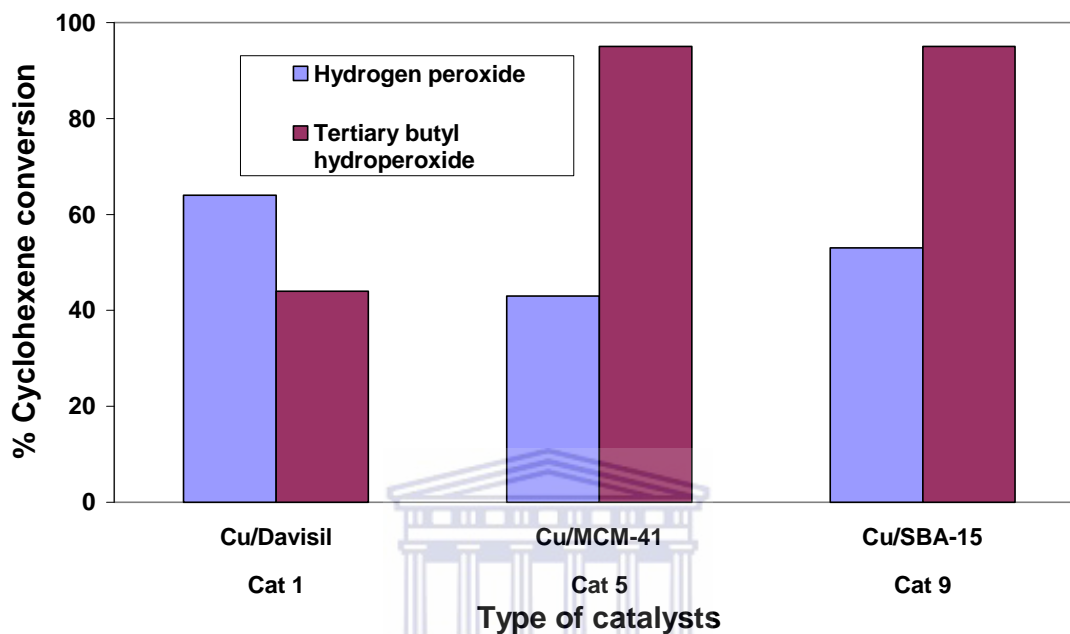
catalysts, it is observed that the most favoured product is 2-cyclohexen-1-ol whereas when a 1:1000:1000 reaction ratio is used, almost equal amounts of 2-cyclohexen-1-ol and 2-cyclohexen-1-one are obtained. In conclusion, when the concentration of substrate is decreased by 50%, the catalysts are more selective to 2-cyclohexen-1-ol. In most cases there is no epoxidation products formed in the reaction except in the case of **Cat 1** where small amounts of cyclohexene oxide are observed.

3.2.6 The effect of changing oxidant

The effect of the nature of the oxidant was evaluated by changing from 30% hydrogen peroxide to tertiary butyl hydroperoxide using a reaction ratio of 1:1000:1000 (metal: cyclohexene: hydrogen peroxide) and employing the unsubstituted Cu catalysts.

Chart 3.11 shows the effect of changing oxidant from hydrogen peroxide to tertiary butyl hydroperoxide. The latter shows higher cyclohexene conversion than hydrogen peroxide for all cases except Davisil silica gel immobilized Cu catalysts (**Cat 1**).

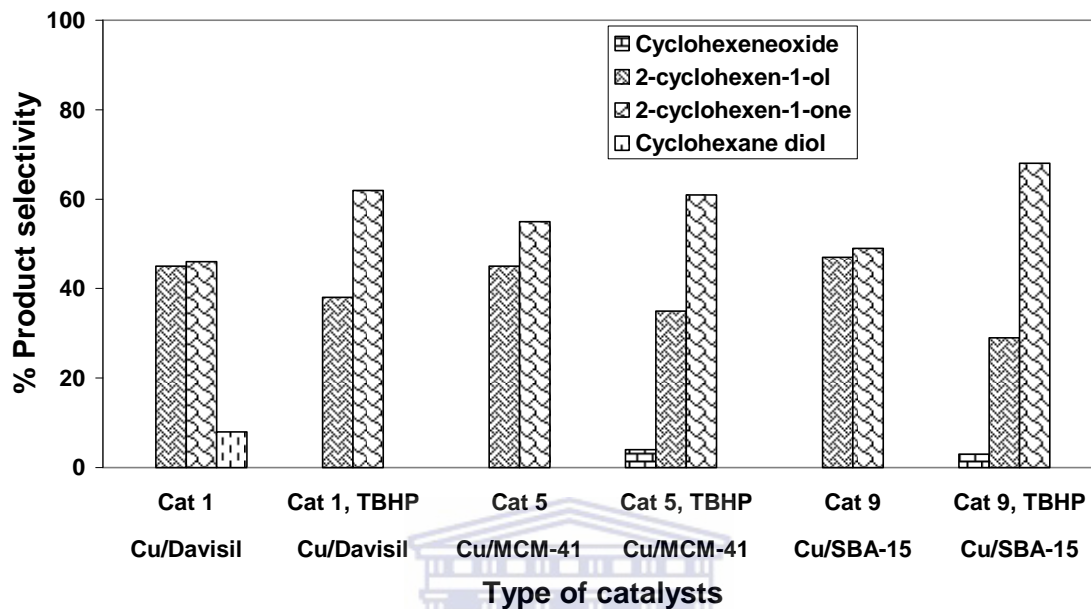
Comparison of H₂O₂ with TBHP on cyclohexene conversion using immobilized Cu catalysts



TBHP = tertiary butyl hydroperoxide

Chart 3.11: Comparison of the use of hydrogen peroxide and tertiary butyl hydroperoxide as oxidants on cyclohexene conversion using unsubstituted Cu immobilized catalysts.

**Effect of H₂O₂ against TBHP on product selectivity
using Cu catalysts**



TBHP = tertiary butyl hydroperoxide

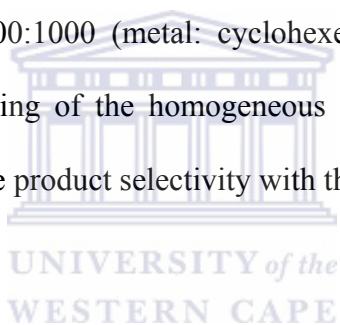
Chart 3.12: Comparison of the effect of hydrogen peroxide against tertiary butyl hydroperoxide as oxidants on product selectivity using immobilized unsubstituted Cu catalysts.

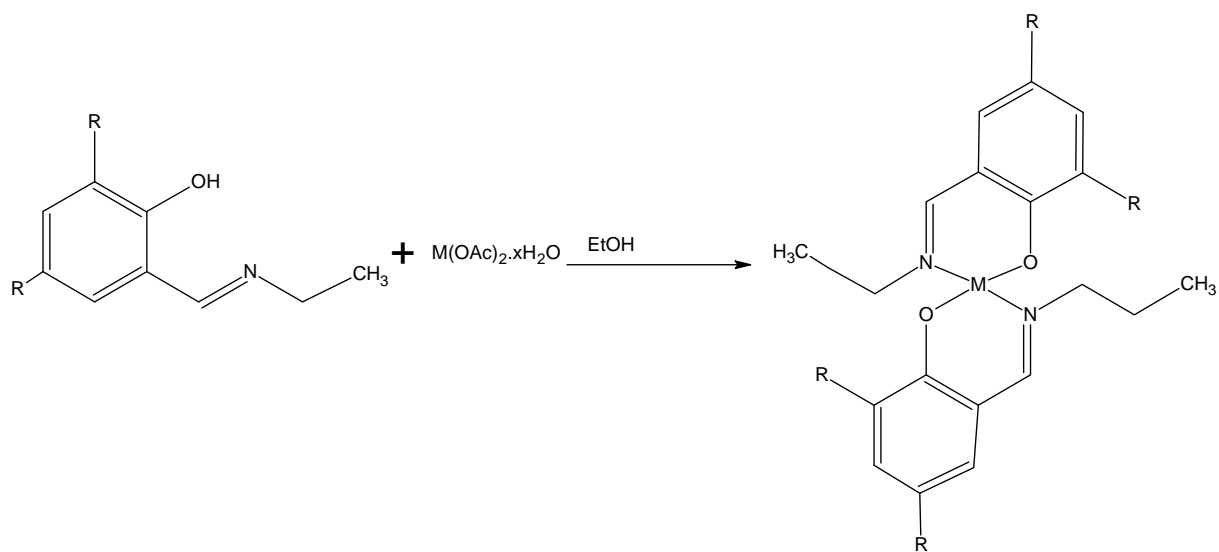
Chart 3.12 shows that when using tertiary butyl hydroperoxide the catalysts tend to favour the formation of 2-cyclohexen-1-one as the major product whereas when using hydrogen peroxide, the catalysts tend to favour almost equal amounts of 2-cyclohexen-1-ol and 2-cyclohexen-1-one as the major products. Chatterjee *et.al.* noticed that their Schiff base chelate Ru complexes showed low yield when using hydrogen peroxide as compared to tertiary butyl hydroperoxide. They claimed that this may be due to the nature of the binding ability of the precursor oxidant. The presence of the methyl groups

in tertiary butyl hydroperoxide makes it a stronger nucleophile as compared to hydrogen peroxide. In their results after 4 hrs they obtained 55% of 2-cyclohexen-1-ol and 5% of 2-cyclohexen-1-one using tertiary butyl hydroperoxide, while in the case of hydrogen peroxide they obtained 13% of 2-cyclohexen-1-ol, 2% of 2-cyclohexen-1-one and 3% of cyclohexene oxide.¹²

3.3 Evaluation of Catalytic Activity using Homogeneous Analogues

Homogeneous analogues of the immobilized catalysts were also evaluated for cyclohexene oxidation using the same reaction conditions as the heterogeneous systems with a reaction ratio of 1:1000:1000 (metal: cyclohexene: hydrogen peroxide) being employed. The reason for using of the homogeneous analogues was to compare the cyclohexene conversion and the product selectivity with the heterogeneous analogues.





Catalyst 5; M = Cu, R = H

Catalyst 6; M = Co, R = H

Catalyst 7; M = Cu, R = ^tBu

Catalyst 8; M = Co, R = ^tBu



Scheme 3.6: Synthetic route of the homogeneous analogues of the immobilized catalysts.

**Effect of homogeneous analogues in conversion using
Cu and Co catalysts after 5 hrs**

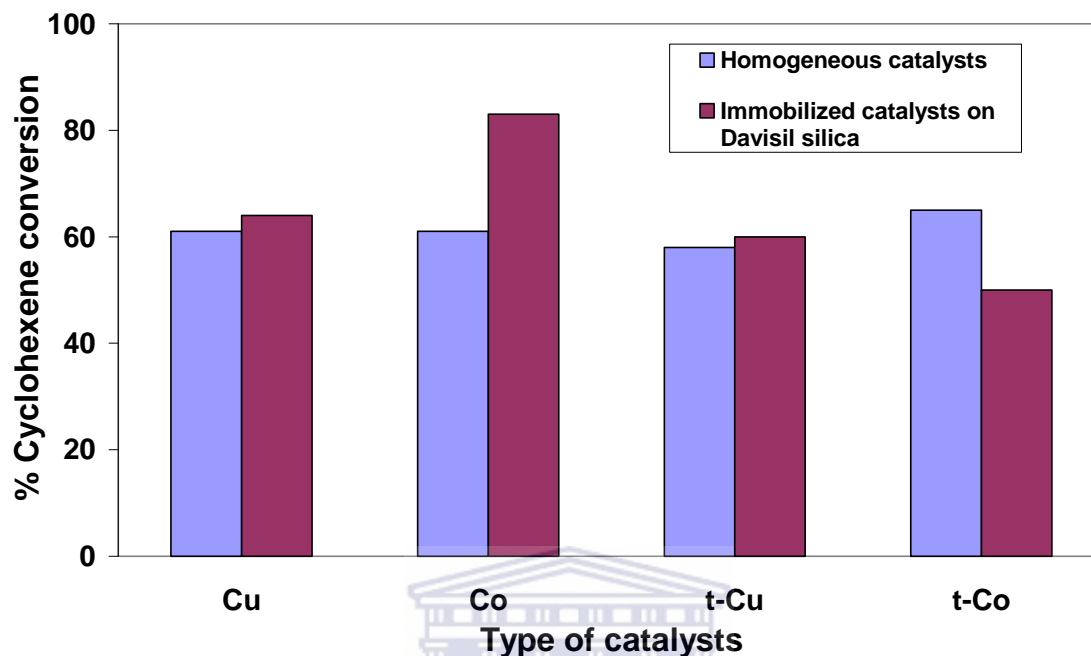


Chart 3.13: Comparison of cyclohexene conversion using homogeneous analogues against heterogeneous analogues.

It was observed that both homogeneous and heterogeneous catalysts convert cyclohexene in relatively moderate amounts. Immobilized Co catalysts convert cyclohexene in higher amounts than the homogeneous catalyst. Immobilized tertiary butyl substituted Co catalyst show the opposite trend where the homogeneous analogues convert cyclohexene in higher amounts than its heterogeneous analogue. It is known that homogeneous catalysts tend to decompose in the reaction mixture leading to low overall conversion.

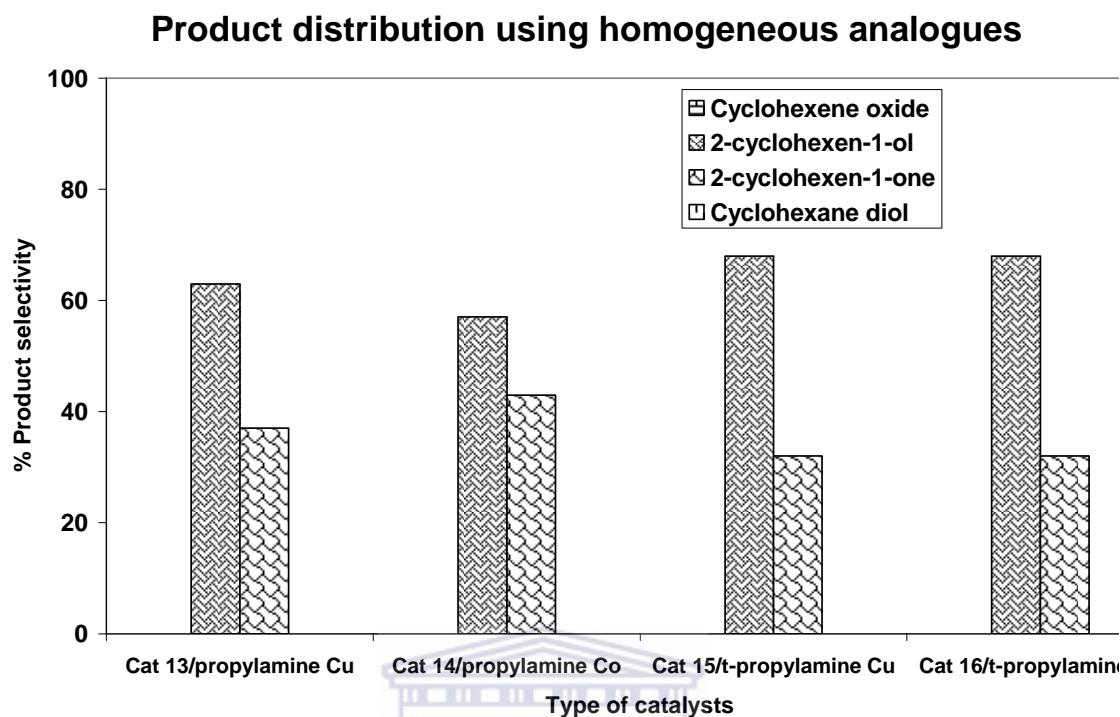


Chart 3.14: Product distribution using homogeneous analogues.

It was observed that homogeneous catalysts show a different selectivity pattern to that of the heterogeneous analogues. The former produce only allylic products whereas heterogeneous analogues produce allylic and some epoxidation products. 2-cyclohexen-1-ol is also produced in higher amounts than was the case for heterogeneous systems. Homogeneous catalysts are very selective as compared to heterogeneous catalysts as observed in our case. Choplin *et.al.* found that heterogeneous catalysts have poorer selectivity than their homogeneous analogues due to the presence of various potential active sites on the surface of the solid that might react with the substrate to form side reactions.¹³

3.4 Conclusion

Cyclohexene oxidation using hydrogen peroxide and tertiary butyl hydroperoxide as potential oxidants in the presence of molecular oxygen as co-oxidant yielded allylic products as the major products. Epoxidation products were obtained as minor products in some cases using heterogeneous catalysts. The effect of substituents was evaluated using heterogeneous catalysts. It was observed that tertiary butyl groups did not have much effect on the immobilized copper(II) catalysts. When using immobilized cobalt(II) catalysts, it was observed that these catalysts favour formation of 2-cyclohexen-1-ol whereas unsubstituted cobalt(II) immobilized catalysts favour formation of 2-cyclohexen-1-one. This difference might be due to steric crowding caused by tertiary butyl groups which cause the immobilized substituted Co(II) catalysts not to behave the same as immobilized substituted Cu(II) catalysts. The effect of support was also investigated, it was found that Davisil silica gel and SBA-15 immobilized catalysts tend to produce similar products. Reducing the substrate concentration changes the selectivity of immobilized catalysts as well as giving higher cyclohexene conversion. Changing the oxidant from hydrogen peroxide to tertiary hydroperoxide shows some improvement in cyclohexene conversion and exhibits a different selectivity profile. Using homogeneous analogues better selectivity was obtained due to the fact that these catalysts were selective only on allylic products irrespective of the substituent whereas the heterogeneous analogues gave both allylic and epoxidation products.

3.5 Experimental Method

3.5.1 Reagents

Most reagents used were purchased from Sigma Aldrich. The following reagents were utilized without further purification; cyclohexene oxide 98%, 2-cyclohexen-1-ol 95%, 2-cyclohexen-1-one 95%, 1,2-cyclohexanediol 98%, cyclohexene, toluene, acetonitrile 99.9% and tert-butyl hydroperoxide solution 70 wt % in water. 30% hydrogen peroxide was purchased from Saarchem uniVAR.

3.5.2 Cyclohexene Oxidation Reactions

A Rodley discovery technologies parallel reactor was used to run cyclohexene oxidation reactions. Catalysts (0.01 mmole), cyclohexene (10 mmole) were transferred to a glass reaction vessel followed by 3ml of acetonitrile. The temperature was set at 60 °C while the solution was stirred, when the desired temperature was reached 30% hydrogen peroxide (10 mmole) was added to the stirred solution. Then the reaction was left to proceed for 5 hrs after which 2ml of sample was withdrawn from the reaction then the reaction was left for 24 hrs after which it was stopped after. All the reactions were carried out in this manner for all the catalysts utilized. The products were analyzed by CP Varian Gas Chromatography using a HP-PONA column.

3.6 References

1. G. A. Barf, R. A. Sheldon, *J. Mol. Catal. A: Chem*, **102** (1995) 23.
2. Oxidation Mechanisms, R. Stewart, W. A. Benjamin, Inc, (1964) 13.
3. S. Jana, B. Dutta, R. Bera, S. Koner, *Langmuir*, **23** (2007) 2492.
4. P. Karandikar, K.C. Dhanya, S. Deshpande, A.J. Chandwadkar, S. Sivasanker, M. Agashe, *Catal. Commun.*, **5** (2004) 69.
5. (a) Z. Yang, Q. Kang, H. Ma, C. Li, Z. Lei, *J. Mol. Catal. A: Chemical*, **213** (2004) 169, (b) H. Weiner, A. Trovarelli, R. G. Finke, *J. Mol. Catal. A: Chem.*, **191**, 3967, (c) J. E. Bennet, D. M. Brown, B. Mile, *Chem. Commun.*, (1969) 504.
6. K. U. Ingold, *Chem. Rev.*, **61** (1961) 563.
7. W. Nam, H. J. Han, S. Y. Oh, Y. J. Lee, M. Choi, S. Han, C. Kim, S. K. Woo, W. Shin, *J. Am. Chem. Soc.*, **122** (2000) 8677.
8. Homogeneous Transition-metal Catalysis: A gentle art, C. Masters, London New York Chapman and Hall, (1981)172.
9. B. S. Lane and K. Burgess, *Chem. Rev.*, **103** (2003) 2457
10. M. Salavati-Niasari, M. Shaterian, M. R. Ganjali, P. Norouzi, *J. Mol. Catal. A: Chem*, **261** (2007) 147.
11. A. Shakthivel, S. E. Dapurkar, P. Selvam, *Appl. Cat. A: Gen.*, **246** (2003), 283.
12. D. Chatterjee, A. Mitra, R. E. Shepherd, *Inorganic Chimica Acta*, **357** (2004) 980.
13. A. Choplin, F. Quignard, *Coord. Chem. Rev*, **178-180** (1998) 1679.

CHAPTER 4



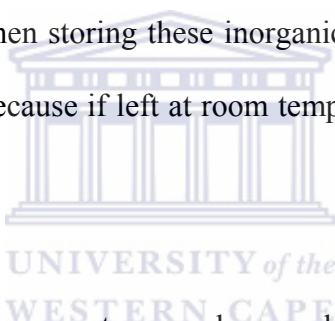
UNIVERSITY *of the*
WESTERN CAPE

SUMMARY

4.1 Summary

Functionalized tertiary butyl substituted and unsubstituted Salicylaldehyde ligands and complexes were successfully synthesized and characterized. Precautions were taken when storing these systems because it was noted that the ethoxy groups of the ligands tend to hydrolyze if left at room temperature for a long time. These systems were stored under vacuum until further use. Some of the synthesized complexes were found to form binuclear species bridged by the phenolic group of the ligand.

Mesoporous silica supports were successfully synthesized and fully characterized. Precautions were also taken when storing these inorganic silica materials. They needed to be stored in the glove box because if left at room temperature for long period of time, the active sites tend to collapse.



Immobilization of metal complexes on to amorphous and mesoporous silica supports was successfully done. The immobilized catalysts were characterized by AAS (metal loading on to the support), FTIR, X-ray diffraction (crystallinity), BET surface analysis (surface area and pore diameter) and SEM (morphology).

The immobilized catalysts were tested for cyclohexene oxidation using molecular oxygen as co-oxidant and hydrogen peroxide as primary oxidant. The following aspects were investigated: i) The effect of metal, ii) The effect of substituents on the ligand, iii) The effect of nature of support material, iv) The effect of decreasing substrate concentration, v) The effect of changing oxidant and vi) Comparison between heterogeneous with their

homogeneous analogues was also investigated in this study. The main products for cyclohexene oxidation under the above investigated aspects were allylic products (2-cyclohexen-1-one and 2-cyclohexen-1-ol). Homogeneous analogues were found to be more selective than the heterogeneous systems. The activity of both of these systems was found to be similar. The binuclear complexes did not play any significant role in catalysis.

